RICE UNIVERSITY

TRANSPORT PHENOMENA AND CHEMICAL REACTION INSIDE A SINGLE CATALYST PELLET

by

Frederick Warren Miller

A THESIS SUBMITTED
IN PARTIAL FULFILLMENT OF THE
REQUIREMENTS FOR THE DEGREE OF

Doctor of Philosophy in Chemical Engineering

Thesis Director's signature:

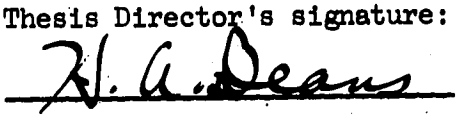

Houston, Texas

October 1964

ACKNOWLEDGEMENTS

The author would like to express gratitude and appreciation to the following persons and organizations for their assistance and support in this work:

Dr. H. A. Deans -- It is an honor to be his first doctoral candidate.

Engelhard Industries ---for gratuitously supplying the catalyst used.

A. B. Stiles and E. I. du Pont de Nemours & Co., Inc. -- for gratuitously determining the surface area and pore volume of the catalyst.

The Production Research Laboratories of the Humble Oil Company -- for use of their facilities to measure the permeability of the catalyst pellets.

The Monsanto Chemical Company -- for their support of the project.

The Pan American Petroleum Corporation -- for their financial support.

The Rice University -- for their financial support.

My wife, Weejee, and our parents.

TABLE OF CONTENTS

TABLE OF CONTENTS (Continued)

TABLE OF CONTENTS (Continued)

LIST OF TABLES

LIST OF FIGURES

LIST OF FIGURES (Continued)

LIST OF ABBREVIATIONS

BTU	British Thermal Unit
cc	Cubic centimeter
cfm	Cubic feet per minute
cm	Centimeter
d.c.	Direct Current
Fig.	Figure
ft	Feet
g	Gram
hp	Horsepower
hr	Hour
I.D.	Inside diameter
in	Inch
m	Meter
min	Minute
ml	Millimeter
mv	Millivolt
No.	Number
O.D.	Outside diameter
ppm	Parts per million
psia	Pounds per square inch absolute
psig	Pounds per square inch gauge
rpm	Revolutions per minute
sec	Seconds

TABLE OF NOMENCLATURE

Symbol	Meaning
A_i, B_i, C_i, B_i	Coefficients in Equation (A-1)
A	Frequency factor, 1/sec
a	Accommodation coefficient
^oC	Degrees centigrade
c_1, c_2	Integration constants
c	Total molar concentration, moles/vol
C_i	Molar concentration of i, moles/vol
C_p	Heat capacity at constant pressure
D_e	Effective diffusivity, cm^2/sec
D_{ij}	Ordinary binary diffusivity, cm^2/sec
D_{AB}^{EFF}	Effective binary diffusivity of A in B, cm^2/sec
D_{im}^{EFF}	Effective diffusivity in a mixture, cm^2/sec
E_i, F_i	Defined by Equation (A-30)
E	Activation energy, cal/mole
E*	Observed activation energy, cal/mole
^oF	Degrees Fahrenheit
F	Volumetric flow rate of hydrogen in diffusivity cell cc/min
f, g	Defined by Equation A-5
Δf	Flow meter pressure reading, in. water
g_i	Body force per unit mass of component i
$\hat{H}$	Enthalpy per unit mass
$\bar{H}_i$	Partial molal enthalpy
$(-\Delta H)$	Negative heat of reaction, cal/mole

TABLE OF NOMENCLATURE (Continued)

Symbol	Meaning
h	Heat transfer coefficient,
I_o	Modified Bessel function of the first kind, of order 0
j_i	Mass flux of i relative to mass average velocity, mass/time, area
j_D, j_H	Chilton-Colburn j-factors for mass and heat transfer
J_i	Molar flux of i relative to mass average velocity, moles/time, area
ka	Specific reaction rate constant with incorporated area, 1/sec
k_{Am}	Mass transfer coefficient
k_e	Effective thermal conductivity
k_D	Thermal conductivity of the discontinuous or solid phase
k_f	Thermal conductivity of the continuous or gas phase as given by Equation (A-44)
k_t	Thermal conductivity contribution of the pellet particles
k_c	Thermal conductivity contribution due to particle contact
^oK	Degrees Kelvin
K	Permeability of the catalyst pellets, millidarcies
K_o	Modified Bessel function of the second kind, of order 0
$\bar{l}$	Mean free path
l	Coordinate distance
L	Length of catalyst pellet
M	Molar flow rate, moles/time
M_i	Molecular weight of i
$(Nu)_h$	Nussult number for heat transfer given by Equation (24)
$(Nu)_m$	Nussult number for mass transfer given by Equation (22)

TABLE OF NOMENCLATURE (Continued)

Symbol	Meaning
n	Reaction order
n^*	Observed reaction order
N	Number of grid increments
N_i	Molar flux of i with respect to stationary coordinates, moles/time, area
P	Porosity
Pr	Prandtl number
p	Pressure
Δp	Micromanometer pressure reading, cm red oil
p_a	Atmospheric pressure
p_m	Mean pressure
q	Energy flux relative to mass average velocity
R	Radius of pellet
R_g	Gas constant
R_i	Molar reaction rate of i, moles/time, vol
^oR	Degrees Rankine
Re	Reynolds number
r	Radio coordinate
$\bar{r}$	Mean pore radius
r_1, r_2	Binary diffusion coefficient ratios
R^*	Observed reaction rate, moles/time, vol
S	Molecular diameter
Sc	Schmidt number
t	Time

TABLE OF NOMENCLATURE (Continued)

Symbol	Meaning
T	Temperature
ΔT	Thermocouple temperature differential measured between reactive and inert catalyst pellets
$(\Delta T)_{max}$	Maximum temperature rise in a pellet according to Prater (32)
v	Velocity
W_1, W_2	Cylinder weights
X_i	Mole fraction of i

GREEK SYMBOLS

α, β, λ	Dimensionless parameters defined by Equation (16)
ξ, ψ, ϕ	Dimensionless variables defined by Equation (16)
γ	Specific heat ratio, C_p/C_v
δ	Geometric diffusion factor
ϵ_a	Macrovoid fraction
ϵ_i	Microvoid fraction
η	Effectiveness factor
θ	Dimensionless temperature
μ	Viscosity, mass/length, time
ρ	Density, mass/vol
σ	Standard deviation
σ_{AB}	Lennard-Jones parameter
τ	Stress tensor (Equation (2) only); dimensionless time
ω	$1 + (N_B/N_A)$
$\Omega_{D_{AB}}$	Mass diffusivity function for Equation (F-1)

TABLE OF NOMENCLATURE (Continued)

SUBSCRIPTS

Symbol	Meaning
A	Oxygen
B	Hydrogen
C	Water
D	Nitrogen
s	Surface of film
ss	Surface of solid
i	Grid point index; component designation
N	N^{th} grid point (solid surface)

I. INTRODUCTION

The heat and mass transfer accompanying a chemical reaction occurring in a porous media has received considerable attention in recent years. Most work has been focused upon proper experimental and theoretical evaluation of diffusion coefficients and effectiveness factors for isothermal systems. Although theoretical treatments of non-isothermal cases have appeared, they have not been followed through experimentally. The highly exothermic water formation reaction on a platinum catalyst has been studied here with the following objectives:

1. To use a recycle system to study a steady state reaction occurring in a porous catalyst pellet.
2. To determine experimentally the magnitude of the temperature rise which occurs in the catalyst during an exothermic reaction.
3. To determine the theoretical concentration and temperature profiles and the effectiveness factor of the catalyst.
4. To compare the measured temperature rise with the predicted temperature rise as a test of the mathematical model.
5. To evaluate the error that results from neglecting catalytic heat effects in the determination of the effectiveness factor.

II. REVIEW OF OTHER WORK

Since Thiele (49) introduced the effect of diffusional impedition of reaction kinetics into the field of heterogeneous catalysis, literature has appeared which has expanded the original insight to encompass the role of heat and mass transfer within porous catalyst pellets. In his work Thiele suggested the use of the ratio of the actual catalytic activity to the activity in the absence of diffusional retardation for an isothermal reaction. This ratio, usually referred to as the effectiveness factor, has received considerable attention since 1939.

Several reviews of advances in the general field of heterogeneous catalysis are available (5, 8, 23). Those of Carberry (8) and Hougen (23) are more directly applicable to the study of individual catalyst particles.

Much attention has necessarily been focused upon the nature of the diffusion of gases through porous solids since diffusive properties may influence the integral reaction rate. Wicke and Kallenbach (61) made the first attempt to measure diffusivities in porous media. Hoogschagen (22) measured the diffusion rate of oxygen through a porous pellet by reacting the diffused gas with copper and noting the resulting weight change. Several comprehensive papers were written on the subject including those of Wheeler (59, 60) and Weisz and Prater (57).

Weisz simplified the Wicke-Kallenbach method of measuring diffusivities in 1957 (54). The basic method of bathing each side of a mounted pellet with different gases and determining the diffusivity by measuring the resultant effluent concentrations by means of a thermal conductivity cell is still popular today (20, 37, 45, 46). Beek (3)

concluded that both component fluxes needed to be measured because of non-equimolar counterdiffusion occurring in the porous media.

Simultaneously, an effective diffusion coefficient for binary diffusion in pores where any combination of Knudsen and bulk diffusion may occur was developed by Evans, et al. (54), Scott and Dullien (46) and Rothfeld (40). These workers and others (33, 50) also showed that the ratio of the molar fluxes of the components must be equal to the square root of the inverse ratio of the molecular weights of the components regardless of the method of transport. Rothfeld's analysis has been extended to the multicomponent case by Butt (6).

Wakao and Smith (52) proposed a model for predicting diffusion rates at constant pressure through "bidisperse" porous media in terms of the porosity and pore size-distribution of the media. The term bidisperse refers to a dual pore system consisting of micropores within the granules making up the pellet and a macropore region between the granules. These authors reached the simple conclusion that in the absence of Knudsen diffusion the diffusivity is porportional to the square of the macropore porosity, i.e., $D_E/D_{AB} = \epsilon_a^2$. This conclusion was also reached by Weisz and Schwartz (58) who investigated numerous porous catalysts.

While the diffusion in porous media has received considerable attention, the thermal conductivity has not. Sehr (47) reviewed the experimental methods available to determine thermal conductivities and compared data taken by these methods on several porous catalysts. The conductivity of alumina pellets was measured by Mischke and Smith (28) under vacuum, in air and in a helium atmosphere. The macropore volume

fraction of the pellets was observed by these authors to be the most influential variable.

The thermal conductivity of the heterogeneous gas-solid mixture is important in determining the magnitude of the temperature gradients which may occur in a catalyst particle due to the non-isothermal nature of the reaction. Damkohler (13) and Wheeler (60) investigated the thermal effects in spherical particles with a first order reaction and found the temperature as a function of concentration to be given by

$$(T - T_s) = \frac{(-\Delta H) D_e}{k_e} (C_s - C)$$

This result was found to be valid for all kinetics and all particle geometries by Prater (32). Obviously, the temperature rise becomes a maximum whenever the concentration in the pellet becomes zero. Temperature measurements within the interior of reactive pellets have not been recorded in the literature.

A number of authors (9, 27, 41, 50, 56) undertook theoretical treatments of porous catalysts under non-isothermal reaction conditions. An analytical solution was presented by Schilson and Amundsen (41). Mingle and Smith (27) introduced micro and macro effectiveness factors to suit the bidisperse model of the catalyst pellet. Reversible reactions (11) and the problem of selectivity in a chain reaction (10) were investigated by Carberry for isothermal reactions in bidisperse catalyst systems. Weisz and Hicks (56), using Prater's relationship, solved the coupled heat and mass transport equations to obtain an overall effectiveness factor in terms of quantities available to the experimentalist.

Scott (44) obtained isothermal effectiveness factors for a first order reaction with any mode of diffusion occurring by introducing his previously mentioned general diffusion equation. Special emphasis was placed by Scott on diffusion under reactive conditions and volume changes accompanying the reaction. Butt (7) further suggested the introduction of a position dependent multicomponent diffusivity into the evaluation of the effectiveness factor.

The problem of diffusion and reaction in light of their bidisperse diffusion model (52) was also the subject of a paper by Wakao and Smith (53). The authors show that the diffusivity in the reaction zone is a function of the microeffectiveness factor. Experimental data on effectiveness factors has to date only been reported by Smith and his co-workers (33, 34, 35). In these studies the isothermal ortho-para-hydrogen conversion reaction was studied in porous glass (34), and on silica and alumina supported nickel oxide (33, 35). The theoretically predicted macroeffectiveness factor agreed very well with the experimentally determined values.

Other aspects of individual pellet catalysis have also been considered. For instance, Aris (1) demonstrated that the effectiveness factor is essentially independent of particle geometry in the case of an isothermal reaction. Additionally, numerous authors have investigated the influence of the boundary layer surrounding the individual pellets (3, 9, 12, 38, 41, 48).

Chambré and Acrivos (12) cautioned against the indiscriminate use of the Frank-Kamenetskiĭ (16) approach to the boundary layer. This principle, which is commonly used in engineering analysis, equates the

rate of mass transfer to the ratio of the driving force to the resistance to mass transfer. Beek (3) and Carberry (9) applied Frank-Kamenetskiĭ's average coefficient approach to their boundary conditions in attacking the non-isothermal reactive catalyst problem. Particular emphasis was also given to the boundary condition by Smith and Amundsen (48) in their analysis of reversible catalytic reactions. Rosner (38, 39) has most recently warned of the pitfalls which may arise due to improper consideration of the pellet boundary layer. He specifically points to the deceptive nature of the apparent activation energy and reaction rate in a surface reacting system.

The thesis of Trotter (51) provided the only available instance of the same reaction being carried out on the same type catalyst as is reported here. Trotter studied the hydrogen-oxygen reaction on a 0.28% platinum on alumina powder which had a considerably higher surface area (203 m^2/g) than that used here.

III. THEORETICAL DEVELOPMENT

The mathematical model used describes an infinitely long cylinder of porous catalyst material with a constant diameter as shown in Fig. 1. A gas stream flowing transverse to the cylinder axis carries the reactants to the surface of the catalyst pellet and removes the product.

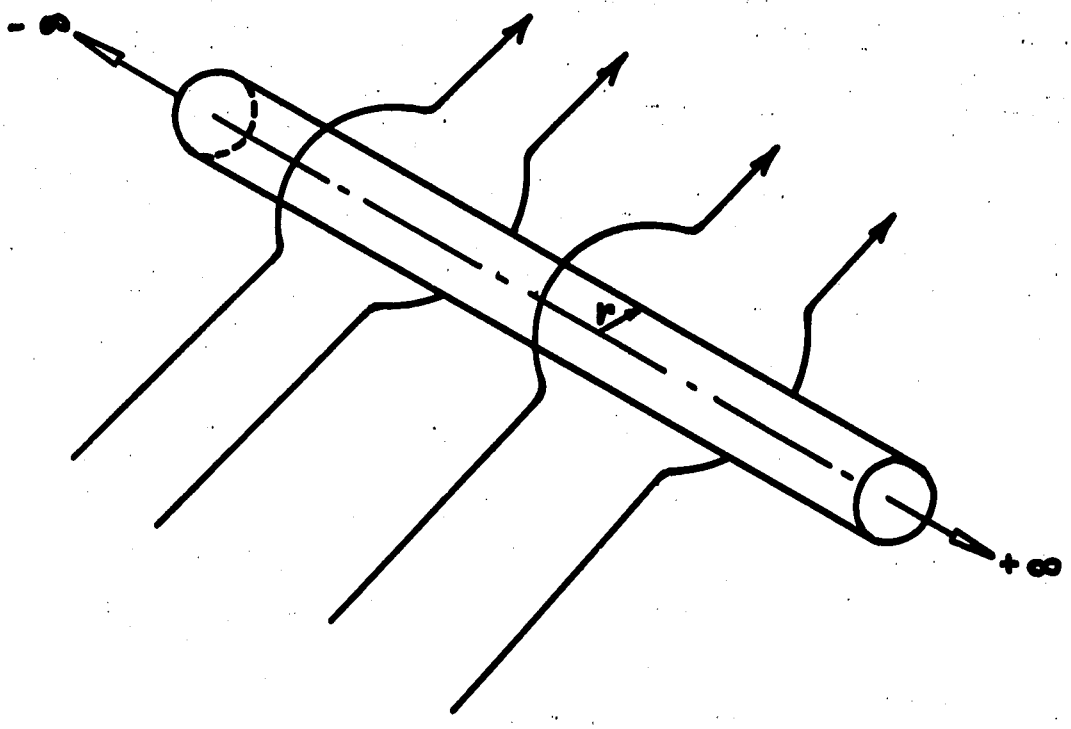

FIGURE 1- THE MODEL

The specific assumptions made are:

1. The cylinder is effectively infinite in length, i.e., no end effects. According to Olsen and Schultz (29) a length greater than four diameters renders the end effects negligible.

2. The surface flow and reaction rate are such that variation of temperature and composition with angular position may be neglected.

3. The diameter of the pellets is large enough relative to the pore size such that diffusion and thermal conduction may be treated as homogeneous phenomena using Fick's and Fourier's laws with effective transport coefficients.

4. The reaction can be expressed as

$$Ae^{-E/RT}(C_A)^n \qquad \text{i.e.,}$$

a) $X_A << X_B$

b) irreversible reaction

c) Arrhenius rate constant.

5. The following effects may be neglected:

a) variations of the diffusivity, thermal conductivity, and heat of reaction with temperature and composition. (See Section V and Appendices F and M.)

b) Pressure change in the pellet due to bulk flow (see Section V).

c) Heat transport due to bulk flow (see Appendix L).

d) Ideal gases

e) Heat generation by viscous dissipation

f) Gravity effects.

The development given here parallels the earlier work of Weisz and Hicks (56), differing in that (a) cylindrical rather than spherical particles are treated, (b) a generalized boundary condition is used and (c) the numerical method of solution is different.

The transport equations in complete form can be written (4)

$$\frac{\partial C_A}{\partial t} + (\nabla \cdot N_A) = R_A \tag{1}$$

for mass transfer of A, and

$$\rho \frac{D\hat{H}}{Dt} = -(\nabla \cdot \mathbf{q}) - (\tau : \nabla v) + \sum_i (j_i \cdot g_i) + \frac{Dp}{Dt} \tag{2}$$

for energy transfer. Since the mass average velocity at any point within the pellet is zero under steady state conditions,

$$\nabla \cdot N_A = R_A \tag{3}$$

and

$$(\nabla \cdot q) = 0 \tag{4}$$

The fluxes are given by the following equations, which serve to define the effective mixture diffusivity and effective thermal conductivity.

$$N_i = - cD_{im}^{eff} \nabla X_i + X_i \sum_{j=1}^{n} N_j \tag{5}$$

$$q = - k_e \nabla T + \sum_i H_i J_i \tag{6}$$

If (6) is combined with (4) and expanded in accordance with assumptions (2) and (5-C) then

$$\nabla \cdot \left(- k_e \nabla T + \sum_i H_i J_i \right) = 0$$

and

$$-k_e \nabla^2 T + \sum_i H_i \nabla \cdot J_i = 0 \tag{7}$$

A A mass balance on the i^{th} component at steady state requires that $\nabla \cdot J_i = R_i$. Thus, in consideration of the reaction being studied, (7) may be rewritten as

$$k_e \nabla^2 T = (-\Delta H) R_A \tag{8}$$

where $(-\Delta H)$ is the negative heat of reaction.

Since the component fluxes are controlled at steady state by the stoichiometry of the reaction, it is seen that

$$N_A = \frac{1}{2} N_B = - \frac{1}{2} N_C; \tag{9}$$

elimination of N_B and N_C from (5), and simplification gives

$$N_A = - \frac{c D_{Am}^{EFF}}{(1-X_A)} \nabla X_A \qquad (10)$$

which is the desired expression.

If the reaction rate is written in accordance with assumption (4) as

$$R_A = - kaC_A^n \qquad (11)$$

then (3) and (8) can be put into the form

$$\frac{1}{r} \frac{d}{dr}\left[\frac{rpD_{Am}^{EFF}}{R_g T(1-X_A)} \frac{dX_A}{dr}\right] = kaC_A^n \qquad (12)$$

and

$$\frac{1}{r} \frac{d}{dr}\left[r\frac{dT}{dr}\right] = - \frac{(-\Delta H)ka}{k_e} C_A^n \qquad (13)$$

The solution of (12) and (13) provide the temperature and oxygen concentration profiles. Another component mass balance is required to describe the system completely, but it is not included here, since one balance is sufficient if the pressure is assumed to be constant.

The specific reaction rate constant can be expressed in Arrhenius form as

$$k = Ae^{-\frac{\epsilon E}{R_g T}}, \qquad (14)$$

and elimination of the frequency factor in favor of the surface temperature rate constant leads to

$$k = k_s e^{\frac{E}{R_g T_s}\left(1 - \frac{T_s}{T}\right)}, \qquad (15)$$

where $k_s = Ae^{-E/R_g T_s}$.

The dimensionless variables and parameters can now be defined

$$\xi = \frac{r}{R};\ \psi = \frac{X_A}{X_{As}};\ \phi = \frac{T}{T_s}$$

$$\alpha^2 = \frac{R^2 k_s a_v C_{As}^{n-1}}{D_{Am}^{EFF}};\ \beta = \frac{E}{R_g T_s};\ \lambda = \frac{(-\Delta H) D_{Am}^{EFF} C_{As}}{k_e T_s} \tag{16}$$

Then, with the aid of (15), the transport equations (12) and (13) can be put into the form

$$\frac{1}{\xi}\frac{d}{d\xi}\left[\frac{\xi}{\phi(1 - X_{As}\psi)}\frac{d\psi}{d\xi}\right] = \alpha^2 e^{\beta\left(1-\frac{1}{\phi}\right)}\left(\frac{\psi}{\phi}\right)^n \tag{17}$$

and

$$\frac{1}{\xi}\frac{d}{d\xi}\left[\xi\frac{d\phi}{d\xi}\right] = -\lambda\alpha^2 e^{\beta\left(1-\frac{1}{\phi}\right)}\left(\frac{\psi}{\phi}\right)^n \tag{18}$$

The boundary conditions at the surface of the pellet are found by equating the solid surface fluxes and the corresponding driving force for transfer of mass and energy between the surface and the flowing gas stream. Thus

$$N_A|_{s.s.} = k_{Am}(C_A - C_{As}) \tag{19}$$

and

$$q|_{ss} = h(T - T_s) \tag{20}$$

With the substitution of (10), (19) becomes in dimensionless form,

$$\psi_{ss} = 1 - \frac{1}{(Nu)_m(1 - X_{As}\psi)}\left.\frac{d\psi}{d\xi}\right|_{\xi=1} \tag{21}$$

where

$$(Nu)_m = \frac{k_{Am}R}{D_{Am}^{EFF}} \tag{22}$$

is the Nussult number for mass transfer. Equation (20) can be written as

$$- k_e \frac{dT}{dr}\Big|_{ss} = h(T - T_s)$$

which is put into the form of (21) to give

$$\phi_{ss} = 1 - \frac{1}{(Nu)_h} \frac{d\phi}{d\xi}\Big|_{\xi=1} \tag{23}$$

where the Nussult number for heat transfer is given by

$$(Nu)_h = \frac{hR}{k_e} \tag{24}$$

The boundary conditions at the pill center express the symmetry of the mass and temperature profiles.

$$\frac{d\psi}{d\xi} = 0 = \frac{d\phi}{d\xi}; \quad \xi = 0 \tag{25}$$

If all of the interior area of the catalyst were exposed to the gas stream concentration and temperature, the integral molar reaction rate could then be expressed as

$$M = - (\pi R^2 L) k_s a C_{As}^n \tag{26}$$

However, diffusional effects may cause the concentration of component A to vary with the pill radius. Likewise, the rate constant varies under non-isothermal conditions existing in the pellet. These combined effects may cause the reaction rate to differ from that given in (26). The actual molar flow at the surface of the pellet is given by

$$M_s = 4\pi R^2 N_A\Big|_s = - \frac{2\pi RLpD_{Am}^{EFF}}{R_g T_s (1-X_A)} \frac{dX_A}{dr}\Big|_{\xi=1} \tag{27}$$

The effectiveness factor is defined in the conventional way as the ratio of this actual molar flow rate to the flow rate which would occur if the entire internal area were exposed to the surface temperature and oxygen concentration.

$$\eta = \frac{2}{\alpha^2 (1 - X_{As}\psi)} \frac{d\psi}{d\xi}\Big|_{\xi=1} \tag{28}$$

The simultaneous heat and mass transfer equations (17) and (18) were put into finite difference form and solved as functions of the parameters X_{AS}, λ, α and β for n = 1. The numerical solutions were carried out on the Rice University Computer. An iterative method of solution was selected to solve the equations. In this method a value of ϕ was calculated for each grid point from the parameters and an assumed ψ grid. The ϕ profile was then used to compute a new ψ profile. These iterations continued until a convergence test was successful on every point of the ψ grid. Details of the computer solution are in Appendix A.

There are three regions of diffusive behavior in porous media, each having different diffusion equation. Scott (44) defined these regions with reference to the magnitude of the ratio of the pore radius to the mean free path. At $\bar{r}/\bar{l}$ ratios of less than 0.1, Knudsen diffusion occurs where wall collisions are more frequent than the intermolecular type. For ratios greater than 10, ordinary diffusion predominates, and the region between has been called the transition zone. The appropriate equation for diffusion in the transition zone has only recently been derived by several authors (40, 46, 54).

In bidisperse porous media the diffusion processes are pictured to occur in series going first from the macropores between granules into the micropores of the granule interior. However, the results of Wakao and Smith (52) indicate that the mass transfer in bidisperse systems is primarily through the macropores, and that micropore diffusion in such systems is only of importance in the case of very fast reactions on large granules.

It is important to know what type of diffusion is prevalent so that proper diffusion equation may be applied to experimentally measured diffusion rates. An estimation of the pore radius controlling flow through a porous media may be obtained from its permeability. Data given in Appendix J indicate that a macropore system controls the diffusion through the pellets used in this work and ordinary diffusion prevails in the macropores. Thus, for the measurements made in this laboratory an effective binary diffusion coefficient may be defined by the equation

$$N_A = - cD_{AB}^{EFF}\frac{dX_A}{dl} + X_A(N_A + N_B) \tag{29}$$

If this equation is integrated with $X_A = 1$ at $l = L$ then

$$N_A = - \frac{cD_{AB}^{EFF}}{\omega L}\ln\frac{1 - \omega}{1 - \omega X_A} \tag{30}$$

where $\omega = 1 + N_B/N_A$. Scott and Dullien (46) and Mason, et al. (54) have shown that

$$\frac{N_B}{N_A} = - \left(\frac{M_A}{M_B}\right)^{\frac{1}{2}} \tag{31}$$

regardless of the prevalent mode of diffusion in the porous media. Equations (30) and (31) were used to calculate the diffusivity of oxygen in hydrogen. (D_{AB}^{EFF}) for pellets used in this work from the experimentally determined fluxes and mole fractions.

The complexion of the diffusive process changes in the presence of the reaction, since multicomponent diffusion occurs, and the diffusive fluxes are controlled by the stoichiometry of the reaction. The

multicomponent diffusion coefficient for ordinary diffusion in porous media defined by (5) is given in terms of the binary diffusion coefficients by

$$D_{im}^{EFF} = \frac{N_i - X_i \sum_{j=1}^{n} N_j}{\delta \sum_{j=1}^{n} \frac{X_j N_T - X_i N_j}{D_{ij}}} \tag{32}$$

where δ is a purely geometric factor which presumably also relates the binary diffusivities

$$\delta = \frac{D_{AB}}{D_{AB}^{EFF}} \tag{33}$$

For the diffusion of oxygen in the reactive pellet mixture (32) may be written

$$\delta \frac{D_{AM}^{EFF}}{D_{AB}} = \frac{D_{AM}^{EFF}}{D_{AB}^{EFF}} = \frac{1 - X_A}{X_B - X_A + r_1(1 + X_A - X_B - X_D) + r_2 X_D} \tag{34}$$

where $r_1 = D_{AB}/D_{AC}$ and $r_2 = D_{AB}/D_{AD}$. If the r's are equal, (34) may be reduced to

$$\frac{D_{AM}^{EFF}}{D_{AB}^{EFF}} = \frac{1 - X_A}{X_B - X_A + r_1(1 - X_A - X_B)} \tag{35}$$

This equation was used to represent the diffusivity under reaction conditions.

Since the theory involved in the experimental determination of the thermal conductivity is well known, it has been included in Appendix A.

IV. EXPERIMENTAL EQUIPMENT

The use of a gas recirculation system to carry out experiments of this nature is unique. The attractive features of this system were that (1) steady state operation was possible and, (2) each run provided a direct measure of the reaction rate.

For convenience the equipment section is subdivided into three sub-sections, each describing a separate piece of equipment used in the study. The sub-sections are: (A) The Reactor System, (B) The Thermal Diffusivity Apparatus, (C) The Diffusivity Apparatus.

A. The Reactor System

The reactor system represents the main experimental facility involved in the program. The purpose of this closed system was to circulate mixtures of hydrogen and oxygen at a controlled steady state temperature and pressure over a platinum on alumina catalyst upon which water was formed. The water produced was collected to obtain a measure of the integral reaction rate at the end of a run. A temperature differential was measured between the geometric centers of the catalyst pellet and a catalytically inert pellet mounted in juxtaposition. A schematic diagram of the equipment used is given in Fig. 2.

The reactor which served as a housing for the catalyst and blank pellets is illustrated in Fig. 3. Its shape is rectangular with the ends rounded to fit circular flanges. Conical expansion and contraction sections coupled the reactor to the remainder of the system.

A 0.05% by weight platinum on porous alumina support was used as

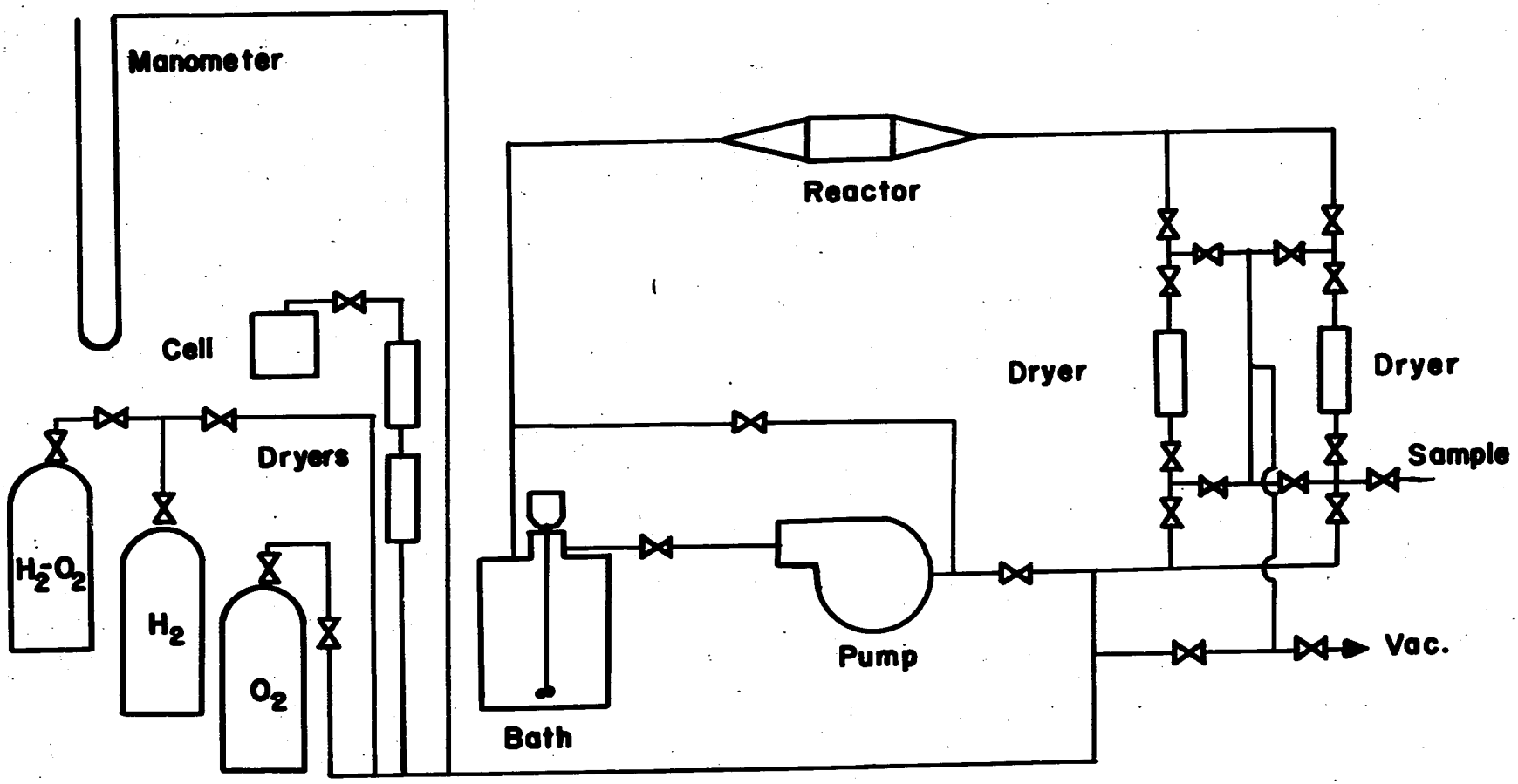

FIGURE 2 - SCHEMATIC DIAGRAM OF SYSTEM

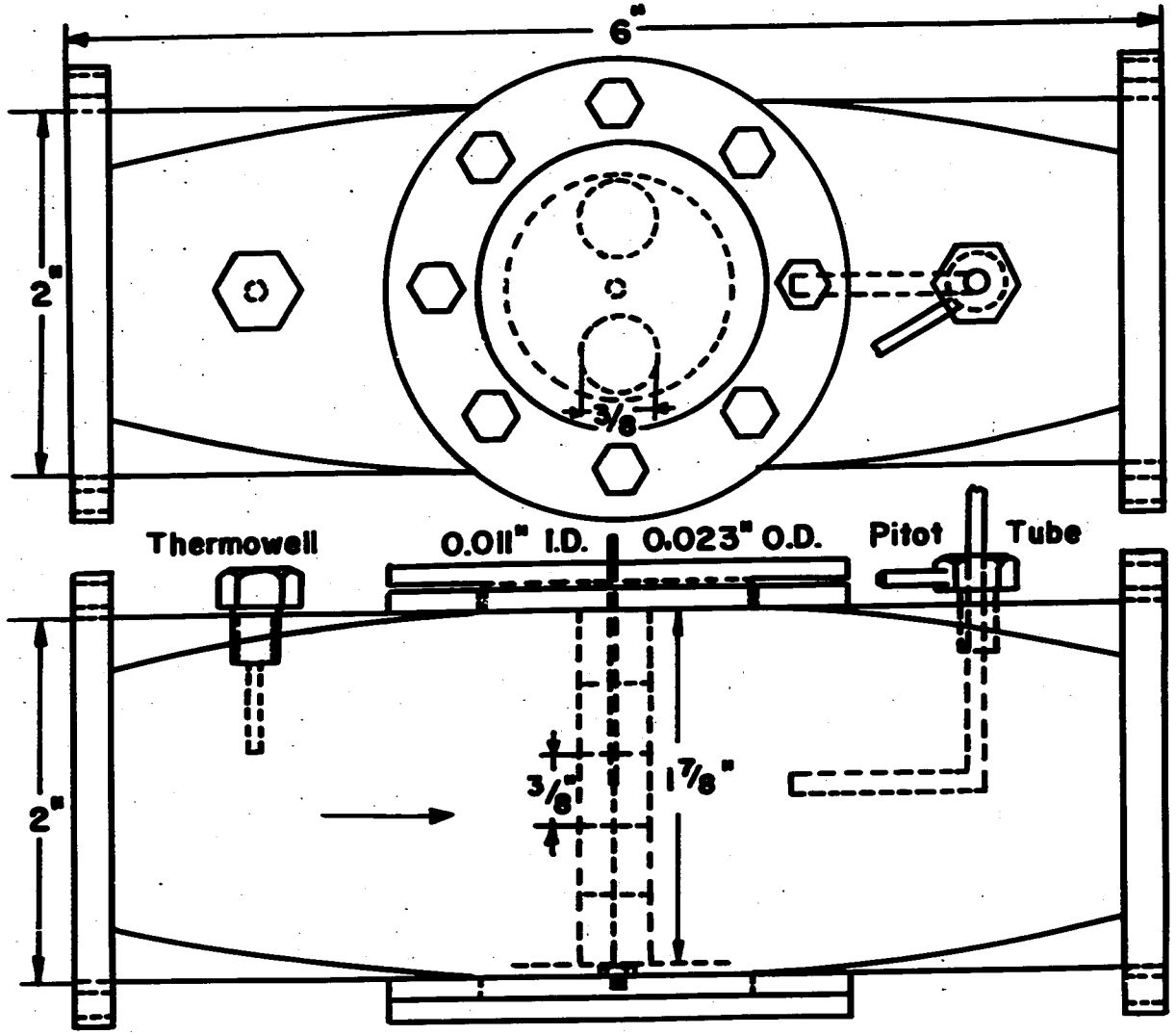

FIGURE 3 - THE REACTOR

the catalyst. The platinum had first been deposited on powdered alumina which was then pelletized into 3/8 x 3/8 inch cylinders. Five pellets were glued end to end with epoxy to serve as the catalyst cylinder in accordance with assumption (1). A blank cylinder consisting of only the alumina support material was made in the same way. The catalyst and blank cylinders were mounted parallel to each other as shown in Fig. 3.

Each pellet was drilled axially to allow insertion of a combination thermocouple-micromanometer into the annulus. The copper-constantan junctions were located at the center of each cylinder and connected in a manner allowing a direct measure of the centerline temperature differential. The copper portion of the thermocouple was a capillary tube notched next to the thermocouple junction to serve as a pressure tap. Pressure differentials were read on a manometer connected to the capillary tubes.

The bulk phase temperature and gas velocity were also measured in the reactor as shown in Fig. 3. Further details of the reactor are given in Appendix B-1a.

A temperature bath controlled by means of a refrigeration unit and a heater maintained the bulk gas temperature in the reactor to within $\pm 0.5^{\circ}C$ for all runs. Details of the temperature bath are given in Appendix B-1b.

Circulation was provided by a double acting diaphram type positive displacement pump as shown schematically in Fig. 4. The pump had a capacity of just under 15 cfm, and flow was regulated by means of a bypass line on the pump. A small amount of air was present in each run,

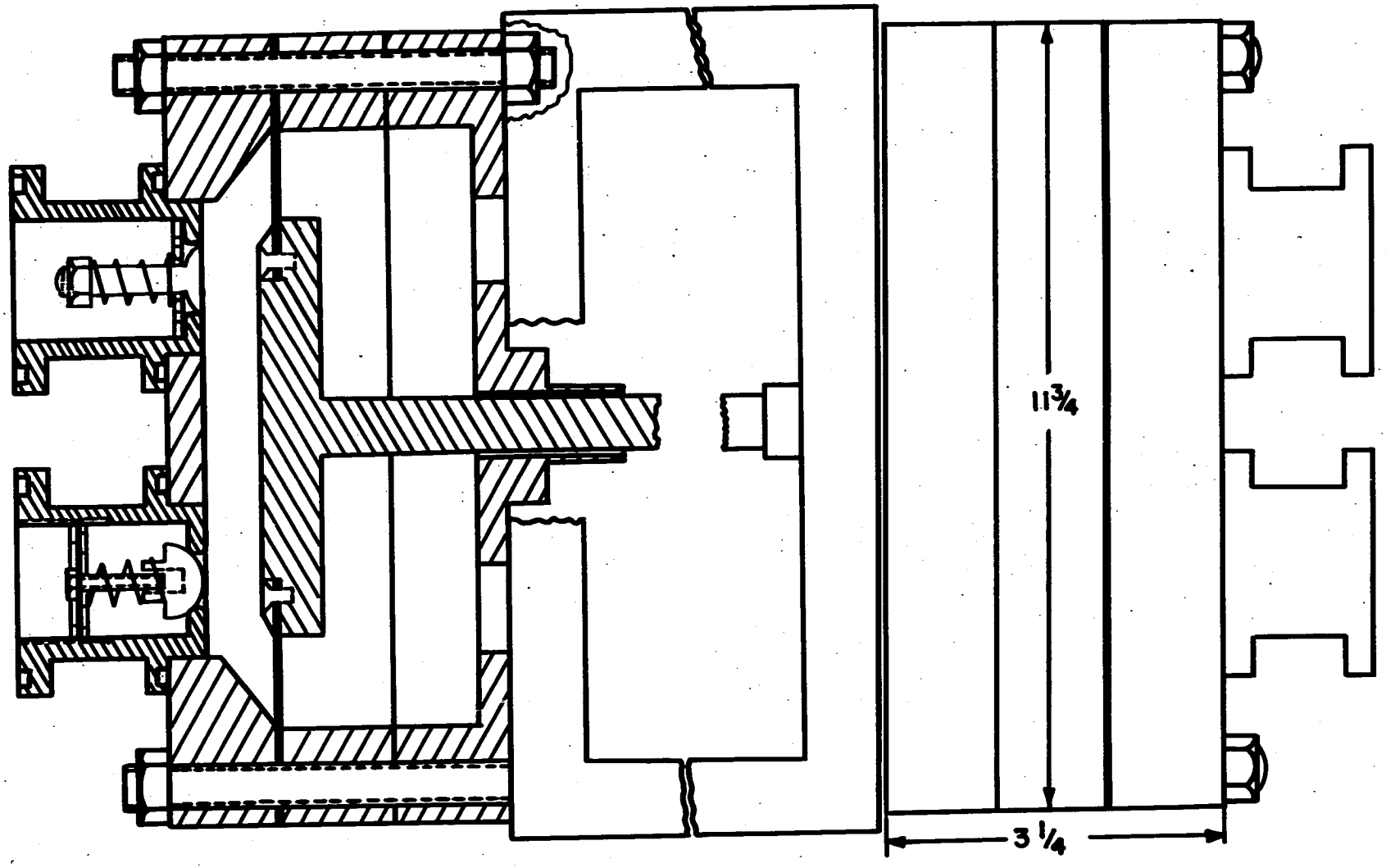

FIGURE 4 - THE CIRCULATION PUMP

because the pump was incapable of maintaining a high vacuum and the system was charged by an evacuation technique. Appendix B-1c gives additional details of the pump.

Water made during the runs was collected on silica gel in two driers mounted in parallel as illustrated in Fig. 2. Flow was directed through one of the driers during the transient stage of equipment startup and switched to the previously weighed secbnd drier to begin the steady state run. At the conclusion of a run the drier was again weighed. The amount of water accumulated during the run furnished a direct measure of the reaction rate. Details of the drying system are found in Appendix B-1d.

Since the product (H_2O) was removed quantitatively, system pressure had to be maintained by continuous makeup; reactant gases were replaced in stoichiometric proportions by water electrolysis. A schematic diagram of the electrical network used to supply power to the electrolysis cell is presented in Fig. 5. Pressure control was automatically maintained by an off-on system which supplied two levels of current to the cell. The pressure control system is further discussed in Appendix B-1e.

Gases were charged into a previously evacuated system from cylinders containing nominal mixtures of one, two, three and four percent oxygen in hydrogen. A sample of the gas in the system was taken at the end of each run from the port shown in Fig. 2. Further discussion of the gas injection system and the gas sampling system is included in Appendices B-1f and B-1g, respectively. The samples were analyzed for oxygen, hydrogen and nitrogen on a Beckman GC-2 gas chromatograph; details of

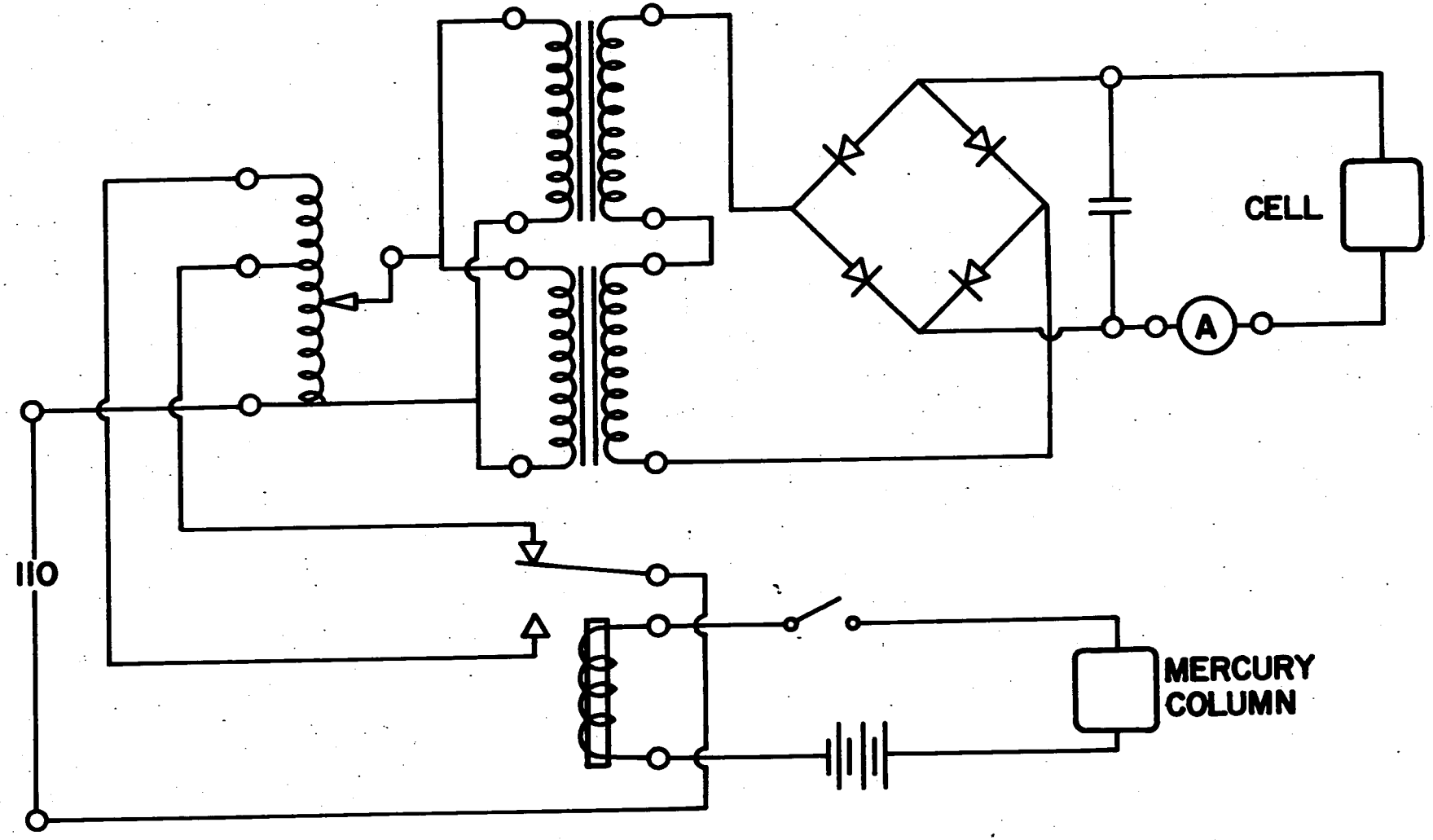

FIG. 5 – THE PRESSURE CONTROL SYSTEM

the analysis are found in Appendix B-2.

B. The Thermal Diffusivity Apparatus

The value of the effective thermal conductivity of the catalyst pellets in hydrogen gas was determined from their thermal diffusivity measured in air. The apparatus is presented schematically in Fig. 6.

Samples of catalyst for these experiments were of the same configuration as described in Section IV-A. In this case four pellets rather than five were fastened end to end after being drilled axially to house a standard copper-constantan thermocouple.

The sample for test was mounted in a holder which could be moved back and forth between hot and cold air circulation chambers. Pellets brought to a steady state temperature in the heating chamber were injected quickly into the cooling chamber where the time response of the centerline temperature was recorded on a 0-1 millivolt recorder. This equipment is further discussed by Park (30), and in Appendix B-3.

C. The Diffusivity Apparatus

The method used to measure the diffusivity is similiar to that used by several authors (20, 40, 55, 61). In this method, illustrated in Fig. 7, different gases are circulated past the ends of a single catalyst pellet arranged in a compartment which prevents leakage of the gases around the sample, thus allowing mixing of the gases to occur only by diffusion through the pellet. Gas flow rates were measured, and samples of the effluent gas were analyzed by gas chromotography to determine the necessary gas fluxes. Additional details may be found in Appendix B-4.

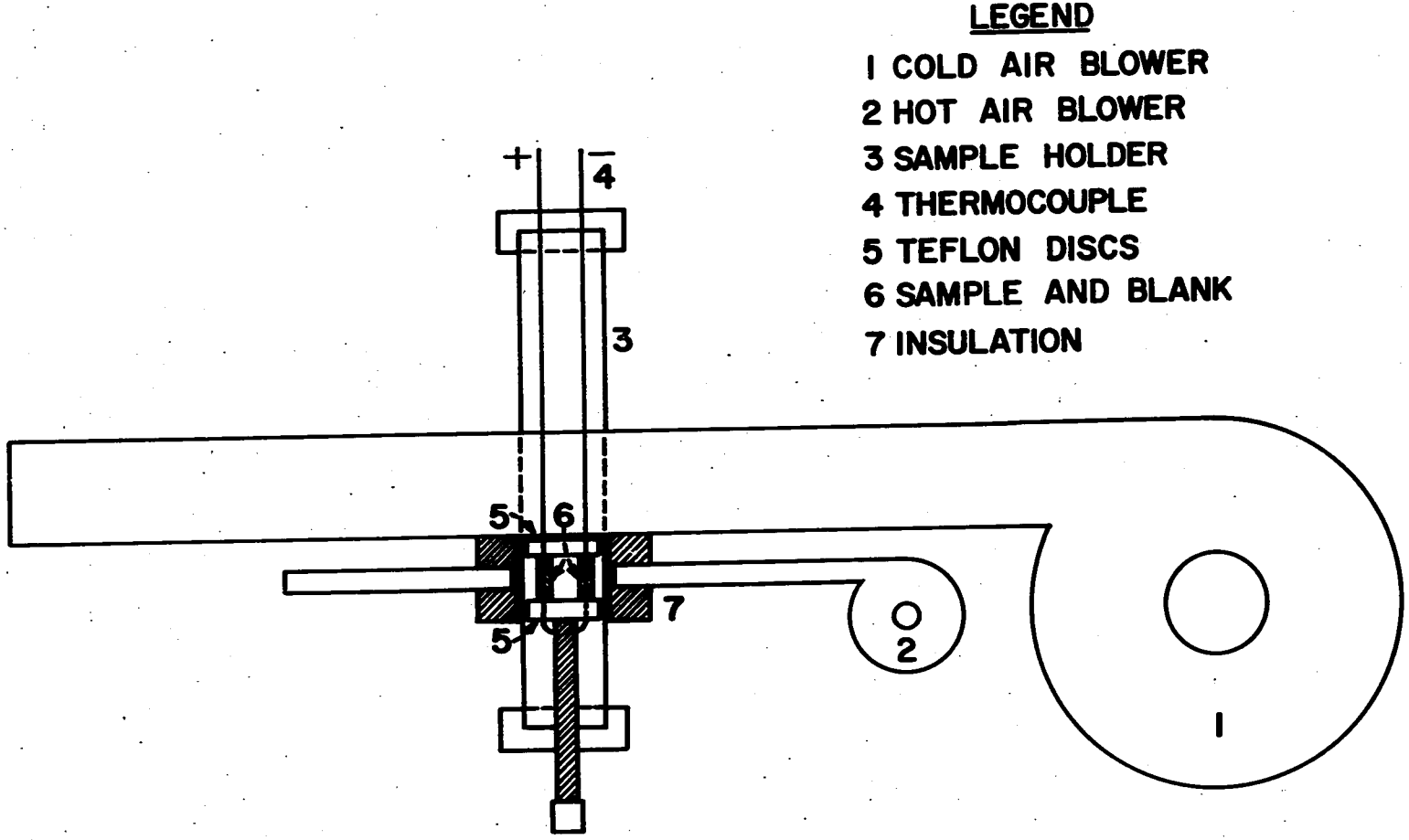

FIG. 6 - THE THERMAL CONDUCTIVITY APPARATUS

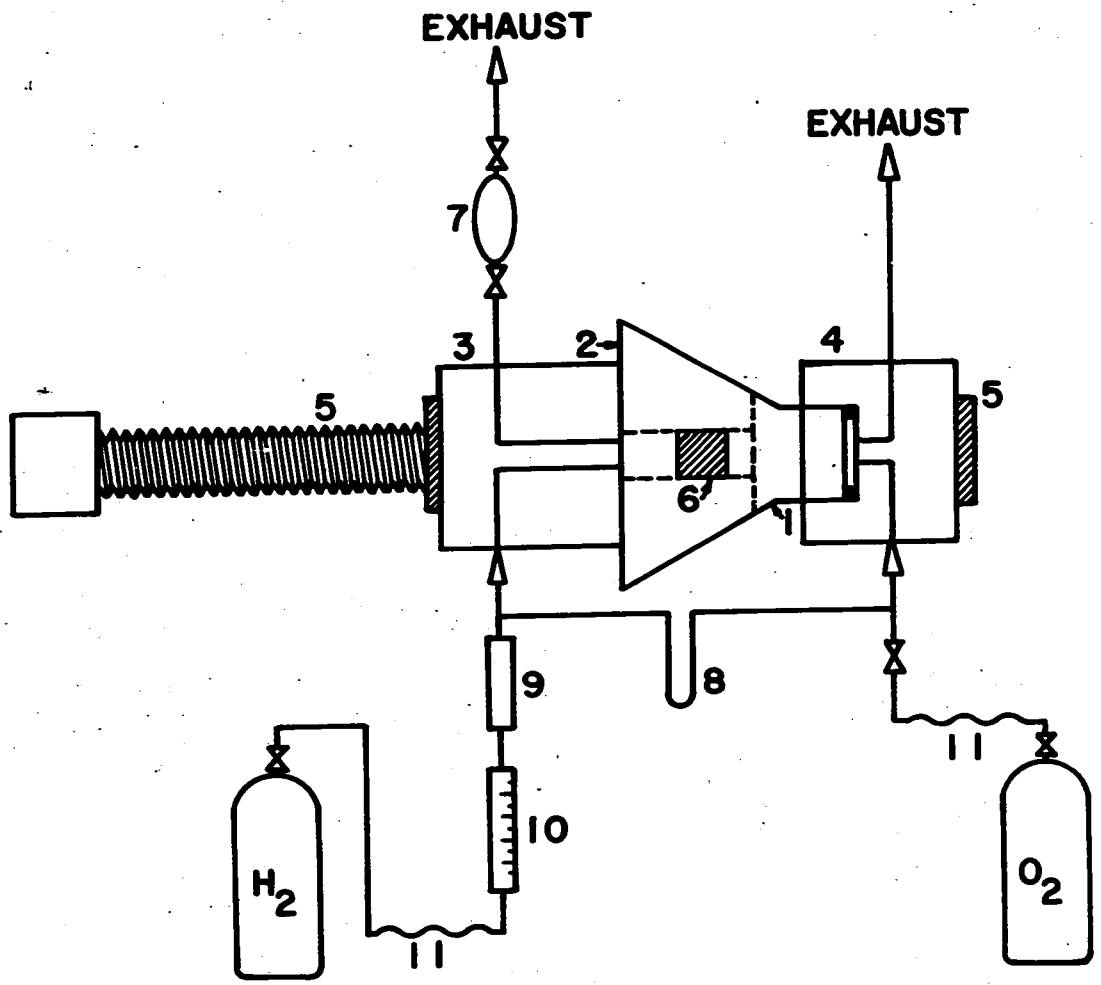

LEGEND

1 MANDRIL
2 STOPPER
3 BRASS SUPPORT
4 LUCITE SUPPORT
5 CLAMP
6 CATALYST
7 SAMPLE
8 MANOMETER
9 DRYER
10 SOAP METER
11 CAPILLARY

FIG. 7- THE DIFFUSIVITY APPARATUS

V. DISCUSSION OF RESULTS

A. The Effective Thermal Conductivity

Centerline temperature-time response data is given in Table 3. These values were converted to the dimensionless quantities given in equation (A-40) by choosing a thermal diffusivity constant for each run which permitted a comparison of the θ vs τ curve so obtained with the theoretical curve for heat loss from a cylinder (42). The experimental value of the Nussult number of the cooling air was 56 based on the velocity data given in Table 2. Schneider's curve for a Nussult number of 20 was used for comparison purposes. Examples of the curve fits obtained are presented in Appendix F, Figs. 19-24. Reproducability of the data is graphically illustrated by comparison of Figs. 19 and 21 and Figs. 20 and 22 which are duplicate runs at two different temperature levels. The particular catalyst type as well as other pertinent data on the samples employed in each run is given in Table 1.

Because of the close correspondence between the theoretical and experimental curves, the theoretical curve was taken to represent all runs, facilitating the calculation of the thermal diffusivities presented in Table 4.

Temperature dependent literature values (25) of the heat capacities of alumina and air were used in the calculation of thermal conductivity. The heat capacities given in Table 5 were calculated according to the equation

$$\overline{\rho C_p} = \sum_i (\text{Volume fraction})_i (\rho C_p)_i$$

Table 6 gives the derived thermal conductivity values at selected values of θ. The mean value for each run is calculated from the portion of the curve which most closely coincides with the theoretical curve. The values chosen in the averaging process are indicated in Table 6.

The more important results implied in Table 6 are the small deviations of the mean thermal conductivity due to changes in temperature and sample type. For this reason, the k_e value was assumed to be a constant independent of sample type and temperature with the value $3.5 \times 10^{-4} \pm 0.1 \times 10^{-4}$ cal sec^{-1} cm^{-1} $^oC^{-1}$. This value agrees with that obtained by Mischke and Smith (28) for a similar material.

The correlation of Godbee (18) was used to convert the conductivity in air to that in hydrogen. His method requires a knowledge of the macropore void volume and the magnitude of the k_D/k_f ratio, values for which are given in Tables 7 and 8. From these values a correction factor was obtained from Godbee's plot and applied to the results of k_f from Schotte equation (A-44). Table 8 presents the data used in evaluating k_f. Also given is the value of k_c, the contact contribution, attained from the data taken in air and k_e^{He}, a value calculated for helium gas to compare with the experimental value of Mischke and Smith.

The uncertainty of these computations lies in the values chosen for the accommodation coefficient and the characteristic diameter of the pellet, since their values strongly influence the results. Pore volume distribution data given in Table 7 indicate a macropore diameter maximum at approximately 900 $\mathring{A}$ which was the value used in (A-44). The accommodation coefficients were taken from the literature (14, 15, 19, 31), and a value of $k_e = 0.13$ BTU $hr^{-1}ft^{-1}{}^oF^{-1}$ was used throughout the remainder of this work.

B. The Effective Diffusivity

Preliminary experiments with hydrogen and nitrogen indicated that equation (31) is applicable to the porous media used here. Thus, equation (30) and (31) were used to calculate the effective binary diffusivity of oxygen in hydrogen. The data and calculated diffusivities are presented in Table 9. The average value of D_{AB}^{EFF} was 0.115 cm^2/sec at one atmosphere and 26.5°C. Using the D_{AB} calculated at these conditions from equation (F-1), the value of δ was computed to be 7.15. For ordinary diffusion in porous media Wakao and Smith (52) offer that

$$\frac{D_{AB}^{EFF}}{D_{AB}} = \frac{1}{\delta} \simeq \epsilon_a^2$$

where $\epsilon_a = 0.345$ is the macrovoid fraction, or in this case

$$0.14 \simeq (0.345)^2 = 0.12$$

which indicates that ordinary diffusion is prevalent.

It must be noted that the flow rate in the experiments was that of hydrogen entering the diffusivity cell (see Fig. 6) and the sample is that of mixture leaving the cell. Therefore, due to the non-equimolar diffusion of the gases through the pellet, the calculated oxygen flux was about 5% high. This discrepancy was ignored because it was considerably smaller than the possible error resulting from neglected thermal effects.

Table 10 gives values of r_1 and r_2 calculated from the binary diffusivities at 20°C and one atmosphere. The proximity of these values allowed the use of (35) to calculate the mixture diffusivity.

The diffusivity predicted by (35) is shown in Table 10 to be virtually independent of the oxygen concentration over the 0-5% range

covered. If it is assumed that nitrogen present in a particular run displaces only hydrogen, then the diffusivity is seen to depend upon the nitrogen concentration. Finally, the values of D_{Am}^{EFF} are given in Table 10 and Fig. 8 as a function of the nitrogen concentration. Values from Fig. 8 were used for other calculations.

C. The Reaction Data and Results

A 4% oxygen run was made with an inert support cylinder in place of the catalytic cylinder. No temperature differential was recorded between the pellets during a one hour run and no weight change had occurred in the drying cylinder, so it was assumed that all reaction occurred in the catalyst pellet.

Data was taken to generate four isotherms between 20-60°C and 0-5% oxygen in hydrogen. The rate data is presented graphically in Fig. 9, and pertinent data for each run is given in Table 12. The negligible size of the radial pressure drop is shown by Table 12. Average values for the Nussult numbers are seen to be $(Nu)_h = 10.8$ and $(Nu)_m = 21.6$. Other data is included in Appendix H. Each run is catalogued first by the isotherm temperature, followed by the nominal oxygen concentration and an indexing number.

Initially, the data was used to evaluate an overall activation energy and reaction order. Then from these, effectiveness factors, rate constants and centerline temperatures were computed for each run.

A similiar approach is used in determining the activation energy and reaction order from the data of Fig. 9 and an alternate definition of the effectiveness factor

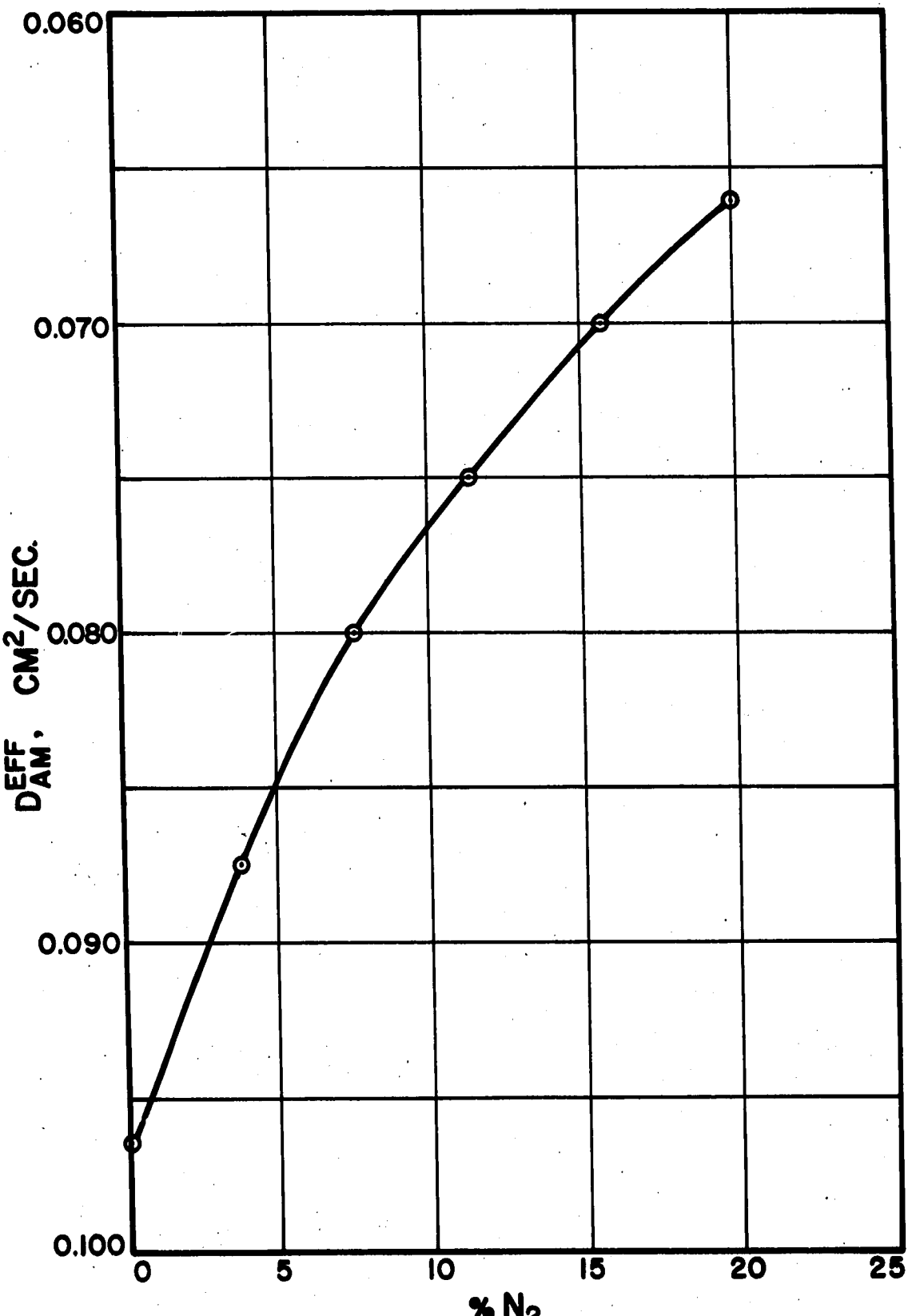

FIG. 8 – EFFECTIVE MIXTURE DIFFUSIVITY vs. PERCENT NITROGEN PRESENT IN RUN

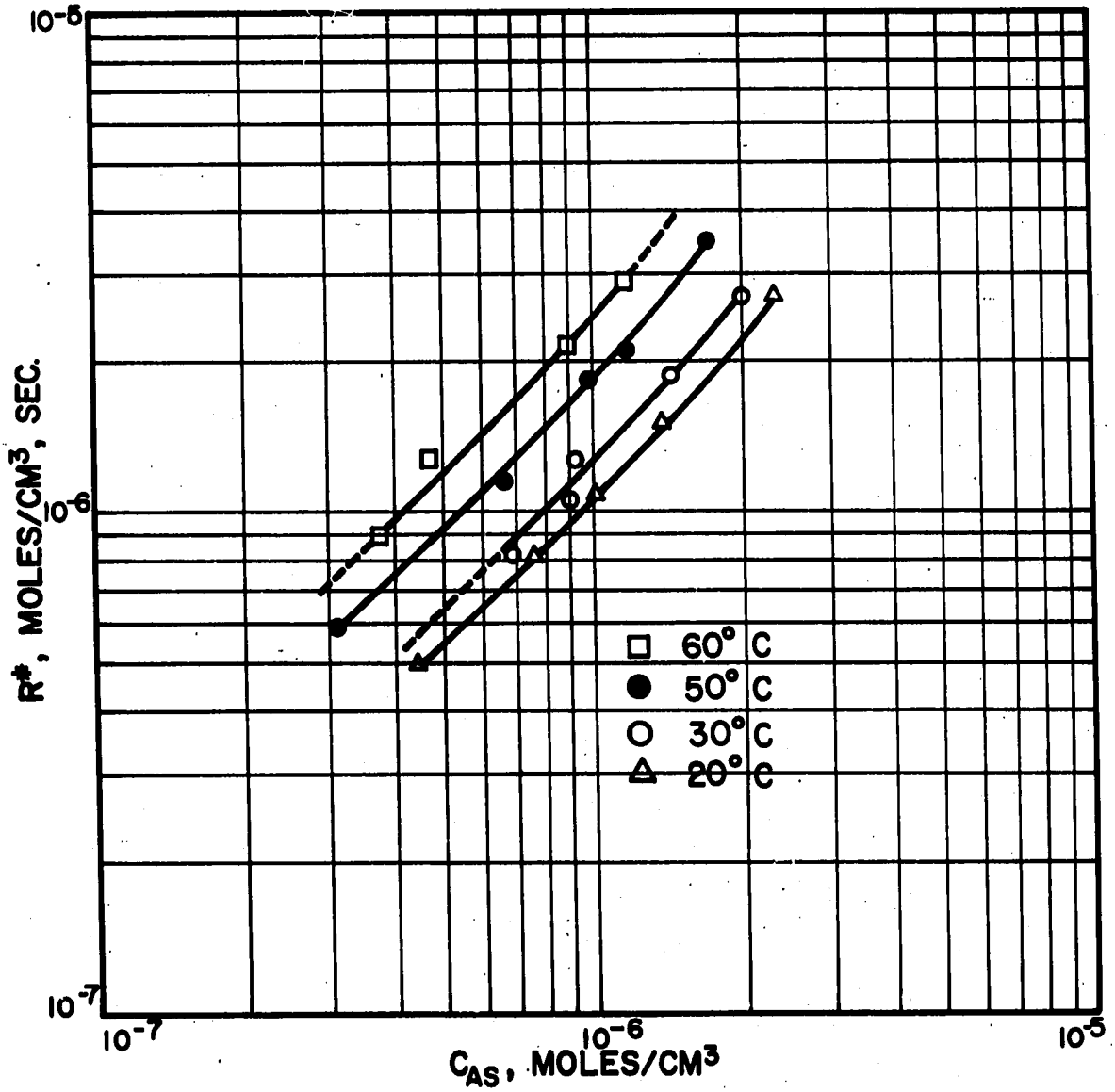

FIG. 9- OBSERVED REACTION RATE vs. OXYGEN CONCENTRATION AT FILM SURFACE

$$R^* = k_s C_{As}^n \eta \tag{36}$$

Slopes of ln k vs $(1/T_s)$ curves are used to obtain the activation energy when an effectiveness factor is not involved. The ln R^* vs $(1/T_s)$ plot shown in Fig. 10 was used here. Equation (36) shows that

$$\left[\frac{\partial \ln R^*}{\partial\left(\frac{1}{T_s}\right)}\right]_{C_{AS}} = \frac{\partial \ln k_s}{\partial\left(\frac{1}{T_s}\right)} + \frac{\partial \ln \eta}{\partial\left(\frac{1}{T_s}\right)}$$

or, using the definition of k_s

$$-\frac{E^*}{R_g} = -\frac{E}{R_g} + \frac{\partial \ln \eta}{\partial\left(\frac{1}{T_s}\right)} \tag{37}$$

The last term in (37) in terms of the system parameters is

$$\frac{\partial \ln \eta}{\partial\left(\frac{1}{T_s}\right)} = \frac{\partial \ln \eta}{\partial \ln \alpha} \cdot \frac{\partial \ln \alpha}{\partial\left(\frac{1}{T_s}\right)} + \frac{\partial \ln \eta}{\partial \beta} \cdot \frac{\partial \beta}{\partial\left(\frac{1}{T_s}\right)} + \frac{\partial \ln \eta}{\partial \lambda} \cdot \frac{\partial \lambda}{\partial\left(\frac{1}{T_s}\right)} \tag{38}$$

From the definitions given in (16), it may be seen that

$$-\frac{E^*}{R_g} = -\frac{E}{R_g} - \frac{E}{2R_g}\frac{\partial \ln \eta}{\partial \ln \alpha} + \frac{E}{R_g}\frac{\partial \ln \eta}{\partial \beta} + \frac{2(-\Delta H) D_{Am}^{EFF} C_{As}}{k_e}\frac{\partial \ln \eta}{\partial \lambda} \tag{39}$$

Prater (32) noted that the group $(-\Delta H) D_{Am}^{EFF} C_{As}/k_e$ represents the maximum temperature rise which may occur in a pellet if surface effects are neglected. Under this supposition (39) may be solved for the real activation energy giving

$$E = \frac{E^* + 2R_g (\Delta T)_{max} \frac{\partial \ln \eta}{\partial \lambda}}{1 + \frac{1}{2}\frac{\partial \ln \eta}{\partial \ln \alpha} - \frac{\partial \ln \eta}{\partial \beta}} \tag{40}$$

The reaction order may be obtained in a similiar fashion from the data of Fig. 9. If the observed reaction order is defined by

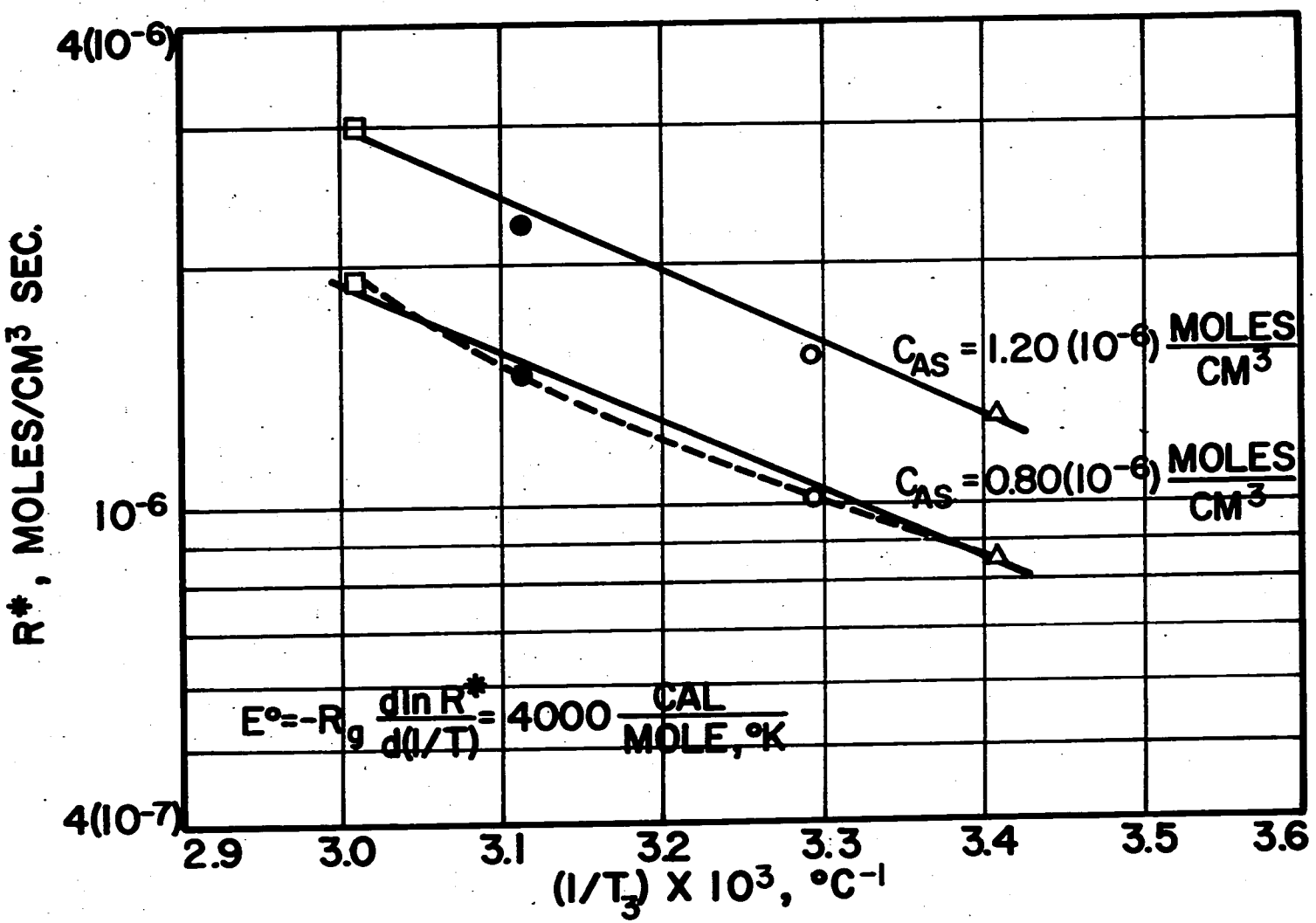

FIG. 10 - OBSERVED REACTION RATE vs. RECIPROCAL SURFACE TEMPERATURE

$$n^* = \left[\frac{\partial \ln R^*}{\partial \ln C_{As}}\right]_{T_s}$$

then (36) gives

$$\left[\frac{\partial \ln R^*}{\partial \ln C_{As}}\right]_{T_s} = n + \frac{\partial \ln \eta}{\partial \ln C_{As}} \tag{41}$$

The total derivative is given by

$$\frac{\partial \ln \eta}{\partial \ln C_{As}} = \frac{\partial \ln \eta}{\partial \ln \alpha} \cdot \frac{\partial \ln \alpha}{\partial \ln C_{As}} + \frac{\partial \ln \eta}{\partial \ln \lambda} \cdot \frac{\partial \ln \lambda}{\partial \ln C_{As}}$$

or

$$\frac{\partial \ln \eta}{\partial \ln C_{As}} = \frac{n - 1}{2} \frac{\partial \ln \eta}{\partial \ln \alpha} + \frac{\partial \ln \eta}{\partial \ln \lambda}$$

Combining this expression with the definition of n^* and (41) gives

$$n^* = n + \frac{(n - 1)}{2} \frac{\partial \ln \eta}{\partial \ln \alpha} + \frac{\partial \ln \eta}{\partial \ln \lambda} \tag{42}$$

From (42) it is evident that n^* will deviate from n by $\partial \ln \eta / \partial \ln \lambda$ for a real first order reaction.

Using average Nussult numbers and n = 1 computer solutions were obtained over a comprehensive range of the parameters α, β and λ. Interpretation of the results given in Figs. 11-13 and Table 13 points out that

(a) $E^* >> 2R_g(\Delta T)_{max} \dfrac{\partial \ln \eta}{\partial \ln \alpha}$

(b) $1 + \dfrac{1}{2} \dfrac{\partial \ln \eta}{\partial \ln \alpha} >> \dfrac{\partial \ln \eta}{\partial \beta}$

(c) $n^* \simeq 1 + \dfrac{\partial \ln \eta}{\partial \ln \lambda}$

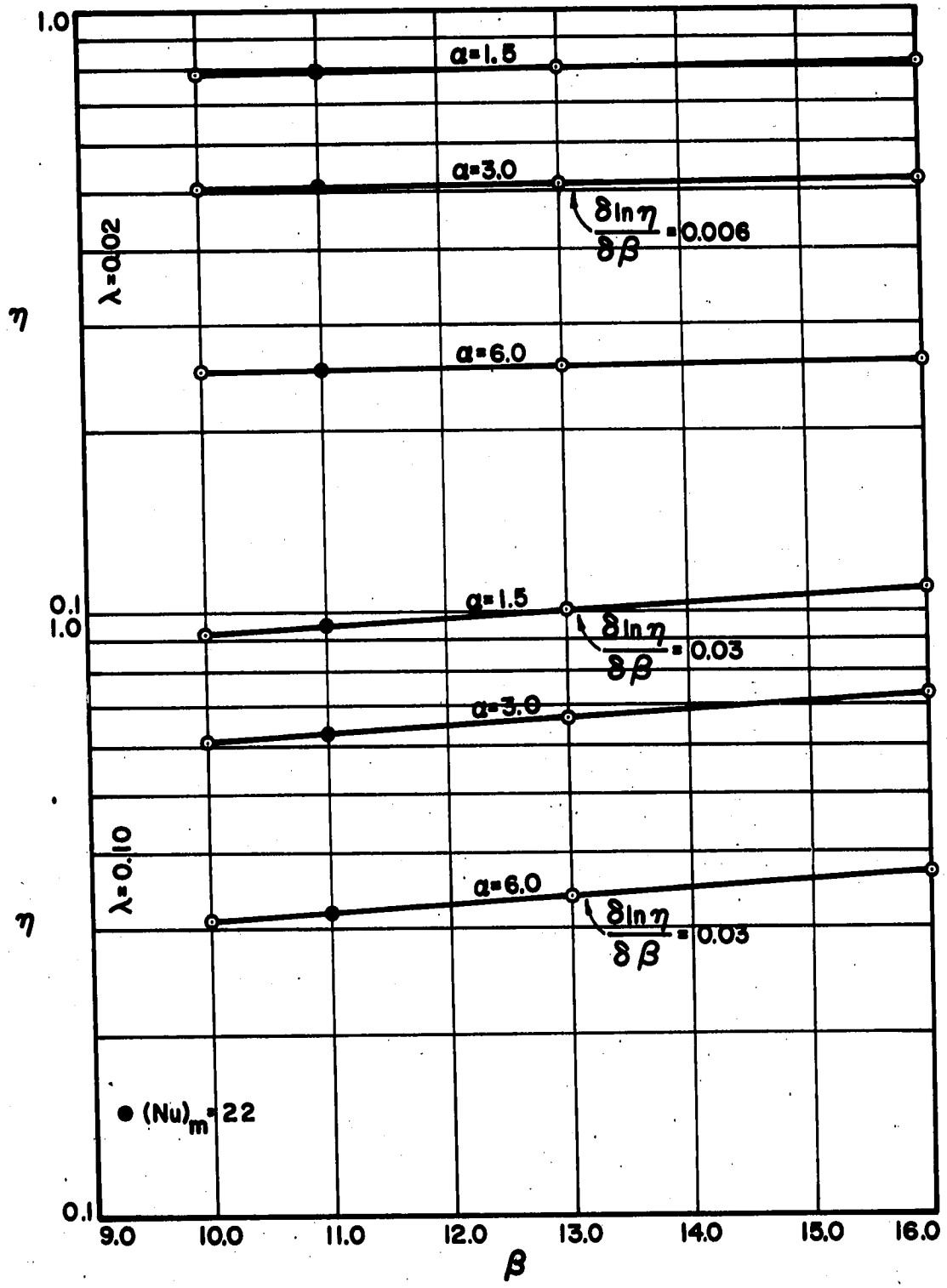

FIG. 11 – EFFECTIVENESS FACTOR vs. β FOR SELECTED λ AND α AT $(Nu)_h = 11$ AND $(Nu)_m = 20$

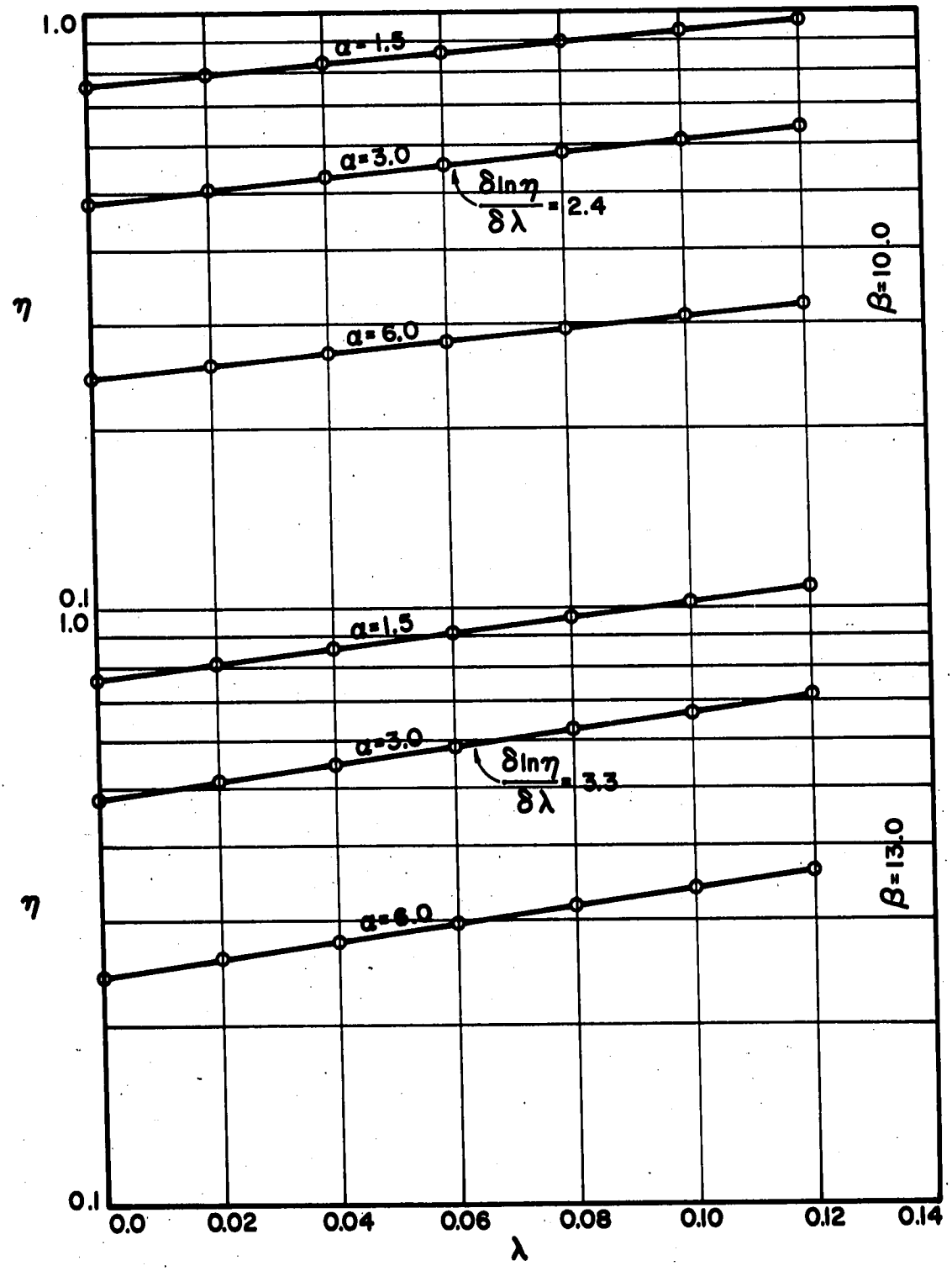

FIG. 12-EFFECTIVENESS FACTOR vs. λ FOR SELECTED β AND α AT $(Nu)_h$ = 11 AND $(Nu)_m$ = 20

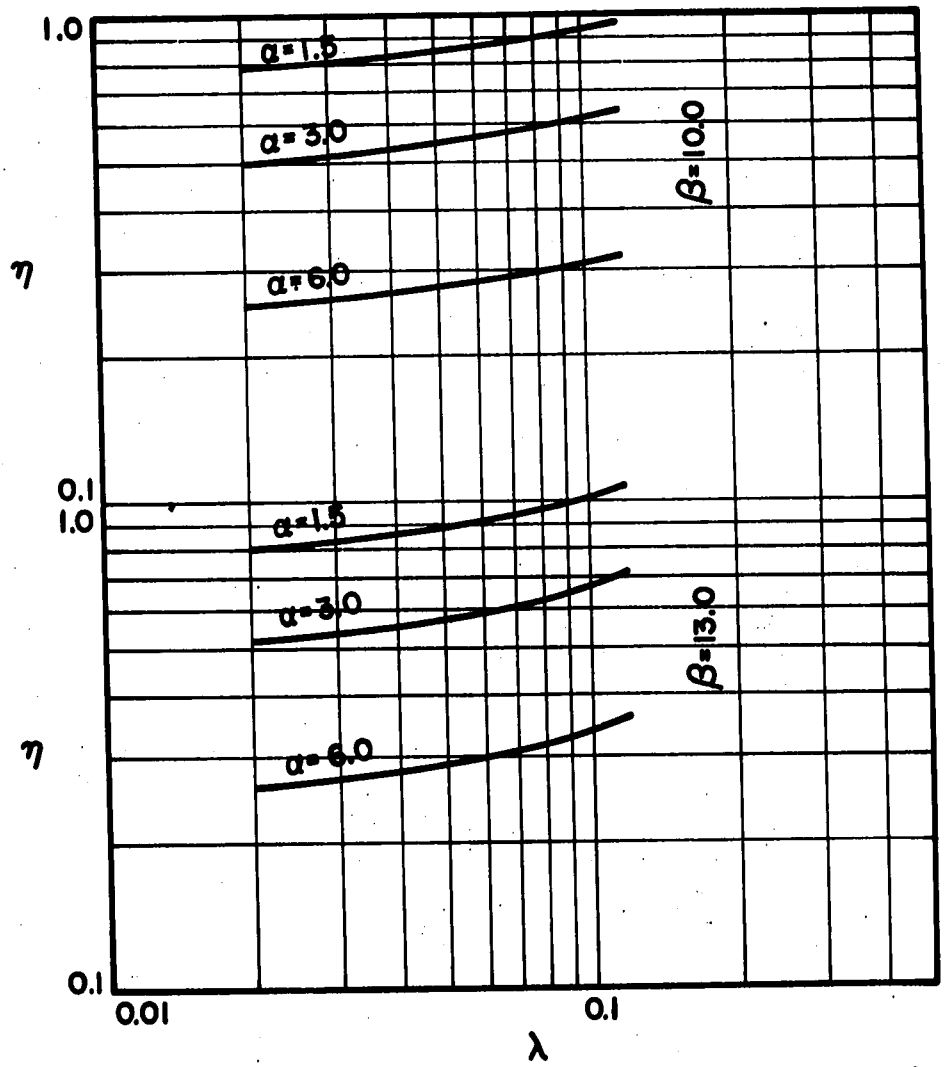

FIG. 13–EFFECTIVENESS FACTOR vs. λ FOR SELECTED β AND α AT $(Nu)_h = 11$ AND $(Nu)_m = 20$

This justified the assumption of a first order reaction and fostered the reduction of (40) to

$$E = \frac{E^*}{1 + \frac{1}{2}\frac{\partial \ln \eta}{\partial \ln \alpha}} \tag{44}$$

A trial and error method was used to evaluate the activation energy from (44). First, a chosen β value was used to obtain curves of η vs α for various λ (see Fig. 14). Activation energies were then determined from (44) for each run which generated a new β in order to repeat the process. Table 14 shows the results of this procedure. Internal consistancy is apparant within each isotherm, but intra-isothermal variations are notable. The mean values are 6500 cal/mol^{o}K for the activation energy and 10.4 for β. This value agrees well with the 6400 cal/mol^{o}K reported by Trotter (51), who worked with a similiar catalyst.

Calculations were made to determine whether experimentally encountered variations in the Nussult numbers, the bulk flow of mass and the activation energy (or β) were significant. The spot results given in Table 15 indicate that a fairly accurate relationship between η and α is obtained for this work from a single set of η vs α curves using constants for the other parameters, i.e. Fig. 14.

To provide a means for determining the effectiveness factor from the experimental data, the Arrhenius constant is eliminated between (36) and the definition of α^2 (16) to give

$$\eta\alpha^2 = \frac{R^2 R^*}{D_{Am}^{EFF} C_{As}} \tag{45}$$

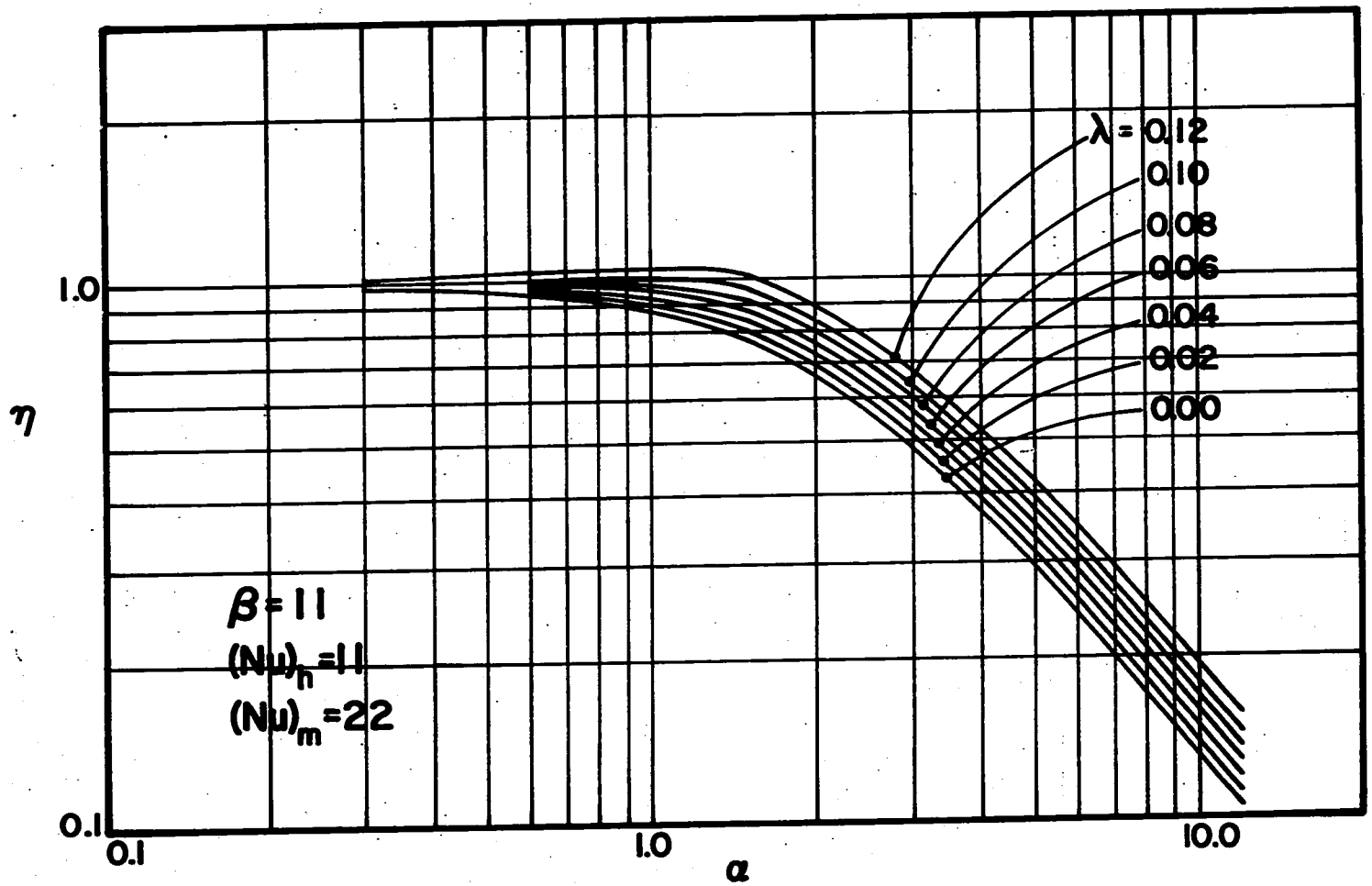

FIG. 14 - EFFECTIVENESS FACTOR vs. α FOR VARIOUS λ AT AVERAGE SYSTEM VALUES OF β, $(Nu)_h$, AND $(Nu)_m$

Quantities on the right side of (45) were measured for each run (see Table 12). Thus, curves of η vs $\eta\alpha^2$ such as Fig. 15 with the appropriate λ yield values of the effectiveness factor which in turn were used to obtain α (and k_s) from Fig. 14. Results of this procedure are presented in Table 16. Differences between η's calculated from the "exact" data and Figs. 14 and 15 never exceeded 0.01. The effectiveness factors in Table 16 are seen to increase as expected with increasing λ at T_s (through increasing C_{As}) and also to decrease with increasing T_s. The η are seen to be independent of C_{As} but dependent upon the surface temperature. Fig. 16 displays the ln k_s vs $(1/T_s)$ curve where the activation energy determined was 7300 cal/mol$^{\circ}$K which is within 15% of the predetermined value.

Radial concentration and temperature profiles were also computed for each set of the parameters. Several representative curves are included in Appendix G. More important than the profiles were the computed temperature differentials which are compared with experimental values in Table 16. Notably, the two methods gave results that were within 13% of each other with only two exceptions.

Table 16 includes values of $(\Delta T)_{max}$ which were calculated by the method given by Prater (32) to insure that the measured temperature rise was within the bounds imposed by this physical limitation. The maximums given were calculated as a guide according to the relation

$$(\Delta T)_{max} = \lambda T_s$$

which fails to account for the effect of the film which envelopes the pellet. A full derivation of the proper equation is given in Appendix I. For the 60°C isotherm the "maximums" are lower than the measured

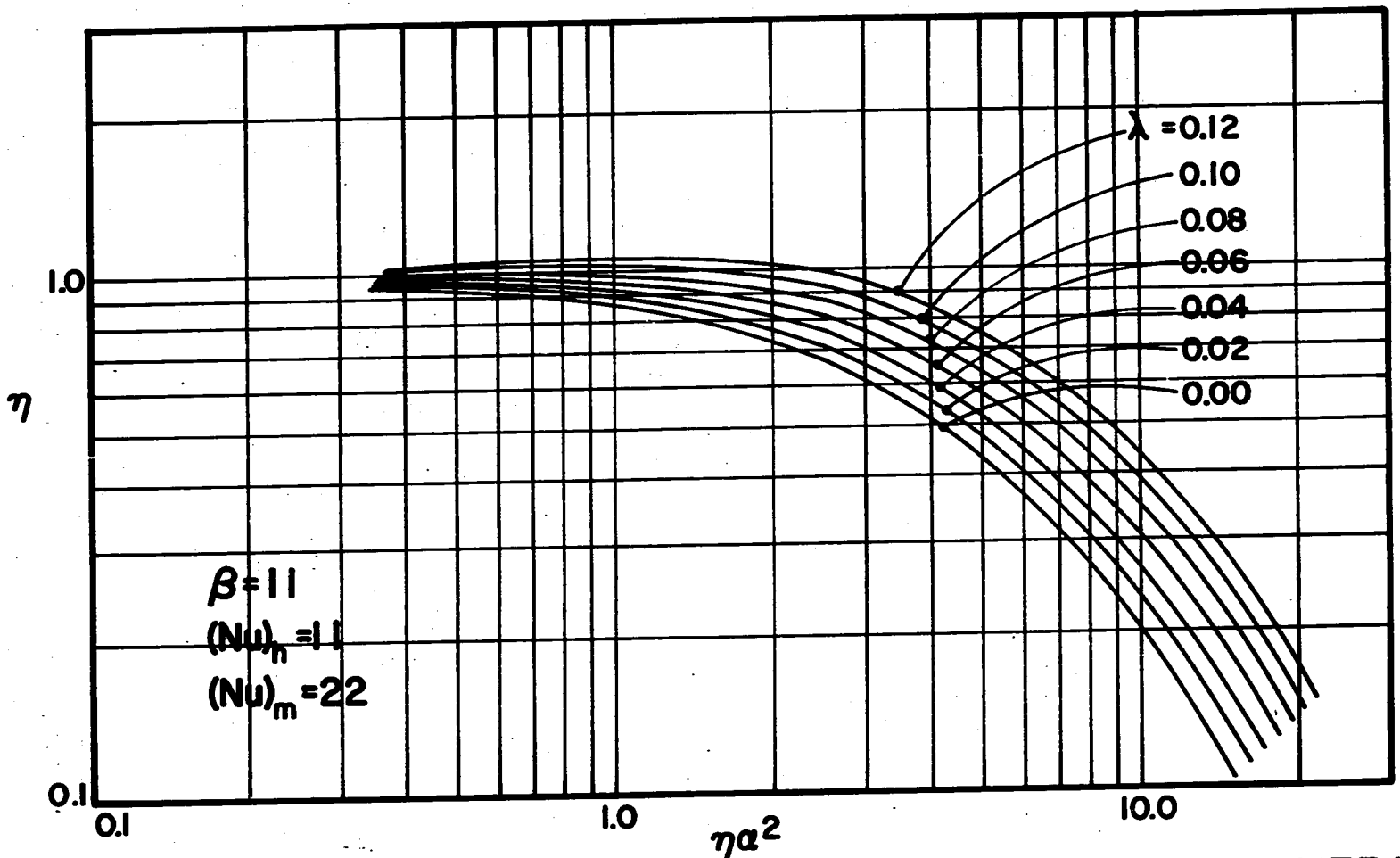

FIG. 15—EFFECTIVENESS FACTOR vs. $\eta\alpha^2$ FOR VARIOUS λ AT AVERAGE SYSTEM VALUES OF β, $(Nu)_h$, AND $(Nu)_m$

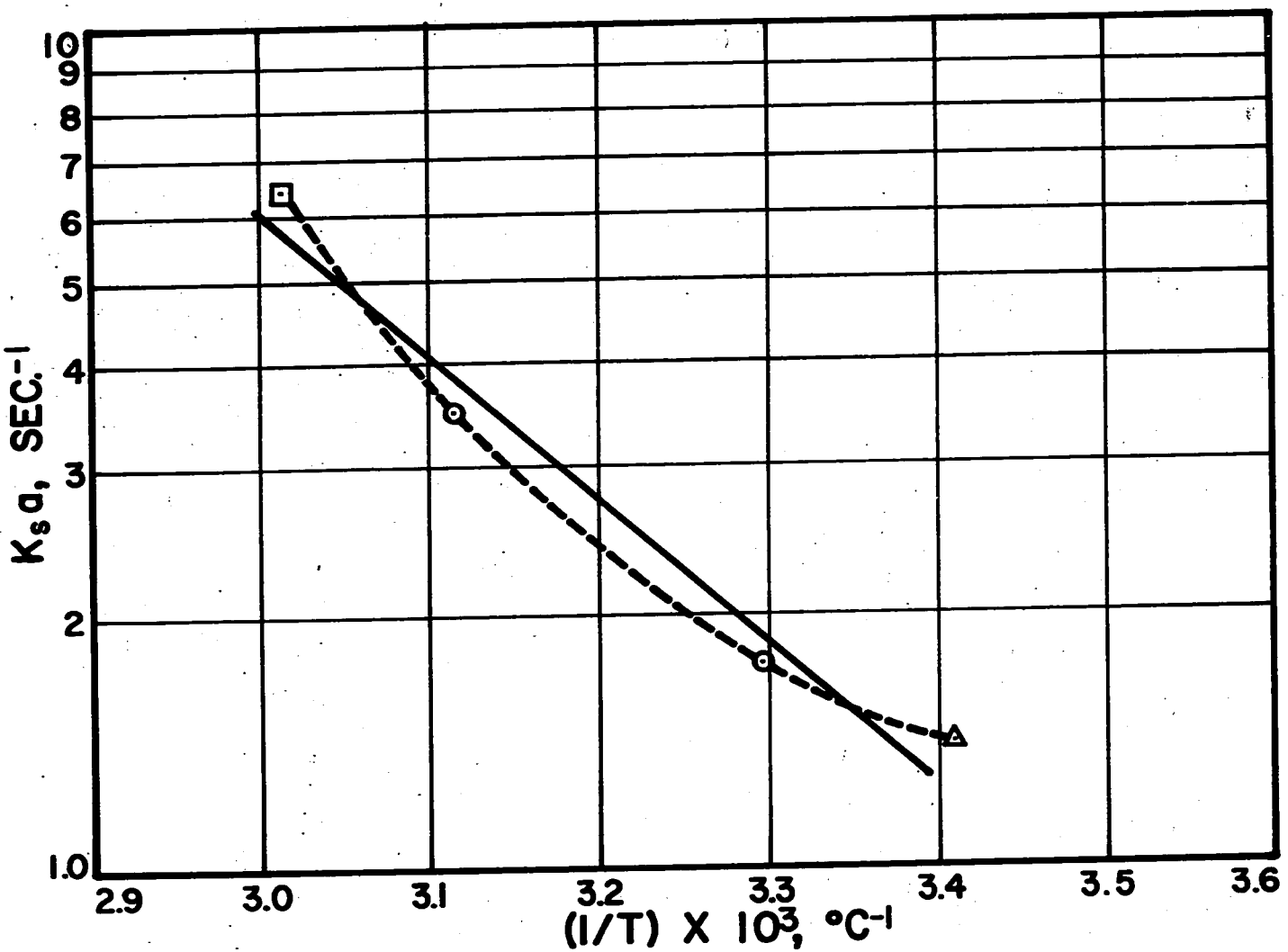

FIG. 16 - RATE CONSTANT vs. RECIPROCAL SURFACE TEMPERATURE

differentials. The corrective term from equation (I-4) increases the maximum differential to a value minimally equal to the measured value in each case.

Effectiveness factors were calculated assuming that the pellet was isothermal. The results in Table 16 point out that the greater the λ, the greater the difference in the effectiveness factors, which is expected since λ represents the ratio of the heat generated in the pill to heat removal. The maximum difference realized was 60%.

Observation of Fig. 10 indicates that the curve may be non-linear. Since the activation energies differed somewhat from isotherm to isotherm, this possibility was investigated assuming that E* was a variable which compensated for changes in the $\partial \ln\eta/\partial \ln\alpha$ term appearing in (44). Two points were significantly discouraging in this regard (1) the maximum deviation from the straight line of any of the points involved is 3-1/2% (2) the slope of the curve is such that it would increase the spread of the mean isotherm activation energies.

VI. CONCLUSIONS

1. Use of a recycle system for measurements of this type was unique and successful, its success hinging upon the acquisition of a satisfactory circulating pump.

2. Experimentally measured temperature rises as high as 33°C were encountered in the porous catalyst pellets during the course of the chemical reaction.

3. The mathematical model predicted the experimental centerline temperature rises to within 13% with two exceptions.

4. Errors in effectiveness factors of up to 60% would result if the heat effects of the reaction were ignored.

TABLE 1

SAMPLE DATA FOR THERMAL DIFFUSIVITY EXPERIMENTS

Sample	Mass, g	Length, in	Diameter, in	$R^2(10^4)$, ft^2	ρ, #/ft^3	Runs
Support	4.154	1.538	0.395	2.71	83.7	7-9
0.05%Pt	4.199	1.589	0.396	2.72	81.7	1-6

TABLE 2

COOLING AIR VELOCITY DATA FOR THERMAL DIFFUSIVITY MEASUREMENT

Reading	1	2	3	4	5	AVG.	σ^2	$(Nu)_h$
Velocity	2730	2730	2745	2730	2717	2731	± 9	56

Velocity given in ft/min

TABLE 3

TIME-CENTERLINE TEMPERATURE DATA

THERMAL DIFFUSIVITY OF CATALYST AND SUPPORT IN AIR

Time min.	Run Number 1	2	3	4	5	6	7	8	9
0.0[a]	76.1	76.8	112.5	53.7	78.2	109.8	59.5	77.8	102.1
0.1	75.8	76.8	112.2	53.6	78.2	109.7	59.4	77.8	102.1
0.2	75.1	76.4	111.4	53.5	78.0	108.9	59.3	76.8	101.7
0.3	72.1	73.5	106.3	53.3	74.6	102.5	58.2	74.6	97.5
0.4	67.3	68.5	99.2	52.0	69.7	94.9	55.4	70.4	90.7
0.5	63.0	63.4	92.2	50.1	64.5	87.1	52.9	65.4	84.2
0.6	58.8	59.6	84.8	48.5	60.2	79.5	50.2	61.4	77.2
0.8	52.4	53.0	71.3	45.2	53.4	67.8	46.4	54.8	66.5
1.0	47.3	48.2	62.6	42.4	48.6	59.2	43.4	50.1	59.2
1.2	42.8[c]	44.6	54.9	40.7	45.0	52.8	41.1	46.5	53.0
1.5	40.0	40.8	49.2	38.6	41.3	46.7	38.7	42.1	47.9
2.0	37.1	37.7	42.3	37.4	38.2	41.4	36.8	38.7	42.0
2.5	35.4	36.0	39.8	36.3	36.3	38.6	35.8	37.5	39.5
5.0[b]	32.9	34.0	36.6	35.0	34.7	35.9	35.0	35.5	36.8
ΔT_o	43.2	42.8	75.9	18.7	43.5	73.9	24.5	42.3	65.3

a T_{max}

b T_o

c Time = 1.25 min

TABLE 4

DIMENSIONLESS TEMPERATURE, θ-THERMAL DIFFUSIVITY, α_d

THERMAL DIFFUSIVITY OF CATALYST AND SUPPORT IN AIR

	θ							
Run	0.900	0.800	0.700	0.600	0.500	0.400	0.300	0.200
1	0.00492	0.00510	0.00520	0.00515	0.00495	0.00480	0.00482	0.00478
2	0.00468	0.00500	0.00510	0.00515	0.00495	0.00490	0.00485	0.00480
3	0.00465	0.00468	0.00478	0.00480	0.00480	0.00482	0.00488	0.00488
4	0.00365	0.00388	0.00405	0.00418	0.00422	0.00430	0.00450	0.00448
5	0.00475	0.00502	0.00518	0.00525	0.00512	0.00498	0.00495	0.00490
6	0.00488	0.00500	0.00515	0.00515	0.00502	0.00495	0.00500	0.00502
7	0.00435	0.00455	0.00468	0.00475	0.00465	0.00462	0.00470	0.00478
8	0.00465	0.00478	0.00485	0.00490	0.00478	0.00468	0.00465	0.00472
9	0.00452	0.00470	0.00475	0.00482	0.00480	0.00475	0.00475	0.00465
τ	0.092	0.123	0.155	0.187	0.219	0.259	0.315	0.392

TABLE 5

DIMENSIONLESS TEMPERATURE, θ-CALCULATED PELLET HEAT CAPACITY IN AIR

	θ							
Run	0.900	0.800	0.700	0.600	0.500	0.400	0.300	0.200
1	0.218	0.217	0.216	0.215	0.213	0.212	0.212	0.210
2	0.218	0.217	0.216	0.215	0.213	0.212	0.212	0.210
3	0.225	0.224	0.222	0.220	0.219	0.217	0.215	0.214
4	0.214	0.213	0.213	0.212	0.212	0.211	0.210	0.210
5	0.218	0.217	0.216	0.215	0.213	0.212	0.212	0.210
6	0.226	0.224	0.223	0.221	0.219	0.217	0.215	0.214
7	0.215	0.215	0.214	0.214	0.213	0.212	0.212	0.211
8	0.218	0.218	0.216	0.215	0.214	0.213	0.213	0.212
9	0.224	0.223	0.221	0.220	0.218	0.216	0.215	0.213

TABLE 6

CALCULATED THERMAL CONDUCTIVITY IN AIR-DIMENSIONLESS TEMPERATURE

	θ								AVG.	
Run	0.900	0.800	0.700	0.600	0.500	0.400	0.300	0.200	k_e	k_e
1	|0.0877	0.0901	0.0915	0.0902	0.0858|	0.0832	0.0834	0.0804	0.0891	
2	|0.0830	0.0883	0.0900	0.0898	0.0861|	0.0845	0.0838	0.0824	0.0874	
3	|0.0852	0.0852	0.0864	0.0860	0.0856	0.0848	0.0858	0.0850|	0.0855	
4	0.0639	0.0675	|0.0702	0.0721	0.0731	0.0741|	0.0771	0.0767	0.0724	0.0854
5	|0.0846	0.0887	0.0911	0.0919	0.0888	0.0861	0.0858|	0.0841	0.0881	
6	|0.0900	0.0912	0.0935	0.0931	0.0899	0.0879	0.0877	0.0877|	0.0901	
7	0.0785	0.0820	|0.0842	0.0854	0.0833	0.0822	0.0825	0.0847|	0.0837	0.0856
8	|0.0853	0.0875	0.0881	0.0884	0.0858	0.0836|	0.0835	0.0841	0.0864	
9	|0.0852	0.0878	0.0883	0.0893	0.0878	0.0861	0.0856	0.0834|	0.0867	

Table values of thermal conductivity in units of BTU/hr ft ^{o}F

$$k_e = 3.5 \times 10^{-4} \pm 0.1 \times 10^{-4} \text{ cal/cm sec } ^{o}\text{C}$$

\| \|values included in averaging process

TABLE 7

SURFACE AREA AND PORE VOLUME DATA*

Sample Designation	Surface Area	Total Pore Volume
Alumina Support	60 m^2/gram	0.3690 ml/g
0.05 % Pt	65 m^2/gram	0.3758 ml/g

	Pore Distribution Cumulation ml/gram	
Pore Size, Å	Alumina Support	0.05% Pt
165,000	0.0000	0.0000
2,000	0.1477	0.1358
1,000	0.1717	0.1387
800	0.1786	0.1662
600	0.1886	0.1761
500	0.1946	0.1810
400	0.2006	0.1889
300	0.2096	0.1987
200	0.2266	0.2154
120	0.2585	0.2479
< 120	0.3690	0.3758

*Courtesy of E. I. du Pont de Nemours and Co., Inc.

TABLE 7 (Continued)

$k_{Al_2O_3}$ (k_0) cal/sec cm °C	Pellet Density g/cm	Total Void Fraction ϵ	Macrovoid Fraction ϵ_a	Microvoid Fraction ϵ_μ
0.065	1.34	0.495	0.346	0.149

TABLE 8

DATA FOR USE IN EQUATION (A-44)

Gas	Air	Helium	Hydrogen
a	0.8	0.5	0.4
γ	1.4	1.67	1.4
T, °R	580	580	58
p, #/ft^2	2120	2120	2120
Pr	0.70	0.70	0.70
d, ft^2	$29.5(10^{-8})$	$29.5(10^{-8})$	$29.5(10^{-8})$
s, ft^2	$10.2(10^{-10})$	$6.25(10^{-10})$	$7.9(10^{-10})$
k_g, cal/sec cm °C	$0.72(10^{-4})$	$3.98(10^{-4})$	$4.99(10^{-4})$
k_f, cal/sec cm °C	$0.110\ (10)^{-4}$	$0.118(10)^{-4}$	$0.192\ (10)^{-4}$
k_t, cal/sec cm °C	$2.5\ (10)^{-4}$	$2.7(10)^{-4}$	$4.4(10)^{-4}$

$Z = 5.08(10^{-24})$ ft-lb/°R Godbee Factor = 22.8

Results Using Above Data

k_c $1.0(10^{-4})$

k_e^{He} $3.7(10^{-4})$

k_e^{H2} $5.4(10^{-4})$

$k_e^{He}(28)$ $4.5(10^{-4})$

TABLE 9

OXYGEN-HYDROGEN DIFFUSIVITY DATA

Run	Vol., cc	t, sec	F, cc/min	% O_2	X_A	D_{AB}^{EFF} cm^2/sec
1	50.0	50.4		2.04		
	50.0	50.4		2.05		
	50.0	50.6		2.05		
AVG.	50.0	50.4	59.5	2.05	0.020	0.1179
2	50.0	50.5		1.94		
	50.0	50.4		1.98		
	50.0	50.4		1.97		
AVG.	50.0	50.4	59.5	1.96	0.020	0.1125
3	50.0	63.6		2.62		
	50.0	63.6		2.50		
	50.0	63.6		2.60		
AVG.	50.0	63.6	47.2	2.58	0.016	0.1186
4	50.0	119.0		4.50		
	50.0	119.2		4.55		
	50.0	119.0		———		
AVG.	50.0	119.0	25.2	4.52	0.045	0.1165
5	50.0	40.6		1.56		
	50.0	40.4		1.53		
AVG.	50.0	40.5	74.0	1.54	0.015	0.1087
AVG.						0.115

p = 1.0 atm T = 26.5 °C

TABLE 10

CALCULATED DIFFUSIVITY RESULTS

Binary Diffusion Coefficients

T, °C	D_{AB}	D_{AC}	D_{AD}	r_1	r_2	p
293 °C	0.74	0.22	0.20	3.4	3.7	1.0 atm

Diffusion Ratio vs Composition

	$D_{Am}^{EFF}/D_{AB}^{EFF}$	
% N_2	$X_A = 0.05$	$X_A = 0.0$
0	0.84	0.85
16	0.61	0.62

Diffusion Ratio and D_{Am}^{EFF} vs % N_2

% N_2	0	4	8	12	16	20
$D_{Am}^{EFF}/D_{AB}^{EFF}$	0.84	0.76	0.70	0.65	0.61	0.57
D_{Am}^{EFF}, cm^2/sec	0.096	0.087	0.080	0.075	0.070	0.066

p = 1.15 atm T = 54 °C δ = 7.15

TABLE 11

CALCULATED VARIATION OF THE DIFFUSION COEFFICIENTS WITH TEMPERATURE

T, °K	293	313	333	353	373	393
D_{AB}	0.684	0.765	0.851	0.940	1.030	1.128
D_{AB}^{EFF}	0.0957	0.1070	0.1190	0.1315	0.1440	0.1578
D_{Am}^{EFF}	0.080	0.1090	0.100	0.110	0.121	0.132

p = 1.15atm % N_2 = 0.0

Diffusivities given in cm^2/sec

TABLE 12

COMPILED REACTION ANALYSIS DATA

Run	$R^* \times 10^7$ $\frac{moles}{cm^3\ sec}$	$C_{As} \times 10^7$ $\frac{moles}{cm^3}$	X^a_{As}	X_{Ds}	X_{Bs}	T_s °C	Measured ΔT, °C	Measured ΔP cm oil	$\rho \times 10^4$ g/cc	D^{EFF}_{Am} $\frac{cm^2}{sec}$	v $\frac{ft}{sec}$	Sc	Re	$j_H = j_D$	$(Nu)_h$	$(Nu)_m$	λ	$(\eta\alpha^2)^b$
20-1-3	4.92	4.41	0.0093	0.0074	0.983	19.9	6.3	0.02	1.16	0.0932	8.8	8.3	328	0.030	8.7	20.0	0.0301	2.72
20-2-3	8.12	7.54	0.0159	0.0215	0.963	20.3	10.1	0.08	1.46	0.0897	8.8	5.1	412	0.027	9.9	24.4	0.0496	3.05
20-2-4	10.74	10.20	0.0215	0.0832	0.895	20.5	13.2	0.10	2.28	0.0782	8.8	6.9	645	0.022	12.6	21.1	0.0585	2.72
20-3-1	15.11	13.67	0.0288	0.0750	0.896	19.8	19.3	0.25	2.35	0.0816	7.1	4.7	518	0.023	10.6	19.9	0.0821	3.07
20-4-1	25.1	23.2	0.0489	0.1634	0.788	20.2	33.4	0.18	3.62	0.0690	5.0	3.6	583	0.022	11.4	19.6	0.1175	3.84
30-1-2	8.27	6.85	0.0152	0.0458	0.939	30.4	7.8	0.04	1.65	0.0862	8.8	5.7	467	0.025	10.4	20.8	0.0397	3.17
30-2-5	10.61	8.93	0.0200	0.0526	0.924	30.0	11.7	0.02	1.81	0.0840	6.5	5.9	389	0.028	9.7	19.7	0.0532	3.21
30-3-5	18.78	14.23	0.0313	0.109	0.860	30.1	20.1	0.06	2.78	0.0759	6.9	4.3	618	0.022	12.1	22.0	0.0768	3.94
30-3-6	12.79	9.18	0.0200	0.050	0.928	30.0	13.0	0.07	1.81	0.0851	8.1	5.4	472	0.025	10.5	20.6	0.0554	3.71
30-4-6	26.8	19.84	0.0434	0.101	0.856	30.7	30.0	0.06	2.71	0.0770	7.0	4.1	641	0.021	12.0	21.5	0.1081	3.98
50-1-1	5.85	3.03	0.0070	0.0279	0.965	48.4	5.7	0.02	1.27	0.0897	8.8	7.9	360	0.029	9.3	20.8	0.0182	4.88
50-2-1	11.47	6.58	0.0152	0.0503	0.934	47.9	11.6	0.05	1.63	0.0851	8.8	6.5	461	0.026	10.6	22.3	0.0375	4.65
50-3-1	18.34	9.74	0.0225	0.1027	0.875	48.1	17.4	0.09	2.32	0.0770	8.8	5.1	657	0.021	12.3	23.7	0.0503	5.54
50-4-1	21.1	11.53	0.0264	0.0656	0.908	48.3	20.6	0.04	1.96	0.0828	8.8	5.5	556	0.023	11.3	22.6	0.0639	5.01
50-4-2	34.7	19.04	0.0390	0.0599	0.901	48.0	33.2	0.10	2.07	0.0840	8.8	5.2	586	0.022	11.4	22.3	0.0958	5.49
60-1-1	8.94	3.69	0.0088	0.0530	0.938	58.5	7.2	0.04	1.53	0.0851	8.8	6.9	434	0.025	9.6	20.6	0.0204	6.46
60-2-1	12.80	4.71	0.0124	0.0207	0.968	58.7	11.1	0.05	1.16	0.0908	8.8	8.5	329	0.030	8.8	20.1	0.0277	6.78
60-3-1	21.3	8.83	0.0209	0.1195	0.860	58.8	17.4	0.09	2.42	0.0748	8.8	5.0	685	0.021	12.8	24.6	0.0427	7.32
60-4-1	28.9	11.60	0.0277	0.0767	0.896	58.6	26.6	0.09	2.02	0.0805	8.8	5.5	572	0.023	11.7	23.3	0.0605	7.02
AVG.															10.8	21.6		

[a]Based on dry stream composition

[b]$R^2 = 0.227\ cm^2$

TABLE 13

COMPARISON OF MAGNITUDES OF TERMS APPEARING IN EQUATIONS (40) AND (42)

Constants: $(Nu)_h = 11$ $(Nu)_m = 20$ $\alpha = 3.0$

(1)

E^* vs $2R_g(\Delta T)_{max}\frac{\partial \ln\eta}{\partial\lambda}$		
β	10.0	13.0
$\frac{\partial \ln\eta}{\partial\lambda}$	2.4	3.3
$2R_g(\Delta T)_{max}\frac{\partial \ln\eta}{\partial\lambda}$	290	400
Maximum % Difference	5.7	10.0

$E^* = 4000$ cal/mole ^oK $(\Delta T)^a_{max} = 30^o$

(2)

$1 + \frac{1}{2}\frac{\partial \ln\eta}{\partial \ln\alpha}$ vs $\frac{\partial \ln\eta}{\partial\beta}$		
λ	0.02	0.10
$\frac{\partial \ln\eta}{\partial\beta}$	0.006	0.03
Maximum % Difference	1%	6%

$$1 \gtrsim 1 + -\frac{\partial \ln\eta}{\partial \ln\alpha} \gtrsim 0.5$$

(3)

n^* vs $1 + \frac{\partial \ln\eta}{\partial \ln\lambda}$		
λ	0.03	0.10
$1 + \frac{\partial \ln\eta}{\partial \ln\lambda}$	1.08	1.22
n^*	1.00	1.20

$\beta = 10$

(a) Largest experimental $(\Delta T)_{max}$. Most runs had considerably smaller ΔT.

TABLE 14

ACTIVATION ENERGY DATA

20 Series		30 Series		50 Series		60 Series	
1-3	5700	1-2	5800	1-1	7100	1-1	7700
2-3	5600	2-5	5600	2-1	6700	2-1	7800
2-4	5300	3-5	5900	3-1	7100	3-1	8000
3-1	5300	3-6	5900	4-1	6800	4-1	7800
4-1	5700	4-6	5800	4-2	6600		
AVG.	5500		5800		6900		7800
β = 9.5		β = 9.6		β = 10.8		β = 11.9	

$\bar{E}$ = 6500 $\bar{\beta}$ = 10.4

TABLE 15

INFLUENCE OF EXPERIMENTAL VARIATION OF PARAMETERS ON THE EFFECTIVENESS FACTOR

$(Nu)_m$	α 1.5	3.0	6.0
10.29	0.904	0.544	0.241
13.27	0.931	0.584	0.273

$(Nu)_h$ = 10.8 β = 9.7 λ = 0.12

$(Nu)_h$	α 1.5	3.0	6.0
8.73	1.024	0.626	0.283
12.77	0.979	0.590	0.264

$(Nu)_m$ = 11.6 β = 9.7 λ = 0.16

β	α 1.5	3.0	6.0
9.1	0.869	0.534	0.244
10.3	0.894	0.549	0.250

$(Nu)_h$ = 10.8 λ = 0.10 $(Nu)_m$ = 11.6

X_{As}	α 1.5	3.0	12.0
0.00	0.997	0.604	0.100
0.04	1.008	0.610	0.100

$(Nu)_h$ = 10.8 λ = 0.16 $(Nu)_m$ = 11.6

$(Nu)_m$	α 1.5	3.0	6.0
10.29	0.904	0.544	0.241
13.27	0.931	0.584	0.273

$(Nu)_h$ = 10.8 β = 9.7 λ = 0.12

TABLE 16

COMPUTED RESULTS

Run	β	η	α	$k_s a$, sec^{-1}	Computed ΔT ^oC [b]	Computed ΔT_{FILM} ^oC	Prater $(\Delta T)_{max}$ ^oC	Measured ΔT ^oC	% Diff.[a]	Isothermal η_I	% Diff.[c]
20-1-3	11.2	0.72	2.0	1.6	6.3	1.4	8.9	6.3	0.0	0.65	10.8
20-2-3	11.2	0.75	2.0	1.6	11.3	2.3	14.7	10.1	8.1	0.61	23.0
20-2-4	11.2	0.78	1.9	1.2	11.5	1.8	7.1	13.2	12.9	0.65	20.0
20-3-1	11.2	0.82	1.9	1.3	18.6	3.5	24.3	19.3	3.6	0.61	34.4
20-4-1	11.2	0.85	2.1	1.3	30.2	5.6	35.1	33.4	9.6	0.53	60.4
AVG.				1.4							
30-1-2	10.8	0.69	2.2	1.8	9.6	1.9	12.1	7.8	23.0	0.60	15.0
30-2-5	10.8	0.72	2.1	1.6	12.7	2.6	16.3	11.7	8.6	0.60	20.0
30-3-5	10.8	0.71	2.4	1.9	20.6	3.9	23.6	20.1	2.5	0.52	36.5
30-3-6	10.8	0.68	2.3	2.0	14.1	2.9	17.0	13.0	8.5	0.54	26.0
30-4-6	10.8	0.80	2.2	1.6	28.7	5.2	32.8	30.0	4.3	0.52	53.9
AVG.				1.8							
50-1-1	10.2	0.48	3.2	4.0	5.9	1.5	5.9	5.7	3.5	0.45	6.7
50-2-1	10.2	0.55	2.9	3.2	11.7	2.6	12.1	11.6	0.9	0.47	17.0
50-3-1	10.2	0.51	3.3	3.7	16.2	3.6	16.3	17.4	6.9	0.40	27.5
50-4-1	10.2	0.58	2.9	3.1	20.1	4.4	20.8	20.6	2.4	0.44	31.8
50-4-2	10.2	0.62	3.0	3.3	31.2	7.3	31.5	33.2	6.0	0.40	55.0
AVG.				3.5							
60-1-1	9.9	0.38	4.1	6.3	7.4	2.2	6.8	7.2	2.8	0.35	8.6
60-2-1	9.9	0.37	4.3	7.4	10.8	3.6	9.3	11.1	2.7	0.33	I2.1
60-3-1	9.9	0.39	4.3	6.1	15.5	4.0	14.3	17.4	10.9	0.29	34.5
60-4-1	9.9	0.43	4.1	6.0	21.7	6.0	20.4	26.6	18.4	0.32	34.4
AVG.				6.4							

[a] Between Computed and Measured ΔT [b] Including Film ΔT [c] Between η and η_I

TABLE 17

PERMEABILITY DATA

Run	Q, cc	t, sec	P_1 psig	P_1 psia	Δp psia	P_2 psia	P_m psia	P_m atm	$\frac{1}{P_m}$, atm	K	L cm	D cm
1	50	42.8	49.8	64.7	49.8	14.86	39.8	2.70	0.370	2.87	1.01	1.02
2	30	35.5	39.8	54.7	39.8	14.86	34.8	2.36	0.423	2.97	1.01	1.02
3	20	34.8	30.1	45.0	30.1	14.86	29.9	2.04	0.491	3.10	1.01	1.02
4	12	35.2	20.2	35.1	20.2	14.86	25.0	1.70	0.589	3.29	1.01	1.02
5	25	37.4	29.8	44.6	29.8	14.84	29.7			3.62	0.98	1.01
6	40	33.5	30.0	44.8	30.0	14.83	29.8			6.54	1.00	1.01
7	40	35.0	29.9	44.7	29.9	14.83	29.8			6.35	0.99	1.01
8	25	36.0	29.9	44.8	29.9	14.85	29.8			3.78	1.01	1.02
9	20	37.0	29.8	44.6	29.8	14.85	29.8			2.96	1.01	1.02
10	20	34.8	29.9	44.8	29.9	14.85	29.8			3.16	1.02	1.02

μ = 0.018 cp

APPENDIX A - THEORETICAL DEVELOPMENTS

1. The Finite Difference Equations

An iterative method of solution was chosen to solve equations (17) and (18). Results of solving one of the profiles was used to calculate the other profile. This result in turn was used to recalculate the first equation, etc., until converged values were obtained.

To do this, both equations were put into the central finite difference form

$$A_i Y_{i-1} + B_i Y_i + C_i Y_{i+1} = D_i \qquad (A\text{-}1)$$

on the discrete axis, $\xi = i\Delta\xi$.

a. The Mass Equation

If (17) is expanded with n = 1, the result can be written as

$$\frac{d^2\psi}{d\xi^2} + \left[\frac{1}{\xi} + \frac{X_{As}}{(1 - X_{As}\psi)}\frac{d\psi}{d\xi} - \frac{1}{\phi}\frac{d\phi}{d\xi}\right]\frac{d\psi}{d\xi} - \alpha^2(1 - X_{As}\psi)e^{\beta\left(1 - \frac{1}{\phi}\right)}\psi = 0 \qquad (A\text{-}2)$$

In central difference form, this equation is

$$\left[\frac{\psi_{i-1} - 2\psi_i + \psi_{i+1}}{\Delta\xi^2}\right] + \left\{\frac{1}{\Delta\xi(i-1)} + \left[\frac{X_{As}(\psi_{i+1} - \psi_{i-1})}{(1 - X_{As}\psi_i)(2\Delta\xi)}\right]^{j-1} - \left[\frac{\phi_{i+1} - \phi_{i-1}}{2\Delta\xi\phi_i}\right]\right\} \cdot \left[\frac{\psi_{i+1} - \psi_{i-1}}{2\Delta\xi}\right] - \alpha^2(1 - X_{As}\psi_i)^{i-1}e^{\beta\left(1 - \frac{1}{\phi_i}\right)}\psi_i = 0 \qquad (A\text{-}3)$$

where

$$\Delta\xi = \frac{1}{N-1};\ \xi = (i-1)\Delta\xi,\ i = 1, 2, 3....N \qquad (A\text{-}4)$$

This equation can be considerably simplified with the aid of the notation,

$$f_i = e^{\beta\left(1 - \frac{1}{\phi_i}\right)};\ g_i = \frac{X_{As}(\psi_{i+1} - \psi_{i-1})}{4(1 - X_{As}\psi_i)} - \frac{\phi_{i+1} - \phi_{i-1}}{4\phi_i} \qquad (A\text{-}5)$$

With these substitutions, terms may be collected in (A-3) giving

$$\psi_{i-1} - \frac{\left[2 + \alpha^2\Delta\xi^2 f_i(1 - X_{As}\psi_i)^{j-1}\right]\psi_i}{\left[\frac{2i-3}{2i-2} - g_i\right]} + \left[\frac{2i-1}{2i-2} + g_i\right]\psi_{i+1} = 0 \qquad (A\text{-}6)$$

which is in the form of (A-1) with the A_i all equal to one.

The boundary conditions must be applied. At the center of the pellet, i.e., $i = 1$; $\xi = 0$, the term $\frac{1}{\xi}\frac{d\psi}{d\xi}$ is seen by L'Hospital's rule to have the limit $\frac{d^2\psi}{d\xi^2}$. Thus, the differential equation (A-2) applying at that point is

$$2\frac{d^2\psi}{d\xi^2} - \alpha^2(1 - X_{As}\psi)e^{\beta\left(1-\frac{1}{\phi}\right)}\psi = 0 \qquad (A\text{-}7)$$

In finite difference form

$$\left[\frac{\psi_0 - 2\psi_1 + \psi_2}{\Delta\xi^2}\right] - \frac{\alpha^2(1 - X_{As}\psi_1)^{j-1}f_1}{2}\psi_1 = 0 \qquad (A\text{-}8)$$

If $d\psi/d\xi$ is zero at the center, then the boundary condition is

$$\psi_0 = \psi_2 \qquad (A\text{-}9)$$

and the difference equation can be written as

$$\left[2 + \frac{\alpha^2\Delta\xi^2 f_1}{2}(1 - X_{As}\psi_1)^{j-1}\right]\psi_1 + 2\psi_2 = 0 \qquad (A\text{-}10)$$

The general difference equation at the other boundary ($i = N$), is written as

$$\psi_{N-1} + B_N\psi_N + C_N\psi_{N+1} = 0 \qquad (A\text{-}11)$$

Also, the boundary condition (21) in finite difference form is

$$\psi_{ss} = \psi_N = 1 - \frac{(\psi_{N+1} - \psi_{N-1})}{2\Delta\xi(Nu)_m(1 - X_{As}\psi_N)} \qquad (A\text{-}12)$$

which is solved for ψ_{N+1} to give

$$\psi_{N+1} = \psi_{N-1} + D_N - D_N\psi_N \qquad (A\text{-}13)$$

where

$$D_N \equiv 2\Delta\xi(Nu)_m(1 - X_{As}\psi_N)^{j-1}$$

Combining (A-13) and (A-11) gives

$$\psi_{N-1} + \frac{B_N - C_N D_N}{1 + C_N}\psi_N = -\frac{C_N D_N}{1 + C_N} \qquad \text{(A-14)}$$

The coefficients B_N and C_N differ from those given in (A-6). From equations (A-2) and (A-5) it is seen that

$$g_N = \left[\frac{X_{As}}{1 - X_{As}\psi}\frac{d\psi}{d\xi} - \frac{1}{\phi}\frac{d\phi}{d\xi}\right]_N,$$

but from the boundary conditions (21) and (23) it is evident that

$$\frac{1}{(1 - X_{As}\psi)}\frac{d\psi}{d\xi}\bigg|_{\xi=1} = (Nu)_m(1 - \psi); \quad \frac{d\phi}{d\xi}\bigg|_{\xi=1} = (Nu)_h(1 - \phi) \qquad \text{(A-15)}$$

The g_N can be put into the finite difference form

$$g_N = \left[X_{As}(Nu)_m(1 - \psi_N) + (Nu)_h\left(1 - \frac{1}{\phi_N}\right)\right]^{j-1}\frac{\Delta\xi}{2} \qquad \text{(A-16)}$$

and used in (A-6).

The set of equations (A-6) with the boundary equations (A-10) and (A-16) represent the complete set of finite difference equations representing the mass transfer of oxygen between the pellet and the main gas stream.

b. The Energy Equation

Equation (18) may be written for the first order case as

$$\frac{d^2\phi}{d\xi^2} + \frac{1}{\xi}\frac{d\phi}{d\xi} + \frac{\lambda\alpha^2 f}{\phi}\psi = 0 \qquad \text{(A-17)}$$

where f is the function described by (A-5). This may be given in central difference form by

$$\left[\frac{\phi_{i-1} - 2\phi_i + \phi_{i+1}}{\Delta\xi^2}\right] + \frac{\phi_{i+1} - \phi_{i-1}}{2(i-1)\Delta\xi^2} + \frac{\lambda\alpha^2 f_i}{\phi_i}\psi_i = 0 \qquad \text{(A-18)}$$

which may be rearranged upon collecting terms to give

$$\phi_{i-1} - \frac{4(i-1)}{2i-3}\phi_i + \frac{2i-1}{2i-3}\phi_{i+1} = -\lambda\alpha^2\Delta\xi^2\left[\frac{2i-2}{2i-3}\right]\left[\frac{f_i\psi_i}{\phi_i}\right]^{j-1} \qquad \text{(A-19)}$$

which is in the form of (A-1).

For the point $\xi = 0$, the limit of the term including the first derivative in (A-17) is seen to be

$$\lim_{\xi \to 0}\left[\frac{1}{\xi}\frac{d\phi}{d\xi}\right] = \frac{d^2\phi}{d\xi^2} \qquad \text{(A-20)}$$

Therefore, (A-17) can be applied at $\xi = 0$ to give

$$\frac{d^2\phi}{d\xi^2} + \frac{\lambda\alpha^2 f}{2}\frac{\psi}{\phi} = 0 \qquad \text{(A-21)}$$

The boundary condition (25) is applied by setting $\phi_0 = \phi_2$ in the finite difference form of (A-21). The result is expressed as

$$-2\phi_1 + 2\phi_2 = -\frac{\lambda\alpha^2\Delta\xi^2}{2}\left[\frac{f_1\psi_1}{\phi_1}\right]^{j-1}. \qquad \text{(A-22)}$$

At the solid-fluid interface, the same procedure is followed as was used for the mass equation. An equation equivalent to (A-1) is

$$\phi_{N-1} + B_N\phi_N + C_N\phi_{N+1} = D_N \qquad \text{(A-23)}$$

where the coefficients are calculated according to (A-19). ϕ_{N+1} is eliminated by use of the boundary condition (23) which is written

$$\phi_{N+1} = \phi_{N-1} - 2(Nu)_h\Delta\xi\phi_N + 2(Nu)_h\Delta\xi. \qquad \text{(A-24)}$$

Combining (A-23) and (A-24), the finite difference equation for the solid-fluid interface is obtained.

$$\phi_{N-1} + \frac{B_N - 2(Nu)_h\Delta\xi C_N}{1 + C_N}\phi_N = \frac{D_N - 2(Nu)_h\Delta\xi C_N}{1 + C_N} \qquad \text{(A-25)}$$

The N equations given by (A-19), (A-22) and (A-25) are solved to give the radial temperature profile of the catalyst pellet.

c. The Effectiveness Factor

Equation (28) defines the effectiveness factor η. To calculate η it is necessary to know the first derivative of the oxygen concentration at the surface. Equation (33) can be rearranged to provide the value of derivative in terms of ψ at the solid surface, or

$$\left.\frac{d\psi}{d\xi}\right|_{\xi=1} = (Nu)_m(1 - X_{As}\psi)(1 - \psi_{ss}) \tag{21}$$

Combining this with (28) gives

$$\eta = \frac{2(Nu)_m(1 - \psi_{ss})}{\alpha^2} = \frac{2(Nu)_m(1 - \psi_N)}{\alpha^2} \tag{A-26}$$

which is the equation used to calculate the effectiveness factor.

2. The Method of Solution

The method employed is described in Richtmyer (36). A brief review of the method is given as it pertains directly to the solution of the equations of this work.

If it is assumed that a solution to the transport equation is available at the i^{th} grid point in terms of the known value at the $i + 1$ grid point, then

$$Y_i = E_i Y_{i+1} + F_i \tag{A-27}$$

For Y_{i-1}

$$Y_{i-1} = E_{i-1} Y_i + F_{i-1} \tag{A-28}$$

Recalling (A-1)

$$A_i Y_{i-1} + B_i Y_i + C_i Y_{i+1} = D_i; \tag{A-1}$$

it is seen by eliminating Y_{i-1}, and noting that the A_i are all one that

$$Y_i = -\frac{C_i}{B_i + E_{i-1}} Y_{i+1} + \frac{D_i - F_{i-1}}{B_i + E_{i-1}} \qquad \text{(A-29)}$$

Comparison of (A-2) with (A-27) shows

$$E_i = \frac{-C_i}{B_i + E_{i-1}}; \quad F_i = \frac{D_i - F_{i-1}}{B_i + E_{i-1}} \qquad \text{(A-30)}$$

where

$$E_1 = -\frac{C_1}{B_1}; \quad F_1 = \frac{D_1}{B_1} \qquad \text{(A-31)}$$

The procedure is to calculate the coefficients B_i, C_i and D_i, then the E_i and F_i, and finally the Y_i from equation (A-27) with

$$Y_N = F_N \qquad \text{(A-32)}$$

A complete block diagram of the program is given in Fig. 17.

3. The Starting Values

To get the iterations started initial values of grids are needed to begin the calculations. For this purpose, approximate values are available from the analytical solution for the case of isothermal equimolar reaction.

The applicable equation is

$$\frac{1}{\xi}\frac{d}{d\xi}\left[\xi\frac{d\psi}{d\xi}\right] - \alpha^2\psi = 0 \qquad \text{(A-33)}$$

which may be written as

$$\xi^2\frac{d^2\psi}{d\xi^2} + \xi\frac{d\psi}{d\xi} - \alpha^2\xi^2\psi = 0 \qquad \text{(A-34)}$$

This is in the form of the modified Bessel function (21) and has the general solution

$$\psi = c_1 I_o(\alpha\xi) + c_2 K_o(\alpha\xi) \qquad \text{(A-35)}$$

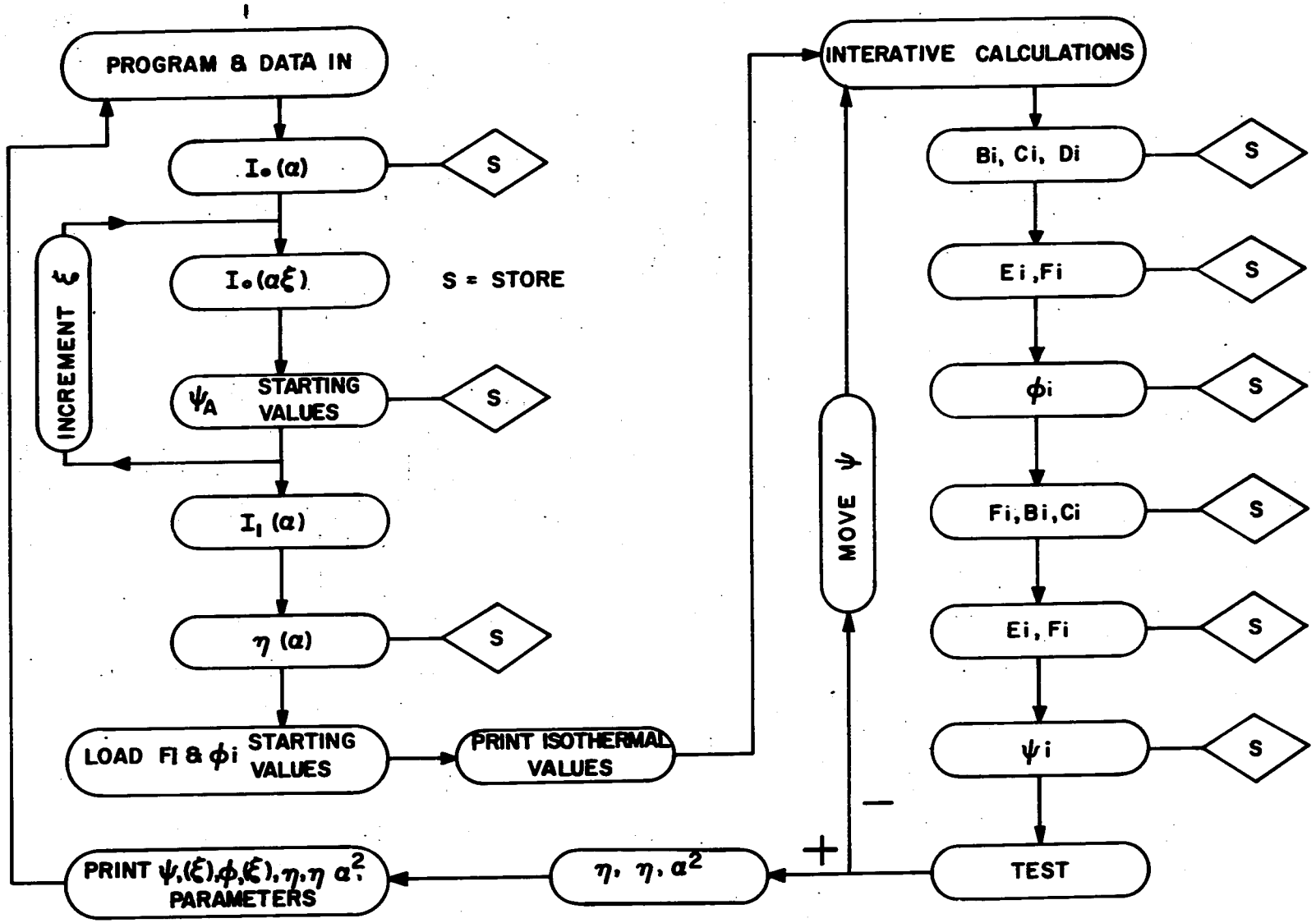

FIG. 17— COMPUTER BLOCK DIAGRAM

Using a boundary condition which requires ψ to be finite at the pellet center forces $c_2 = 0$, since $K_0(0)$ is infinite. An approximate boundary condition of $\psi = 1$ at $\xi = 1$ is used to obtain the final solution

$$\psi = \frac{I_0(\alpha\xi)}{I_0(\alpha)} \qquad \text{(A- 36)}$$

where

$$I_0(\alpha\xi) = \sum_{k=0}^{\infty} \frac{\left[\frac{\alpha\xi}{2}\right]^{2k}}{(k!)^2} \qquad \text{(A-37)}$$

Using (A-36) and (A-37), initial values of ψ were calculated for the N grid points between $0 \leq \xi \leq 1$. Simple perturbations of λ and α at a particular β value were used to obtain converged solutions over the desired range of values in subsequent calculations.

4. The Computational Procedure

The calculations were made on the Rice University Computer. A block diagram or flow sheet of the computational method is shown in Fig. 17.

The calculations were begun by calculating a grid of starting values for a small value of α as states above. This grid was used in turn to compute the corresponding isothermal case ($\lambda = 0$) for the system equations. With the X_{As} and β constant, λ was brought in small increments to the desired value using the last calculated values as starting values for the new λ. Then with λ held constant, the α value was similarly incremented stepwise to any preselected level. For each converged profile a value of the effectiveness factor was calculated. All data changes on the computer were made externally.

Two tests were necessary in the course of the calculations. First, the Bessel functions used to calculate the starting values are infinite

series. The series was cut off when two successive terms failed to differ by more than 0.001. A convergence test was used on successive $\bar{\psi}$ iterations. Each point in the grid was tested against its corresponding value from the previous iteration. If any of the values differed by a value greater than 10^{-5}, the test failed and another complete iteration was made.

When convergence was achieved, the profiles along with the data and effectiveness factor were printed out, or one of the parameters was incremented to restart the calculations. Another option available in the program is the print of successive iterations.

5. The Computer Program

The program used to solve the equations mentioned in the past sections is reproduced below.

6. The Thermal Diffusivity and Conductivity

The centerline temperature response of an infinitely long cylinder (initially at a uniform temperature) to forced convection flow over its surface of a gas at another temperature can be used to compute the mean thermal diffusivity of the cylinder.

An energy balance applied to a differential element of the cylinder yields the necessary equation for solution. The following assumptions are made in the derivation:

1) The cylinder is circular, homegeneous and is infinite in length.

2) The surface transfer group is independent of temperature.

3) Radiative losses from the cylinder are negligible.

4) An effective thermal conductivity for the heterogeneous gas-solid system can be defined which is independent of position and temperature.

```
                                                                    1
210                 ORG                                             2
          PF        RPA       EXIT                                  3
                    TRA       CC+2                                  4
                    CLA       DELSW,U+T4                            5
                    TRA       NUDAT                                 6
                    SBI       a10                                   7
                    STX       a2                                    10
                    CLA       #240                                  11
                    STO       TEST2                                 12
                    SBI       a2                                    13
                    CLA       #240,U+T4                             14
                    ABI       a4                                    15
                    CLA       #240,U+T5                             16
                    STO       EN                                    17
                    LT7       000004310000000131                    20
                    TSR       #126                                  21
                    SB2       a2                                    22
          T5        LDR       022000000005000000                    23
                    LLS       d39,U+T6                              24
                    TSR       #126,U+T7                             25
          IZI       ADD+      T6                                    26
                    TSR       #126,U+T7                             27
          B2        IF(NZE)TRA  CC-3,B2-1                           30
          T6        ADD       a4,U+T6                               31
                    SB2       a2,B1+1                               32
          IZI       ADD+      T6                                    33
                    TSR       #126,U+T7                             34
          B2        IF(NZE)TRA  CC-3,B2-1                           35
                    CLA       250,U+B4                              36
                    CLA       251,U+B3                              37
                    CLA       252,U+B2                              40
                    CLA       #240,U+T6                             41
                    TSR       #220                                  42
NUDAT     T4        STO       DELSW,U+T5                            43
                    SBI       a3                                    44
                    CLA       #240,U+T4                             45
                    ABI       a3                                    46
                    CLA       #240,U+T6                             47
                    TSR       #221                                  50
          T4        STO       DLSW2                                 51
          T5        STO       ALFA2                                 52
                    CLA       DELSW,U+T5                            53
                    SBI       a5                                    54
                    CLA       #240,U+T6                             55
                    ABI       a1                                    56
                    CLA       #240,U+T7                             57
                    TSR       #222                                  60
                    SBI       a1                                    61
YEA                 CLA       #260,U+T4                             62
                    CLA       #262                                  63
                    FSB       T4                                    64
          IUI       FSB       TEST2                                 65
                    IF(POS)TRA  B00                                 66
          B1        IF(ZER)SKP  EN                                  67
                    TRA       YEA,B1+1                              70
                    CLA       262                                   71
                    LDR+      260                                   72
          R         STO       262                                   73
```

```
                SBI         a2                          74
                CLA         *240,U-T4                   75
                ABI         a3                          76
                CLA         *240                        77
                FMP         TWO,U-T5                    100
                SBI         a*EN                        101
                CLA         *260                        102
          -U    FAD         ONE                         103
                FMP-        T5                          104
                SBI         a12                         105
          T5    STC         *240                        106
                FDV         ALFA2,B1-1                  107
                STO         *240                        110
                CLA         ALFA2,B1+X                  111
                STO         *240                        112
                IF(SLF)SKP  a20000                      113
                TRA         EXIT                        114
                CLA         0000440100000000000         115
                BAU         aLABEL,U-T7                 116
                TSR         *126                        117
                SPA         aZ                          120
                LT7         0000542300001000240         121
                TSR         *126                        122
                SPA         aZ                          123
                CLA         0000540100000000000         124
                BAU         aMABLE,U-T7                 125
                TSR         *126                        126
                SPA         aZ                          127
                LT7         0000542300006000240         130
                TSR         *126                        131
                SPA         aZ                          132
                CLA         0000240100000000000         133
                BAU         aTABLE,U-T7                 134
                TSR         *126                        135
                SPA         aZ                          136
                LT7         0000242300013000240         137
                TSR         *126                        140
                SPA         aZ                          141
                CLA         0000340100000000000         142
                BAU         aSABOL,U-T7                 143
                TSR         *126                        144
                SPA         aZ                          145
                CLA         EN                          146
                LDR         4230000000060000000         147
                LLS         a39,U-T6                    150
                TSR         *126,U-T7                   151
          121   ADD         T6,U-T7                     152
                TSR         *126                        153
EXIT            TRA         (PF)                        154
800             CLA         262                         155
                LDR-        260                         156
          R     STO         262                         157
                IF(SLF)SKP  a40000                      160
                TRA         PRINT                       161
HOUSE     --    IF(SLF)SKP  a10000                      162
                TRA         WEIGHT                      163
HOME            CLA         DELSW,U-T4                  164
                TRA         NUDAT                       165
PRINT           CLA         EN                          166
```

```
                    LDR     4230000000600000        167
                    LLS     d39,U→T6                170
                    TSR     *126,U→T7               171
              1.Z1  ADD     T6,U→T7                 172
                    TSR     *126                    173
                    TRA     HOUSE                   174
WEIGHT              SB1     a1                      175
AVGUUP              CLA     *260                    176
                    FAD     *262                    177
                    FDV     TWO                     200
                    STO     *262                    201
              B1    IF(ZER)SKP  EN                  202
                    TRA     AVGUUP,B1+1             203
                    TRA     HOME                    204
LABEL               BCD     LAMBDA, ALPHA,          205
                            BETA, (NU)↓H↑, (NU)↓M↑  206
MABLE               BCD     EN, S, V, TEST, PSI     207
                            TEST, ETA, ETALFA2      210
TABLE               BCD     ALPHA SQUARED, XAS      211
SABOL               BCD     PSI AND PHI VECTORS     212
TEST2               OCT     0                       213
EN                  OCT     0                       214
DELSW               OCT     0                       215
DUSW2               OCT     0                       216
ALFA2               OCT     0                       217
TWO                 DEC     2.0000                  220
ONE                 DEC     1.0000                  221
                    END                             222
                                                    223
```

```
                                                                    1
220                 ORG                                             2
          PF        RPA       EXIT                                  3
                    SBI       @15                                   4
                    CLA       #240                                  5
                    STO       ENF                                   6
          T6        STO       TEST                                  7
          T5        STO       EN                                    10
          T4        STO       ALPHA                                 11
                    FDV       TWO,U→T4                              12
                    LT5       ONE                                   13
          T5        LT6       T5,U→T7                               14
          T4        FMP*      T4                                    15
INOT      T6        FMP       T6                                    16
                    VDF       T4                                    17
                    FMP*      T7                                    20
                    FAD*      T5                                    21
          T6        FAD       ONE,U→T6                              22
          T7        IF(NEG)SKP  TEST                                23
                    TRA       INOT                                  24
          T5        STO       DEN                                   25
                    SBI       @1                                    26
                    LT6       ONE                                   27
                    CLA       ENF                                   30
                    FSB       ONE                                   31
                    VDF       ONE                                   32
                    STO       DELSW                                 33
KART                LT7       ONE                                   34
                    LT5       ONE                                   35
          T5        STO       TEMP1                                 36
          T6        FSB       ONE                                   37
                    FMP       DELSW,U→T4                            40
                    CLA       ALPHA                                 41
                    DMR       @1                                    42
                    FAD       @2                                    43
                    FMP       T4                                    44
                    FMP       U,U→T4                                45
BALLY     T7        FMP       T7                                    46
                    VDF       T4                                    47
                    FMP*      TEMP1                                 50
                    FAD*      T5                                    51
          T7        FAD       ONE,U→T7                              52
                    CLA       TEMP1                                 53
                    IF(NEG)SKP  TEST                                54
                    TRA       BALLY                                 55
          T5        FDV       DEN                                   56
                    STO       #260                                  57
          T6        FAD       ONE,U→T6                              60
          B1        IF(ZER)SKP  EN                                  61
                    TRA       KART,B1+1                             62
                    LT6       ONE                                   63
                    CLA       ALPHA                                 64
                    DMR       @1                                    65
                    FAD       @2,U→T4                               66
                    LT5       T4,U→T7                               67
                    FMP*      T4                                    70
IONE      T6        FAD       ONE                                   71
                    FMP       T6                                    72
                    VDF       T4                                    73
```

```
                FMP*        T7                          74
                FAD*        T5                          75
        T6      FAD         ONE,U*T6                    76
        T7      IF(NEG)SKP  TEST                        77
                TRA         ICNE                        100
        T5      FAD         U                           101
                FDV         ALPHA                       102
                FDV         DEN                         103
                STO         ETA                         104
                SBI         @*EN                        105
                CLA         ONE,U*T4                    106
        T4      STO         *261                        107
                STO         *253,B1-1                   110
        B1      IF(NZE)TRA  CC-3                        111
                CLA         000024010000000000          112
                BAU         @LABEL,U*T7                 113
                TSR         *126                        114
                SPA         @Z                          115
                CLA         000014030000000000          116
                BAU         @ETA,U*T7                   117
                TSR         *126                        120
                SPA         @Z                          121
                CLA         000024010000000000          122
                BAU         @MABLE,U*T7                 123
                TSR         *126                        124
                CLA         EN                          125
                LDR         423000000006000000          126
                LLS         @39,U*T7                    127
                TSR         *126                        130
                CLA         DELSW,U*T4                  131
EXIT            TRA         (PF)                        132
EN              OCT         0                           133
ENF             OCT         0                           134
LABEL           BCD         ETA ISOTHERMAL              135
MABLE           BCD         PSI ISOTHERMAL              136
ALPHA           OCT         0                           137
ONE             DEC         1.00000                     140
TWO             DEC         2.00000                     141
TEST            OCT         0                           142
DEN             OCT         0                           143
TEMP1           OCT         0                           144
DELSW           OCT         0                           145
ETA             OCT         0                           146
                END                                     147
                                                        150
```

```
                                                                    1
221                 ORG                                             2
          PF        RPA       EXIT                                  3
          T6        STO       EN                                    4
          T4        STO       BETA                                  5
          T5        STO       DELSW                                 6
                    FMP       T5                                    7
                    STO       DLSW2                                 10
                    SBI       a4                                    11
                    CLA       #240                                  12
                    STO       NUH                                   13
          IZI       LT4       ONE,U→B1                              14
                    CLA       TWO                                   15
                    STO       B2+B1                                 16
          -U        STO       B3+B1                                 17
                    CLA       #240,B1+1                             20
                    STO       LAMDA                                 21
                    CLA       #240,U→T5                             22
                    FMP       T5,B1-1                               23
                    STO       ALFA2                                 24
                    FMP       LAMDA                                 25
                    FMP       DLSW2,U→T6                            26
                    FMP       #260                                  27
                    FMP       HALF,U→T7                             30
                    FDV       #261                                  31
          -T7       FMP       #253                                  32
                    STO       B4+B1,B1+1                            33
FELUP     T4        FAD       ONE,U→T4                              34
          T4        FAD       U                                     35
                    FSB       ONE,U→T7                              36
                    FSB       TWO,U→T5                              37
                    VDF       T7                                    40
                    STO       B2+B1                                 41
          T7        FSB       ONE                                   42
                    FDV-      T5                                    43
                    FAD       U                                     44
          -U        STO       B3+B1                                 45
          T6        FMP       #260,U→T7                             46
          T5        FMP       T7                                    47
          -U        FMP       #253                                  50
                    FDV       #261                                  51
                    STO       B4+B1                                 52
          B1        IF(ZER)SKP  EN                                  53
                    TRA       FELUP,B1+1                            54
                    CLA       DELSW                                 55
                    FMP       TWO                                   56
                    FMP       NUH,U→T7                              57
                    FMP       B2+B1,U→T7                            60
                    CLA       B2+B1                                 61
                    FAD       ONE,U→T5                              62
                    CLA       B3+B1                                 63
                    FSB       T7                                    64
                    FDV       T5                                    65
                    STO       B3+B1                                 66
                    CLA       B4+B1                                 67
                    FSB       T7                                    70
                    FDV       T5                                    71
                    STO       B4+B1                                 72
                    SBI       a1                                    73
```

```
                CLA       B3+B1,U→T4                74
                CLA       B2+B1                     75
          -U    FDV       T4,U→T6                   76
                STO       B2+B1                     77
                CLA       B4+B1                     100
                FDV       T4,U→T7                   101
                STO       B3+B1,B1+1                102
YNU             CLA       B3+B1                     103
                FAD       T6,U→T4                   104
                CLA       B2+B1                     105
          -U    FDV       T4,U→T5                   106
                STO       B2+B1                     107
          T5    LDR       B4+B1,U→T6                110
          R     FSB       T7                        111
                FDV       T4,U→T7                   112
                STO       B3+B1                     113
          B1    IF(ZER)SKP  EN                      114
                TRA       YNU,B1+1                  115
                CLA       B3+B1,U→T4                116
                STO       #261,B1-1                 117
FEE             CLA       B2+B1                     120
                FMP*      T4                        121
                CLA       B3+B1                     122
                FAD*      T4                        123
                STO       #261                      124
          B1    IF(ZER)SKP  a1                      125
                TRA       FEE,B1-1                  126
                CLA       DLSW2,U→T4                127
                CLA       ALFA2,U→T5                130
EXIT            TRA       (PF)                      131
EN              OCT       0                         132
BETA            OCT       0                         133
DELSW           OCT       0                         134
DLSW2           OCT       0                         135
NUH             OCT       0                         136
LAMDA           OCT       0                         137
ALFA2           OCT       0                         140
ONE             DEC       1.00000                   141
TWO             DEC       2.00000                   142
HALF            DEC       0.500000                  143
                END                                 144
                                                    145
```

```
                                                                    1
222                 ORG                                             2
          PF        RPA       EXIT                                  3
          T4        STO       DLSW2                                 4
          T5        STO       DELSW                                 5
          T6        STO       NUM                                   6
          T7        STO       EN                                    7
                    SBI       a2                                    10
                    CLA       #240,U+T4                             11
                    FMP       T4,B1+1                               12
                    FMP       DLSW2,U+T4                            13
                    CLA       #240,U+T5                             14
                    SBI       a1                                    15
FUUP                CLA       #261                                  16
                    VDF       ONE                                   17
          -U        FAD       ONE                                   20
                    FMP       T5,U+T6                               21
                    TSR       #203                                  22
          T6        STO       #253                                  23
          B1        IF(ZER)SKP  EN                                  24
                    TRA       FLUP,B1+1                             25
                    SBI       a14                                   26
                    CLA       #240,U+T6                             27
                    STO       XAS                                   30
                    FDV       d4.0000,U+T7                          31
                    SB5       #EN                                   32
                    SBI       a4                                    33
                    CLA       #240                                  34
                    STO       NUM                                   35
                    STX       a2                                    36
                    SBI       a1,B5-1                               37
GEEUUP              CLA       #260,U+T5                             40
                    ABI       a2                                    41
                    CLA       #260,B1-1                             42
                    FSB+      T5                                    43
                    CLA       #260                                  44
                    FMP       T6                                    45
          -U        FAD       ONE                                   46
                    VDF       T5                                    47
                    FMP       T7                                    50
                    STO       TEMP1,B1-1                            51
                    CLA       #261,B1+X                             52
          -U        FAD       #261,B1-1                             53
                    FDV       #261                                  54
                    FDV       d4.0000                               55
          -U        FAD       TEMP1                                 56
                    STO       #262                                  57
          B1        IF(ZER)SKP  aB5                                 60
                    TRA       GEEUUP                                61
                    ABI       a1                                    62
          T7        FMP       NUM,U+T7                              63
                    FMP       #260                                  64
          -U        FAD       T7                                    65
                    FMP       DELSW                                 66
                    FAD       U                                     67
                    STO       TEMP2                                 70
                    CLA       #261                                  71
                    VDF       ONE                                   72
          -U        FAD       ONE                                   73
```

```
                    FMP         NUH                 74
                    FMP         DELSW               75
                    FDV         TWO                 76
                    FAD         TEMP2               77
                    STO         *262                100
                    SBI         a1                  101
               T4   FMP         *253                102
                    DMR         a1                  103
                    FAD         a2                  104
                    STO         TEMP2               105
                    CLA         *260                106
                    FMP         XAS                 107
               -U   FAD         ONE                 110
                    FMP         TEMP2               111
                    FAD         TWO                 112
               -U   STO         B3+B1               113
                    CLA         ONE,U+T7            114
               T7   FAD         ONE                 115
                    STO         B2+B1,B1+1          116
STAR           T7   FAD         ONE,U+T7            117
               T7   FAD         U                   120
                    FSB         ONE,U+T5            121
                    FSB         ONE,U+T6            122
                    VDF         T5                  123
                    FAD         *262                124
                    STO         B2+B1               125
               T6   FSB         ONE                 126
                    FDV         T6                  127
                    FSB         *262                130
                    STO         TEMP1               131
               T4   FMP         *253                132
                    STO         TEMP2               133
                    CLA         *260                134
                    FMP         XAS                 135
               -U   FAD         ONE                 136
                    FMP         TEMP2               137
                    FAD         TWO                 140
                    FDV         TEMP1               141
               -U   STO         B3+B1               142
                    CLA         B2+B1               143
                    FDV         TEMP1               144
                    STO         B2+B1               145
               B1   IF(ZER)SKP  EN                  146
                    TRA         STAR,B1+1           147
                    CLA         NUM                 150
                    FMP         DELSW               151
                    FAD         U,U+T4              152
                    CLA         *260                153
                    FMP         XAS                 154
               -U   FAD         ONE                 155
                    FMP*        T4                  156
                    FMP         B2+B1,U+T4          157
                    CLA         B2+B1               160
                    FAD         ONE,U+T5            161
                    CLA         B3+B1               162
                    FSB         T4                  163
                    FDV         T5                  164
                    STO         B3+B1               165
              -T4   FDV         T5                  166
```

```
                    STO     DEEN                    167
                    SBI     a1                      170
                    CLA     B2+B1,U+T4              171
                    CLA     B3+B1                   172
                -U  VDF     T4,U+T5                 173
                    STO     B2+B1,B1+1              174
ULOOP               CLA     B2+B1,U+T4              175
                    CLA     B3+B1                   176
                    FAD     T5,U+T6                 177
                -U  VDF     T4,U+T5                 200
                    STO     B2+B1                   201
                B1  IF(ZER)SKP  EN                  202
                    TRA     ULOOP,B1+1              203
                    CLA     DEEN,U+T4               204
                    FDV     T6,U+T4                 205
                    STO     *262,B1-1               206
PSI             T4  FMP     B2+B1                   207
                    STO     *262,U+T4               210
                B1  IF(ZER)SKP  a1                  211
                    TRA     PSI,B1-1                212
EXIT                TRA     (PF)                    213
ONE                 DEC     1.00000                 214
TWO                 DEC     2.00000                 215
XAS                 OCT     0                       216
TEMP2               OCT     0                       217
DUSW2               OCT     0                       220
DELSW               OCT     0                       221
NUM                 OCT     0                       222
BETA                OCT     0                       223
TEMP1               OCT     0                       224
EN                  OCT     0                       225
DEEN                OCT     0                       226
                    END                             227
                                                    230
```

The energy balance gives

$$\frac{1}{r}\frac{\partial}{\partial r}\left[rk_e\frac{\partial T}{\partial r}\right] = \rho C_p\frac{\partial T}{\partial t} \qquad \text{(A-38)}$$

with the boundary conditions

$$t \leq 0,\ T = T_M;\ r = 0,\ \frac{\partial T}{\partial r} = 0;\ r = R,\ -k_e\frac{\partial T}{\partial r} = h(T - T_o) \qquad \text{(A-39)}$$

If dimensionless quantities are defined as

$$\xi = \frac{r}{R};\ \theta = \frac{T - T_o}{T_M - T_o};\ \alpha_d = \frac{k_e}{\rho Cp};\ \tau = \frac{t\alpha}{R^2}, \qquad \text{(A-40)}$$

then the equation can be written

$$\frac{\partial^2\theta}{\partial\xi^2} + \frac{1}{\xi}\frac{\partial\theta}{\partial\xi} = \frac{\partial\theta}{\partial\tau} \qquad \text{(A-41)}$$

with the boundary conditions

$$\tau \leq 0,\ \theta = 1;\ \xi = 0,\ \frac{\partial\theta}{\partial\xi} = 0;\ \xi = 1,\ \theta = -\frac{1}{(Nu)_h}\frac{\partial\theta}{\partial\xi} \qquad \text{(A-42)}$$

The solution of this equation for constant α_d at $\xi = 0$ for various values of $(Nu)_h$ can be found in Schneider (42). From these curves, the thermal diffusivity α_d is calculated. Then, if the heat capacity and density of the cylinder are known, the thermal conductivity can be calculated.

Experimental evidence was necessary to show that the above theory applied to the heterogeneous pellets used in this work. However, assuming that this model was satisfactory, a method was further required to convert the thermal conductivity calculated in air to its corresponding value in a hydrogen atmosphere.

A model is chosen which relates the thermal conductivity of the heterogeneous solid to that of its solid and gas phase constituents and to the volume fraction of these constituents. Such models generally include empericisms which tailor the results to agree with experimentally measured values, wherein lies their value. The model chosen was suggested by Fulkerson (17).

In this model the gas phase is chosen as the continuous phase and the solid phase as the discontinuous phase. The effective thermal conductivity, k_e is expressed in the form

$$k_e = k_t(k_f,\ k_D,\ V_D) + k_c \qquad \text{(A-43)}$$

where

k_t = thermal conductivity contribution of the pellet particles

= (Godbee factor)(k_f)

k_c = thermal conductivity contribution due to particle contact

k_d = thermal conductivity of the discontinuous or solid phase

V_d = volume fraction of the discontinuous phase.

In this equation k_c is obtained from the difference between the measured values of k_e in air and k_t. Changing the gas affects only k_t.

The correlation developed by H. W. Godbee (18) is applied to values of k_f in the computation of k_t. Values of k_f are calculated from the expression developed by Schotte (43)

$$k_f = \frac{k_g}{1 + Z\left[\frac{2-a}{a}\right]\left[\frac{\gamma}{1+\gamma}\right]\left[\frac{T}{pdS^2(Pr)}\right]} \qquad \text{(A-44)}$$

where k_g = bulk phase thermal conductivity of the gas.

In media containing small pores, the thermal conductivity of a gas

is reduced as the pore diameter becomes comparable in size with the molecular mean free path. Another important phenomena occurring in small pores is the reaction between the solid and gaseous phases. The extent to which a molecule striking a surface comes into thermal equilibrium with the surface is given by a factor known as the accommodation coefficient, a. Its value is greater than zero and equal to or less than one, if equilibrium is achieved for all molecules striking the surface. Experimental values of the accommodation coefficient (14, 15, 19, 31) provide a means of estimating its value.

Godbee's correlation is based on a graphical relationship from which the ratio k_t/k_f can be obtained from a knowledge of the volume fraction of the discontinuous phase. If this ratio is multiplied by k_f as procured from equation (A-44), a value of k_t results which is then corrected by an emperical factor dependent on the fraction k_b/k_f.

APPENDIX B - EXPERIMENTAL EQUIPMENT

1. The Reactor System

a. The Reactor

Construction of the entire reactor was of 316 stainless steel. A 2.0 inch cross section for gas flow was provided in the reactor. The flanges shown in Fig. 3 on the top and bottom of the reactor were used to mount and gain access to the catalyst.

Connecting the reactor to the rest of the system were two conical sections, eight inches in length, used for expansion and contraction. The large end of each cone was fitted with a flange to connect it to the reactor. On the small end the cones were connected to 1/2 inch stainless steel tubing.

The catalyst and blank were mounted parallel to each other, as shown in Fig. 3 and compressed axially between the top flange on the reactor and a mounting plate. A rod attached to the center of the top flange was threaded on the free end, making it possible to secure the mounting plate by means of a retaining nut.

Each pellet was drilled axially before the cylinders were assembled and the annulus served to house a combination thermocouple-micromanometer. Copper-constantan thermocouples were snug-fit at the center of each cylinder. When the constantan ends were enjoined a direct reading of the centerline temperature differential was available. The copper portion of the thermocouple was a 0.023 inch O.D. by 0.011 inch I.D. capillary tube of thermocouple grade copper. A notch in each capillary tube next to the thermocouple junction served as a pressure tap. Both

cylinder ends were sealed with epoxy. The capillary tubes were connected to a red oil manometer which was read with a cathetometer.

A thermocouple, positioned upstream of the catalyst, measured the bulk phase temperature of the circulating gas mixture. Downstream of the catalyst cylinders was a pitot tube connected to an inclined manometer. Pressure drops recorded for each run were converted to gas velocities as shown in Appendix K.

The bulk phase temperature and the centerline temperature differential were measured through use of a Leeds and Northrup Model 8686 potentiometer.

b. Temperature Control System

The temperature bath was constructed in the following manner. An inner liner of 18 gauge stainless steel was formed into a cylinder 17 inches in length and 10-3/4 inches O.D. One end of the cylinder was closed. A similiar vessel 18-1/2 inches long and 14-3/4 inches I.D. served as the outer shell of the bath. The space between the inner and outer shells was lined with a two inch thickness of Johns-Manville thermobestos insulation. The top of the bath was a 17-1/2 inch circular plate of 304 stainless steel which rested on the inner shell separated from it by a rubber gasket. Four bolts through slotted pieces of angle iron welded to the outside of the exterior shell compressed the top onto the bath.

Mineral oil was used throughout as the bath fluid, as the temperature of the system was only varied between the limits of 20°C and 60°C.

To control the system at an equilibrium temperature during the runs, both a heater and a refrigeration unit were required.

Refrigeration was supplied continuously by a Tecumseh Air-Cooled

Condensing unit, Model C4414HTK, with a rating of 1/4 hp which employed Freon 12 as the refrigerant. A Detroit Model 905-c-50 expansion valve was used preceeding 50 feet of flow through a 3/8 inch O.D. copper tubing coiled in the temperature bath.

To supply heat to the system and maintain the bath temperature at a given level, a 500 watt immersion heater was used.

The final temperature control was attained through the use of a Thermotrol, Model No. 1053-A equipped with a nickel resistance thermometer bulb Model 1060-A, both of which were manufactured by the Hallikainen Instrument Co. The 500 watt heater was connected to the Thermotrol so that its operation was governed by the Thermotrol. The bath temperature was adjusted to maintain a constant bulk phase temperature of the gas as measured in the reactor. Control was maintained to within $\pm 0.5^{\circ}C$ with only minor adjustments to the Thermotrol necessary during the runs.

To insure a uniform bath temperature, the bath fluid was constantly circulated by means of a motor driven stirrer mounted on a 3/8 inch shaft. The two inch propeller was located about one inch from the bottom of the bath.

The heat transfer area of the system was provided by a 20 foot length of 1/2 inch O.D. aluminum tubing coiled in the temperature bath.

c. The Gas Circulation Pump

Gases were circulated about the system by means of a single-stage, double-acting diaphram type, positive displacement pump shown in Fig. 4. The pump chambers were constructed of aluminum and mounted on an angle iron frame. Each chamber consisted of a head plate, a spacer and an end plate. The diaphrams were of neoprene rubber. They were attached

to the plunger by means of a retainer plate. A shaft guide mounted to the end plate aligned the plunger and its shaft with the pump chamber. The chambers were synchronized with each other by means of a link rod connecting the plunger shafts.

The pump was driven by a 3 hp Dayton Motor, Model No. 2N860-B with the motor speed reduced to 267.4 rpm through the use of a Boston Gear Reducer, Model No. H1350.

A connecting rod fitted with roller bearings at both ends coupled the gear reducer and one of the plunger shafts. The plunger displacement was fixed at one inch by means of an offset connector between the connecting rod and the gear reducer. This particular combination of stroke length and pump speed led to a design capacity of just under 15 cfm.

The intake and exhaust ports of the pump were equipped with spring loaded check valves which had been designed especially for this pump to minimize the amount of dead volume involved. One intake and one exhaust valve were mounted on each head plate.

The pump was equipped with a valve regulated bypass line as shown in Fig. 2. In most runs the opening of the bypass valve was the same. One-half inch stainless steel Rockwood Ball Valves, Model 204, were located on the intake and discharge lines of the pump so that the pump could be separated from the system.

The pump was not capable of maintaining a high vacuum. This required that precautions be taken during operation to prevent a vacuum from forming in the chambers. Preliminary tests showed that operation at pressures slightly greater than atmospheric was sufficient to prevent pump starvation. However, since the system was charged by an evacation

technique, a small amount of air was present in each run.

d. The Drying System

Water made during the runs was collected on silica gel in two driers mounted in parallel as shown in Fig. 2. Flow was directed through one of the driers during the transient stage of equipment startup. To begin the steady state run, flow was switched to the second drier which had been previously weighed. At the conclusion of a run the drier was again weighed. The amount of water accumulated during the run furnished a direct measure of the reaction rate for that run.

The driers were cylindrical tubes two inches in diameter and six inches long. Each was fitted at one end with a screw-on cap which was sealed with a neoprene gasket. Aluminum was used as the material of construction in order to keep the total weight to a minimum.

At each end of the cylinders a pair of 1/2 inch stainless steel Rockwood Ball Valves, Model 204, were set in series. The valves nearest the cylinders were used to close off the ends of the drying chambers, while those farthest from the cylinders were to isolate the cylinders from the remaining part of the system whenever the cylinders were to be removed from the system.

A provision was made to evacuate only the dead volume located between the pairs of valves, as well as the entire system. For all purposes throughout the reactor system the vacuum was provided by a Welch Duo Seal Vacuum Pump, Series No. 1405-6.

The cylinders were removed from the system through the use of standard 1/2 inch Swagelok fittings.

Weighings were made on a Model 106 August Sauter Heavy Duty

Analytical Balance with 10 kilogram capacity. The sensitivity of the balance as determined in this laboratory was approximately eight milligrams per scale division. The manufacturer quotes the balance as reproducible within $\pm 1/4$ scale division, so that weighings could be taken to be accurate within ± 2 milligrams.

Since an absolute mass measurement of the cylinders was unecessary, a tare weight of 2300 grams was used in conjunction with a small analytical weight set. The five swing rest point determination method was employed for all weighings.

e. The Pressure Control System

Due to the non-equimolarity of the reaction, the system pressure dropped as the reaction proceeded. Since the reacting gases removed water stoichiometrically, they were replaced by a water electrolysis technique in order to maintain a constant pressure.

A one quart capacity glass jar sealed with a neoprene stopper served as an electrolysis cell. One inch square platinum electrodes were used in distilled water whose conductivity was enhanced by the addition of about 33% sulfuric acid.

Power was supplied to the cell by means of a d.c. power supply built in this laboratory. A schematic diagram of the electrical network is presented in Fig. 5. Two levels of current were made available to the cell through the utilization of both output voltage levels available on a powerstat. The levels were adjusted by the powerstat setting to make the pressure of the system increase at the high current level and decrease at the lower level. The adoption of the high or low level of cell current was controlled by a relay operated by a mercury-nichrome

sensing switch located in a mercury manometer equipped with a 10 micron snubber to dampen oscillations. The manometer was of the open end U-tube type and was used to measure the system pressure. When the pressure of the system decreased, contact was broken in the sensing switch and the high level of current passed through the cell. When the mercury-nichrome contact in the manometer was reestablished, the low level of current prevailed.

Vapors from the electrolysis cell passed through a two stage drying chain before entering the main circulating system. The driers were of the same construction as those used in the drying system described in the previous section.

The first drier contained Ascarite* which is a highly basic compound used to remove any sulfuric acid that carried over as well as water vapor. A second drier containing silica gel was used to insure the delivery of dry gases to the system. The gases were injected into the circulating system at the intake of the pump to provide maximum mixing.

f. The Gas Injection System

Four gas mixtures were prepared. They nominally contained one, two, three and four percent oxygen in hydrogen. The cylinders were initially charged to approximately four atmospheres pressure. These gases were introduced by expansion into a previously evacuated system.

Facilities were available to inject the gas mixtures, hydrogen or oxygen into the system. The hydrogen and the hydrogen rich mixtures used a common manifold, and the oxygen was separately introduced. The valves used for control of the injections were Whitey Valves, Model

*Registered Trademark

No. 1KS4, featuring Kel-F* stem tips.

The hydrogen and oxygen was let down from the high pressure cylinders through the use of Victor pressure regulators. Any oxygen in the pure hydrogen was catalytically removed by means of a series of three Engelhard Deoxo Hydrogen Purifiers. Silica gel drying tubes were used to remove water vapor from any gases being introduced into the system.

g. The Gas Sampling System

A 250 cc sample of the system gas was collected for analysis at the close of each run. A tee located between the two ball valves on the discharge side of the steady state drying chamber served as a sample port.

A 250 cc glass gas holder with stopcock valves was suitable as a sample bomb. It was attached on one end to the system vacuum source and on the other end to the system through the use of tubing and clamps. A 1KS4 Whitey Valve which served to keep the system closed during the run separated the sample bomb and the tee.

The sample was collected by expansion into the sample bomb which had previously been evacuated to 20 microns or less absolute pressure. Precautions were taken to exclude gases in the vapor line from the electrolysis cell which were oxygen rich. Gases in the pump were also excluded from the sample.

2. The Gas Analysis System

The samples of gas from each run were analyzed for oxygen, hydrogen and nitrogen on a Beckman GC-2 gas chromatograph. Complete

*Registered Trademark

details of this unit are available elsewhere (2). (See Fig. 18.)

A 10 foot, 1/4 inch O.D. stainless steel tube was used as a chromatographic column. The packing used was molecular sieve, type 13X. Screened 50-60 mesh material which had been roasted at 400°C for six hours was packed into the column. The column was further baken out in the system by purging with helium carrier gas at 150°C for 24 hours. This insured the removal of moisture from the column.

The chromatographic unit was equipped with a flow regulation system, a gas sampling valve, a thermal conductivity detector cell and a temperature bath which housed both the column and the cell. Carrier gas flow was split into two equal parts in the flow regulation system where capillary tubes restricted the flow to the desired rate. One part being preheated in the temperature bath en route, passed directly into the reference side of the detector cell. The other portion flowed first through the sample valve where the sample was injected and then through the column before passing through the sensing side of the detector cell. The gas flow rate was measured through the use of a soap film bubble meter affixed to the effluent of the sample side on the detector cell. Both sides of the detector were maintained at one atmosphere pressure at all times. The temperature bath was kept at 100°C for all measurements.

Helium was used as the carrier gas for the entire program, and its flow to the thermal conductivity cell was never interrupted. A helium flow rate of approximately 15 cc/min was maintained by adjusting the pressure regulator until the pressure gauge on the unit read 10.0 psig. The helium was taken from a high pressure cylinder fitted with a Victor pressure regulator. A silica gel drier was inserted in the helium line

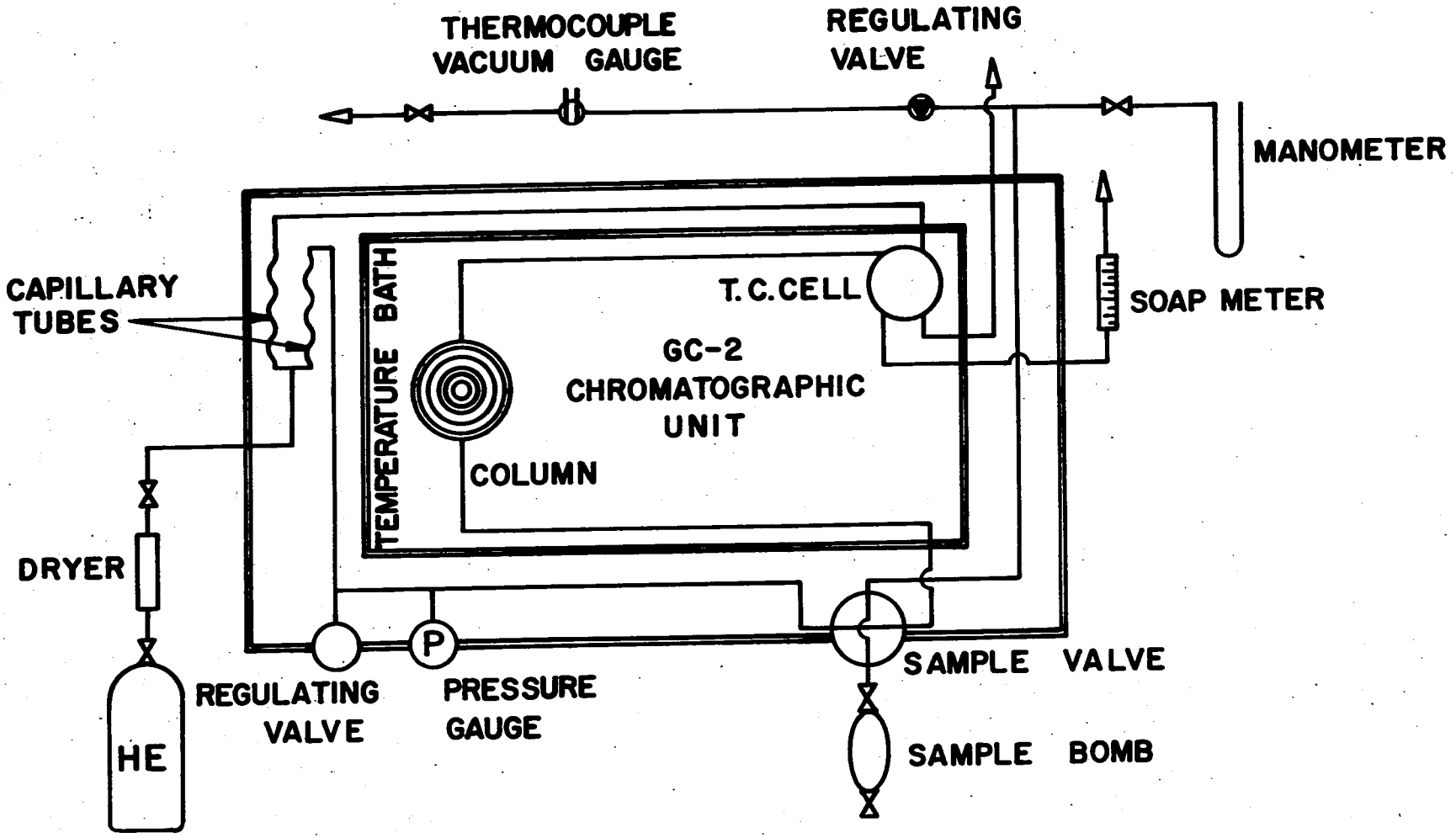

FIG. 18—SCHEMATIC OF GAS ANALYSIS SYSTEM

to prevent water vapor from contaminating the molecular seive.

The samples were introduced from the sample bomb to the sample valve by means of a nozzle located on the front of the GC-2 for that purpose. A rubber hose and clamps were used to link the bomb and the nozzle. The gas sample valve was of the dual position variety. With the valve in either position, one of the two sample loops was in the system. Meanwhile, the other sample line could be made ready with the next sample. Both sample lines were made of 1/8 inch stainless steel tubing which was 0.069 inches I.D. The volumes were adjusted to 1/4 cc by measuring the lengths with a micrometer.

The thermal conductivity cell was comprised of two pairs of filaments mounted in a stainless steel body. One pair served as the sample or sensing side while the other pair was the reference side. Heat was supplied to the filaments by a current which was manually adjusted. The filaments were arranged in a standard thermal conductivity cell bridge circuit which converted temperature changes in the sensing filaments to a voltage differential across the bridge. Temperature changes were due to varying amounts of heat being removed from the sensing filaments by gases of differing thermal conductivities flowing over them. The voltage differential was applied across an attenuator before being applied to the recorder.

The recorder was a Texas Instruments servo/riter* Integrating Recorder, Model PWS, with a 0-5 millevolt range. The span of the recorder was 10 inches, and the span step response time was 0.5 seconds. A chart speed of 0.75 in/min was used throughout.

*Registered Trademark

The design of the gas sampling valve permitted admission of the gas samples by a means of a vacuum technique. A vacuum system was connected to the exhaust line on the sample valve. A Welch Duo Seal Vacuum Pump, Model No. 1402 furnished the vacuum. The vacuum was measured prior to sample injection at 15 microns or less on a Veeco Thermocouple Vacuum Gauge, Type RG-3A. A regulating valve was used to arrest the vacuum system in order to introduce the sample. Once the sample was roughly inserted the system pressure was then adjusted with this valve. The sample pressure was measured before and after the sample was introduced to the sample loop by means of a U-tube mercury manometer read with a cathetometer.

3. The Thermal Diffusivity Apparatus

The value of the effective thermal conductivity, k_e, of the pellets in hydrogen gas was determined from the thermal diffusivity which was measured in air. These experiments were carried out on equipment described by Park (30) and modified for this work.

Samples of catalyst for these experiments were of the same structure as those described earlier. In this case four pellets rather than five were fastened end to end after being drilled axially. Standard Leeds and Northrup 24 B & S gauge copper-constantan thermocouple wire was used for the thermocouple which was located at the geometric center of the sample. Two types of samples were used; 0.05% Pt on alumina and an alumina support.

The sample for test was mounted in a holder which could be moved back and forth between heating and cooling chambers. Pills heated to a steady state temperature in the heating chamber were injected quickly

into the cooling chamber. Cooling curves were obtained by recording the variance of the centerline temperature with time.

The equipment used consisted primarily of a speciman holder for the catalyst sample, heating and cooling chambers and recording equipment for the temperature response measurements. The major equipment change from that described by Park (30) was the use of a Spencer Gas Booster with a 50 cfm capacity to increase the turbulence in the cooling chamber. Other modifications were minor, consisting largely of remodeling equipment used by Park.

The samples were mounted perpendicular to two teflon disks which were machined to fit tightly into an 18 inch length of 1-1/2 inch aluminum tubing. The tubing served as the sample holder which could be switched back and forth between the heating and cooling chambers. The samples sat in a section of the aluminum tubing which had been milled away leaving only three strips of metal as supports. One teflon end disk was held in place by set screws, the other by means of an externally operated screw mechanism.

The thermocouple wire was threaded through one of the teflon disks, the catalyst pellet and the other teflon disk before being reversed through the teflon disks and a teflon spacer between the disks. Both thermocouple leads were insulated with teflon spagetti.

The cooling chamber was a four foot section of two inch steel pipe. A hole at the approximate center of the length allowed the sample holder to slide into the cooling chamber. Room air was blown through the pipe by the gas booster.

The heating chamber was a four inch length of two inch pipe fitted

with inlet and outlet lines for the hot air. The two inch pipe was welded at a right angle onto the cooling chamber. The ends of the chamber were fit snuggly around the sample holder through the use of brass bushings. This physical structure accorded the rapid transfer of the speciman from the heating to the cooling chamber.

Hot air was supplied to the heating chamber by means of an electric heat gun. The temperature in the chamber was controlled by a Powerstat transformer which allowed coverage of the 20-100°C temperature range. A thermocouple probe was used to measure the temperature of the heating chamber. Various locations in the chamber were checked to assure the absence of thermal gradients. This temperature was also matched with the centerline temperature of the sample. The temperatures were measured on a Leeds and Northrup Potentiometer, Model 8686.

The time response of the centerline temperature was measured on a 0-1 millevolt Texas Instruments servo/riter Recorder, Model PWS. The recorder had a 10 inch span and a 0.5 second span sweep response time. The chart speed used was 2 in/min.

Air velocities in the cooling chamber were measured with a Taylor Anemometer, No. 14423.

4. The Diffusivity Apparatus

The method adopted to measure the diffusivity is similar to that used by several authors (22, 54, 58, 60). In this method different gases are circulated past the ends of a catalyst pellet arranged in a compartment which prevents leakage of the gases around the catalyst, thus allowing mixing of the gases to occur only by diffusion through the pellet. Gas flow rates are measured, and samples of the gas are analyzed

to determine the necessary gas fluxes.

The apparatus was comprised of a compartment to house the sample, a bubble meter for flow measurement, and a manometer to balance the pressure on both sides of the sample. The gas samples were analyzed on the Beckman GC-2 gas chromatograph described earlier. The equipment is diagrammed schematically in Fig. 7.

The samples for this work were cylindrical alumina pellets, 3/8 inch x 3/8 inch O.D. from the same lot as those used for the other work described here. A rubber stopper with a 3/8 inch hole centered on its axis served as a holder for the sample speciman. The stopper was mounted into a brass mandril beveled to match the taper of the stopper. The mandril was fitted on the narrow end into a cylindrical lucite support fitted with a neoprene O-ring which served as a seal between the two pieces. The rubber stopper at the wide end of the mandril was mounted against a cylindrical brass support with a lip around its circumference to seal against the stopper. An anchored C-clamp was used to compress the three piece ensamble and form the seals. This also squeezed the rubber stopper into the mandril and prevented gas seepage around the sample.

Both the brass and lucite supports had inlet and outlet lines for gases which opened into the 3/8 inch hole in the rubber stopper. An in-line moving film bubble meter provided a method of measuring the flow rate of hydrogen prior to its inlet to the brass support. Samples of the exhaust gas from the brass support were captured by passing this gas through a 250 cc glass gas holder with stopcock valves at each end. Pure oxygen gas passed through the lucite. Its flow rate was regulated

to balance the pressure on both sides of the porous pellet which were linked by a red oil manometer.

Gases were supplied from high pressure cylinders. Victor pressure regulators were used to reduce the gas pressure. The hydrogen flow was controlled by a model 2S Nupro metering valve. An Engelhard Deoxo Hydrogen Purifier converted any oxygen in the hydrogen to water. A silica gel drier installed after the in-line bubble meter removed the moisture from this gas.

APPENDIX C - EXPERIMENTAL PROCEDURES

1. The Reactor System

Since the reactor system was of necessity a closed unit, frequent pressure tests were required. An accepted pressure test was one in which no manometer changes were detectable over a minimum period of two hours. The tests were conducted with hydrogen gas at 6 psig prior to each run. This pressure exceeded any pressure developed in the system during a run. Any leaks which were detected were repaired until a satisfactory pressure test resulted.

Prior to beginning each isotherm a rough temperature adjustment was made on the thermotrol unit. For the high temperature isotherms, the amount of refrigeration was also reduced. Final adjustment was deferred until starting the first run of the isotherm.

Freshly dried silica gel was used to replace that in the system minimally before every other run. The silica gel was prepared by drying under vacuum overnight at 150°C. Several runs were ruined because the drying agent was not dried under vacuum and the silica gel became saturated while in use. The ascarite was replaced at the same time as was the silica gel.

Following the pressure test, the drying cylinder for the steady state portion of the run was weighed. The weighing was made with the cylinder charged with hydrogen to the approximate run pressure.

With the drying chamber re-installed, the entire system with the exception of the electrolysis cell was evacuated. Since the pump could

not withstand a high vacuum, it was only partially evacuated by rapidly opening and closing one of the ball valves separating it from the rest of the system. The entire system was then charged with the proper gas mixture by overpressuring the remainder of the system before expanding the gases into the pump. The system was then again evacuated and recharged. On this occasion with the electrolysis cell open to the system, the desired static pressure was fixed, and the pump by-pass valve was completely opened.

After proper valve alignment to direct flow through the transient drying chamber and activation of the electrolysis cell, the pump was turned on to start a run. The nichrome contact on the manometer was set to the desired pressure, and as the system pressure increased due to the gas generated by the electrolysis cell, the pump by-pass valve was gradually closed, circulating more of the gases through the reactor. In this manner, the by-pass valve and the pressure settings were achieved.

Temperature equilibrium was generally achieved from three-quarters of an hour to an hour after the pump was turned on. Minor adjustments were made as necessary to maintain the reactor temperature to within $\pm 0.5^{\circ}C$. For the initial run of each isotherm the temperature had to be adjusted by means of the thermotrol.

When no changes in the bulk phase temperature and the centerline temperature differential had occurred for five minutes, the drying cylinders were changed and the run begun.

The only changes made to the system during the steady state portion were to the thermotrol as described above. Measurements were recorded at frequent intervals of the bulk phase temperature, centerline

temperature and pressure differentials, pressure at the pump intake and pitot tube flow pressure. Most runs were terminated after an hour, but this was not a fixed policy. During the last five minutes of each run, the sample bomb was evacuated.

To end a run the pump was shut down; the electrolysis cell de-energized; and the static pressure of the system was measured. This value was used for computational purposes. Before taking the sample, the section of the system from below the sample line to the discharge of the pump was removed from the system. This excluded from the sample the line connecting the electrolysis cell and the circulating system. Finally, the cylinder to be weighed was valved off from the rest of the system and removed.

2. The Gas Analysis System

Prior to sample analysis, the chromatograph and recorder had to be warmed up. Therefore, a few hours before analyzing this equipment was activated. Improper warmup led to a zero drift in the recorder.

When a sample bomb was fitted into position, the system vacuum pressure was read on the cathetometer. The vacuum was then cut off, and a sample admitted. When the sample pressure had been adjusted to approximately 40 cm absolute (20 cm as measured on one side of the manometer), the sample was injected into the column and the exact pressure read. The vacuum system was then opened to prepare the next sample.

The total elution time for a three component sample was about 12 minutes. Hydrogen was the first gas to come out at about 4.5 minutes after injection. Oxygen and nitrogen followed in that order. There was

a highly satisfactory signal zero between peaks.

Leakage in the system usually occurred at the gas sampling valve and was detectable on the thermocouple gauge. Replacing the grease seal on the valve corrected these leaks. As a further test for leaks, the vacuum system was periodically shut off. After waiting 1.5 minutes with the valve closed, the false sample was injected into the column. This time lapse represented a longer period than was necessary to inject a normal sample. No integrator disturbances were ever detected on the recorder in this fashion.

From three to five samples were run from each sample bomb, depending primarily upon the temperment of the recorder.

The chromatographic column was calibrated for oxygen and nitrogen. A pure component method was used for the calibrations. Samples of the pure gases at varying measured pressures were injected into the column. Resulting plots of curve area versus component pressure served as calibration curves. In a sample analysis the area of a given peak was used to find the partial pressure of the component from the calibration curve.

Hydrogen determinations were effected by difference. The oxygen and nitrogen partial pressures were subtracted from the total sample pressure, and the difference was assumed to be the partial pressure of hydrogen.

3. The Thermal Diffusivity Apparatus

A sample was mounted into the holder and located in the heating chamber. Preliminary work showed that a particular position of the holder in the heating chamber gave an even temperature distribution

throughout the chamber. This position utilized the aluminum support strips of the holder as baffles for the heated air.

The samples were heated until steady state was reached as indicated by the recorder. The absence of radial gradients was assured by comparison of the ambient and centerline temperatures before inserting the sample holder into the cooling chamber.

Time zero was taken as the moment of insertion of the sample into the cooling chamber. Time temperature plots were recorded for each run. Approximately five minutes were required for the centerline temperature to arrive at its new steady state at which time the run was terminated.

The air velocity in the cooling chamber was measured after all runs were completed. An average value of 45.5 ft/sec was assessed.

4. The Diffusivity Apparatus

Gases were admitted to each side of the catalyst pellet. First, the hydrogen flow was adjusted with the regulating valve, then the manometer pressure was balanced by adjusting the oxygen flow. Preliminary tests showed that equilibrium was reached in the cell within ten minutes. In these tests the effluent from both sides of the diffusivity cell passed through a thermal conductivity cell where steady state was detected by the leveling off of the recorded voltage.

Based on this information the time for each run was set at ten minutes plus the time necessary to allow five volume changeovers in the sample bomb.

The samples were analyzed on the gas chromatography unit used throughout this project.

APPENDIX D - MATERIALS

Catalyst

The catalyst was supplied through the courtesy of Engelhard Industries, Incorporated. Platinum was deposited on finely divided alumina particles in two amounts, 0.05% and 0.3% by weight. The material was then separately pelletized. Several pellets of the alumina support material were also donated by Engelhard. Only the 0.05% material was used for reaction purposes.

Hydrogen

Big Three Welding Co.; prepurified grade; stated purity of 99.91%; Impurities; 15 ppm oxygen, 30 ppm hydrocarbons, 810 ppm nitrogen.

Oxygen

Big Three Welding Co.; stated purity of 99.70%; Impurities; 0.25% argon, 0.05% nitrogen, 25 ppm methane, < 0.1% ethane, < 5 ppm water.

Nitrogen

Big Three Welding Co.; prepurified grade; stated purity 99.998%.

Helium

Big Three Welding Co.; stated purity 99.99%.

Silica Gel

Davidson Chemical Co.; Grade 40; 6 to 12 mesh size.

Ascarite

Arthur H. Thomas Co.; 8 to 20 mesh; purchased from W. H. Curtin Co.

Water

Walker's Distilled Water Co.

Sulfuric Acid

J. T. Baker Chemical Co.; specific gravity—1.84; purchased from W. H. Curtin Co.

APPENDIX E - EXPERIMENTAL DIFFICULTIES

The major difficulty encountered was in purchasing a satisfactory gas circulation pump which would deliver approximately 10 cfm at 5 psig which were the requirements of this system. Pumps with this combination of capacity and pressure rating were commercially uncommon. Several models of vane type positive displacement pumps were available, one of which was tried in the system. An attempt was also made to use a 15,000 rpm blower in the system. Both of these ventures failed because of gas leakage at the pump shaft seals.

Very few diaphram pumps were available commercially. Those that were adequate were prohibitive for reasons of cost or delivery time. Thus, the pump was designed and built here.

Inconsistancies were noticable in the early runs made with the circulation pump. It appeared as though the pump delivery was inconsistant, and the fault was found in one of the check valves. The springs on the exhaust valves were held in place by a back-up plate threaded to the valve body. One of the back-up plates worked its way loose during operation until there was no spring compression in the valve. This was corrected with a retainer threaded in series with the back-up plate.

Several runs were lost at one point due to the silica gel driers becoming saturated during the process of a run. This was corrected by drying the silica gel under vacuum rather than at atmospheric pressure.

Measurement of the system velocity was another experimental problem. The snubber damped flowmeter provided a reasonable relative pressure drop

from run to run, but pitot tubes are not accurate in pulsating systems. Thus, an absolute system velocity measurement was made with the pump intake open to the atmosphere. The velocity was measured with an anemometer at the exhaust flange of the reactor. The pump bypass valve was opened to its usual setting during this measurement. This method is admittedly questionable, but the measured velocity was consistant with design specifications, and subsequent calculations are somewhat insensitive to velocity changes. A correlation between the pressure drop and gas density at the known valve setting was used to calculate new velocities for other valve settings.

APPENDIX F - TEMPERATURE DEPENDANCE OF THE DIFFUSIVITY

If it is assumed that the effective diffusivity is influenced by temperature changes in the same way as binary diffusivities, then Bird's equation (4) can be modified to give

$$D_{AB} = \delta D_{AB}^{EFF} = 1.858(10^{-3})\sqrt{\frac{T^3\left(\frac{1}{M_A} + \frac{1}{M_B}\right)}{p\sigma_{AB}^2\Omega_{D_{AB}}}} \qquad \text{(F-1)}$$

This equation was used to calculate δ as well as the effect of temperature of the value of the diffusivity. The temperature, pressure, and average D_{AB}^{EFF} given in Table 9 were used to compute δ. Several values of $D_{AB}^{EFF}(T)$ are given in Table 11 for p = 1.15 atm which was the approximate reactor pressure.

Over the range of isotherms examined, this could lead to an error of ± 10%. The maximum ΔT for any run was approximately 30°C leading to a diffusivity which may be as much as 25% low.

It is evident that the assumption of a diffusivity independent of temperature is not a good one. The diffusivity should be incorporated as a function of temperature in further work.

APPENDIX G

THERMAL DIFFUSION AND PELLET PROFILE CURVES

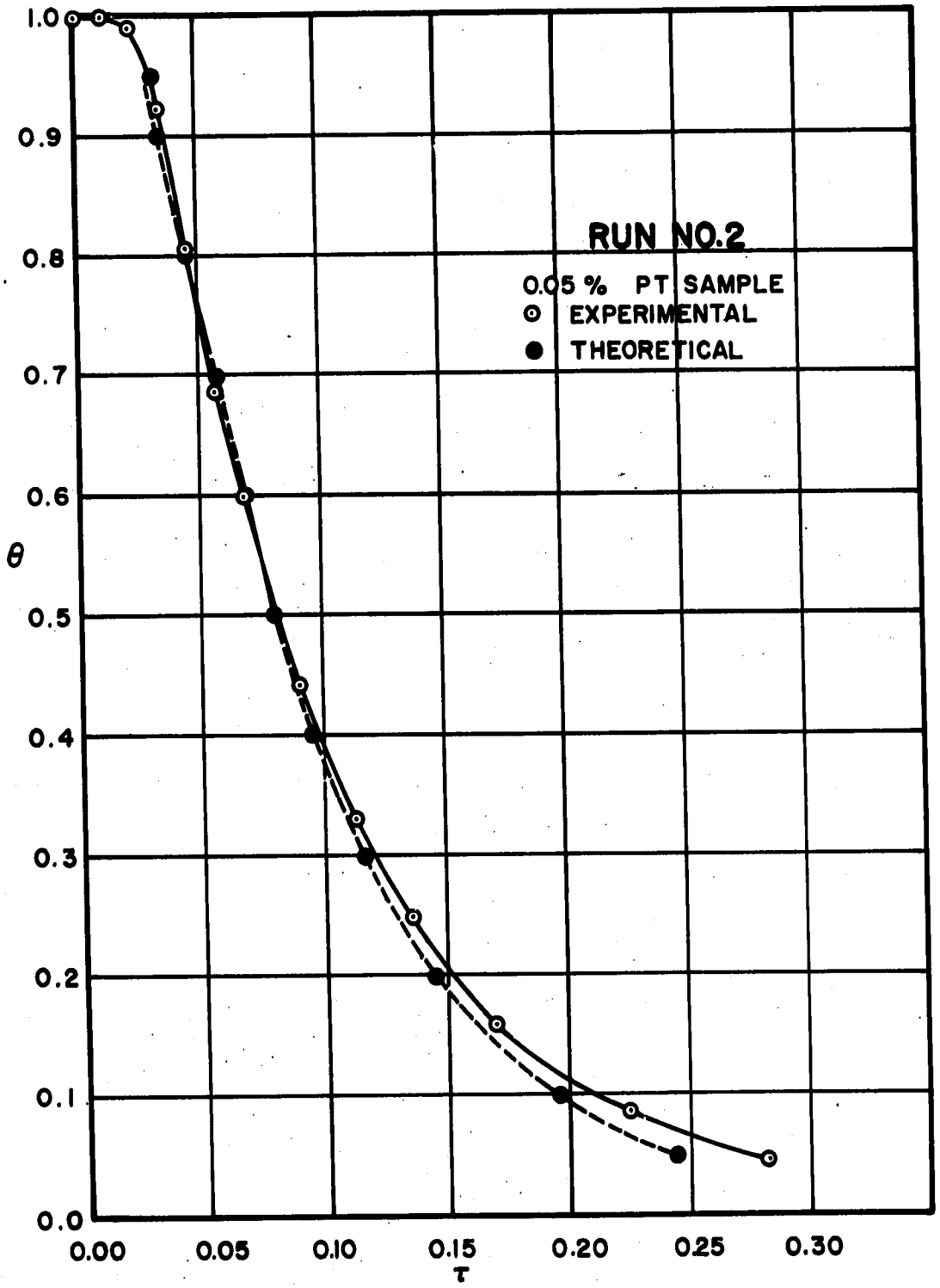

FIG 19- DIMENSIONLESS CENTERLINE TEMPERATURE TIME CURVES FOR HEAT LOSS FROM A CYLINDER

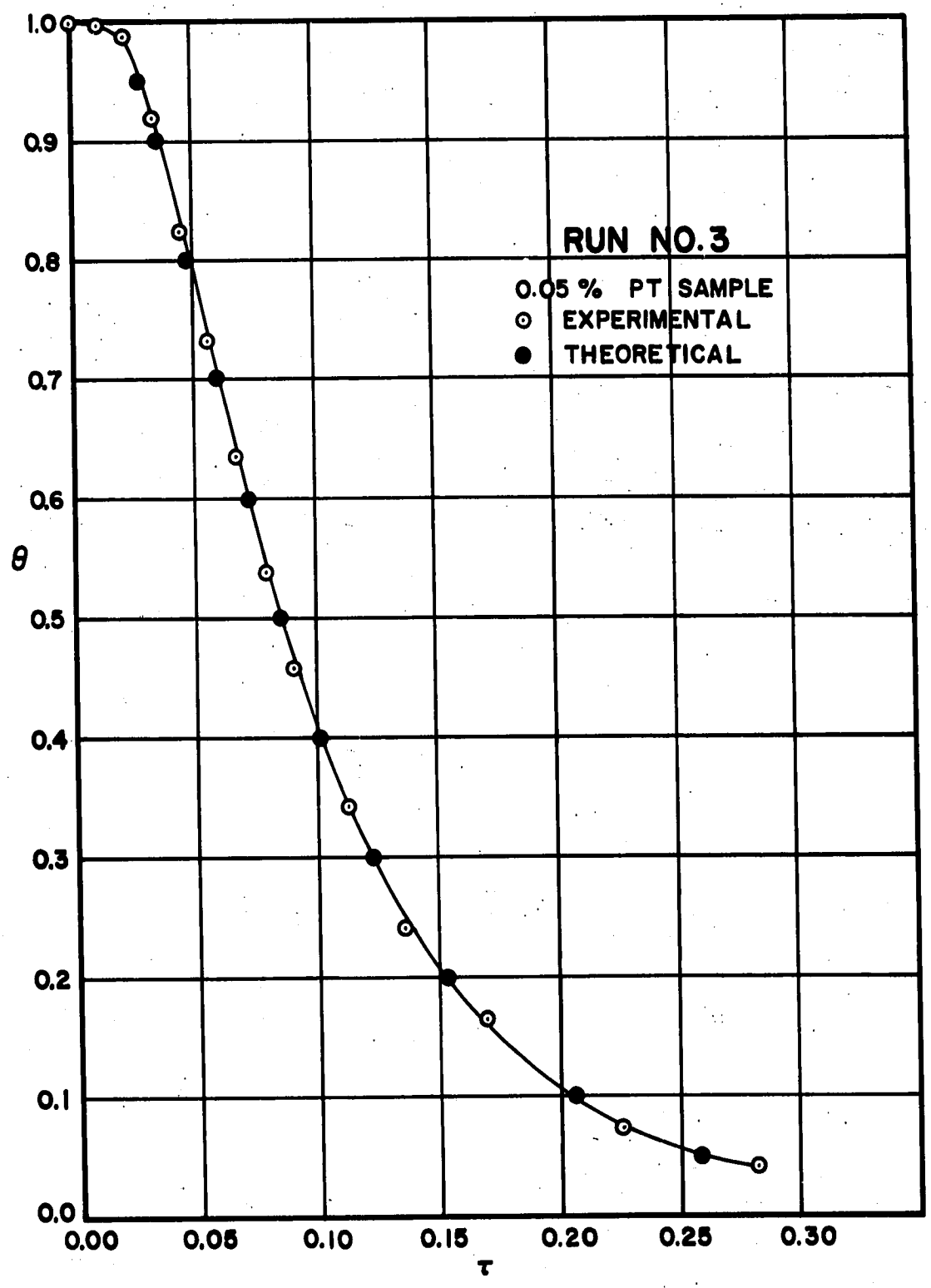

FIG 20-DIMENSIONLESS CENTERLINE TEMPERATURE-TIME CURVES FOR HEAT LOSS FROM A CYLINDER

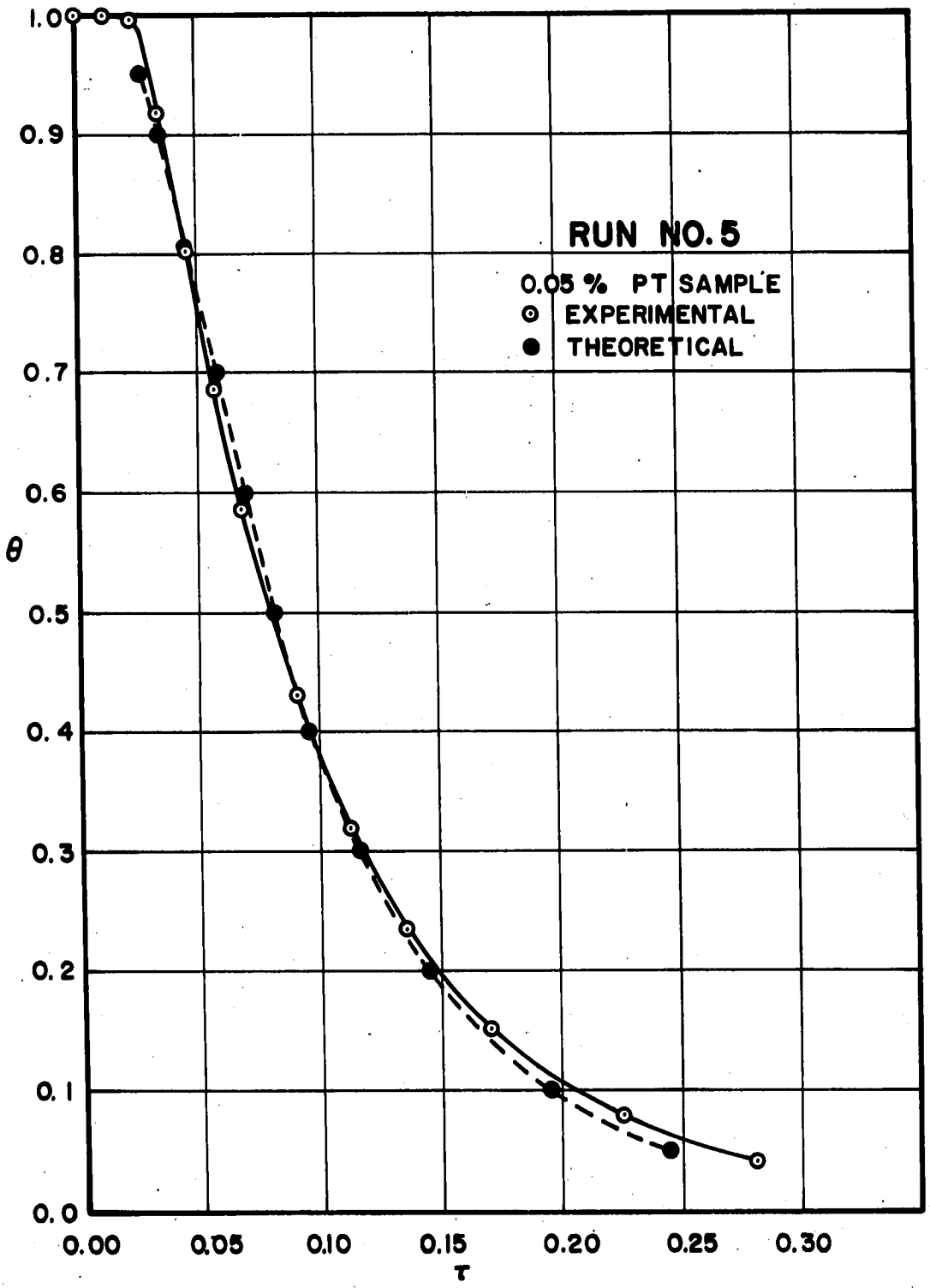

FIG 21- DIMENSIONLESS CENTERLINE TEMPERATURE TIME CURVES FOR HEAT LOSS FROM A CYLINDER

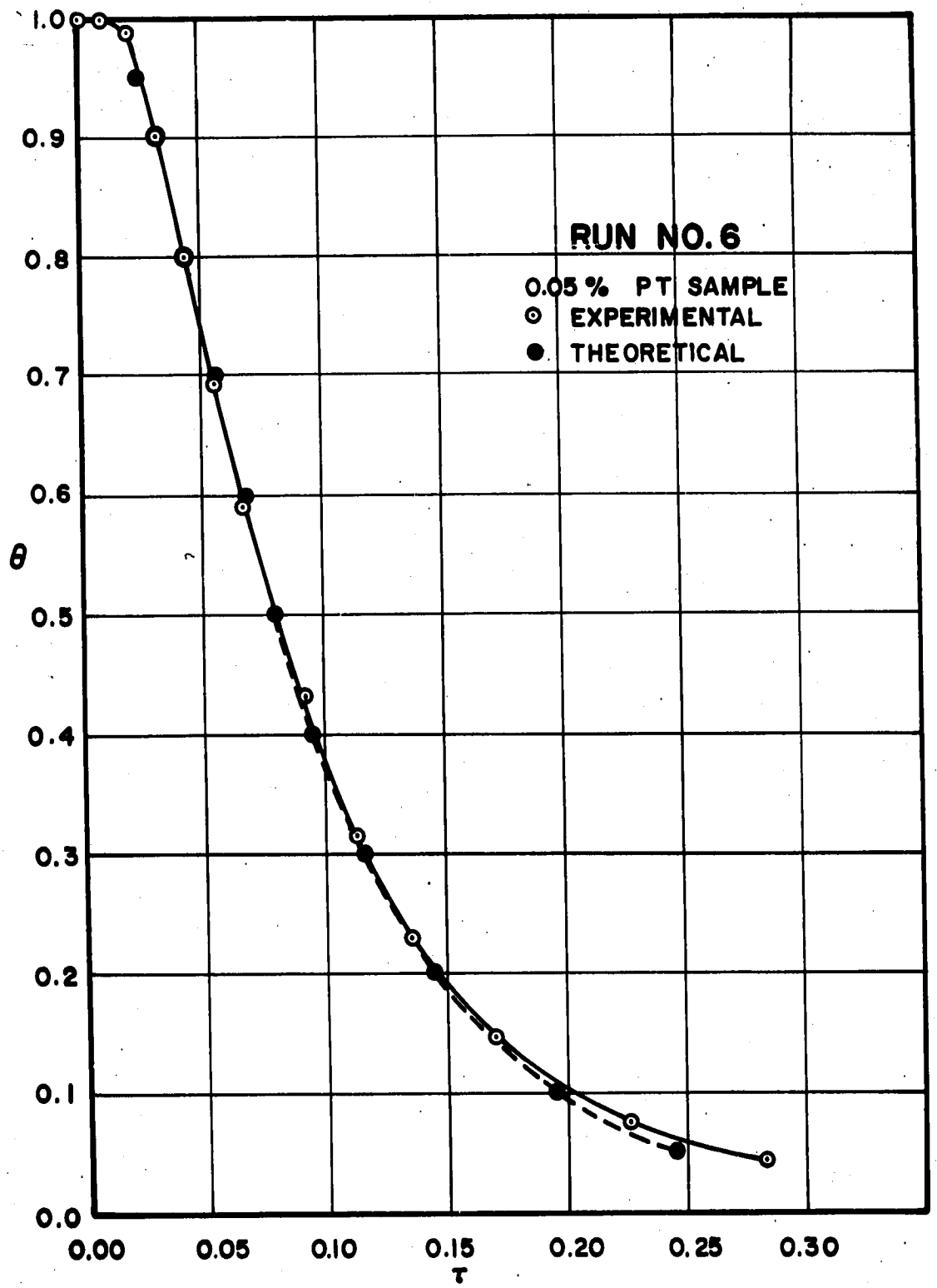

FIG 22-DIMENSIONLESS CENTERLINE TEMPERATURE TIME CURVES FOR HEAT LOSS FROM A CYLINDER

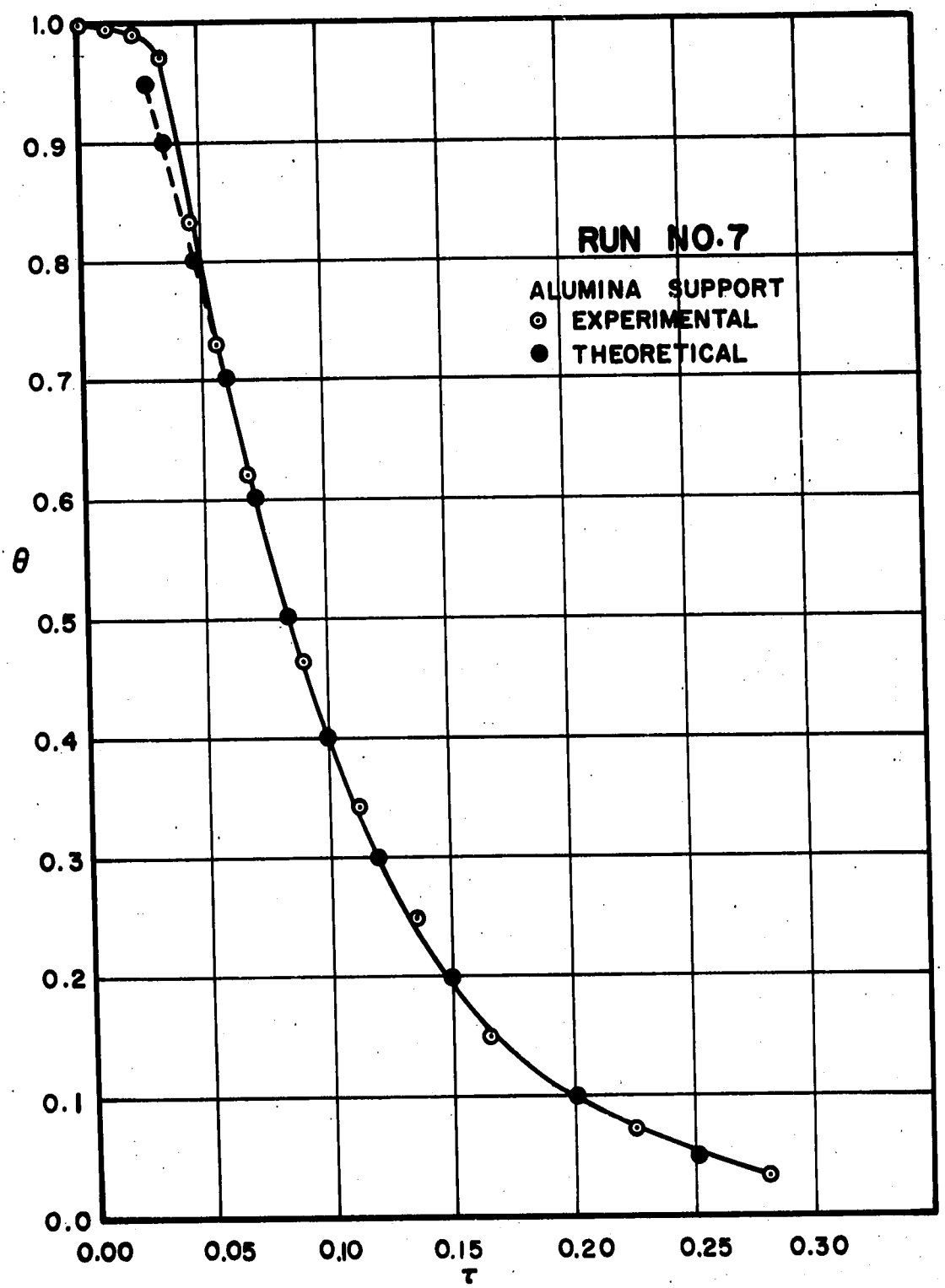

FIG 23-DIMENSIONLESS CENTERLINE TEMPERATURE TIME CURVES FOR HEAT LOSS FROM A CYLINDER

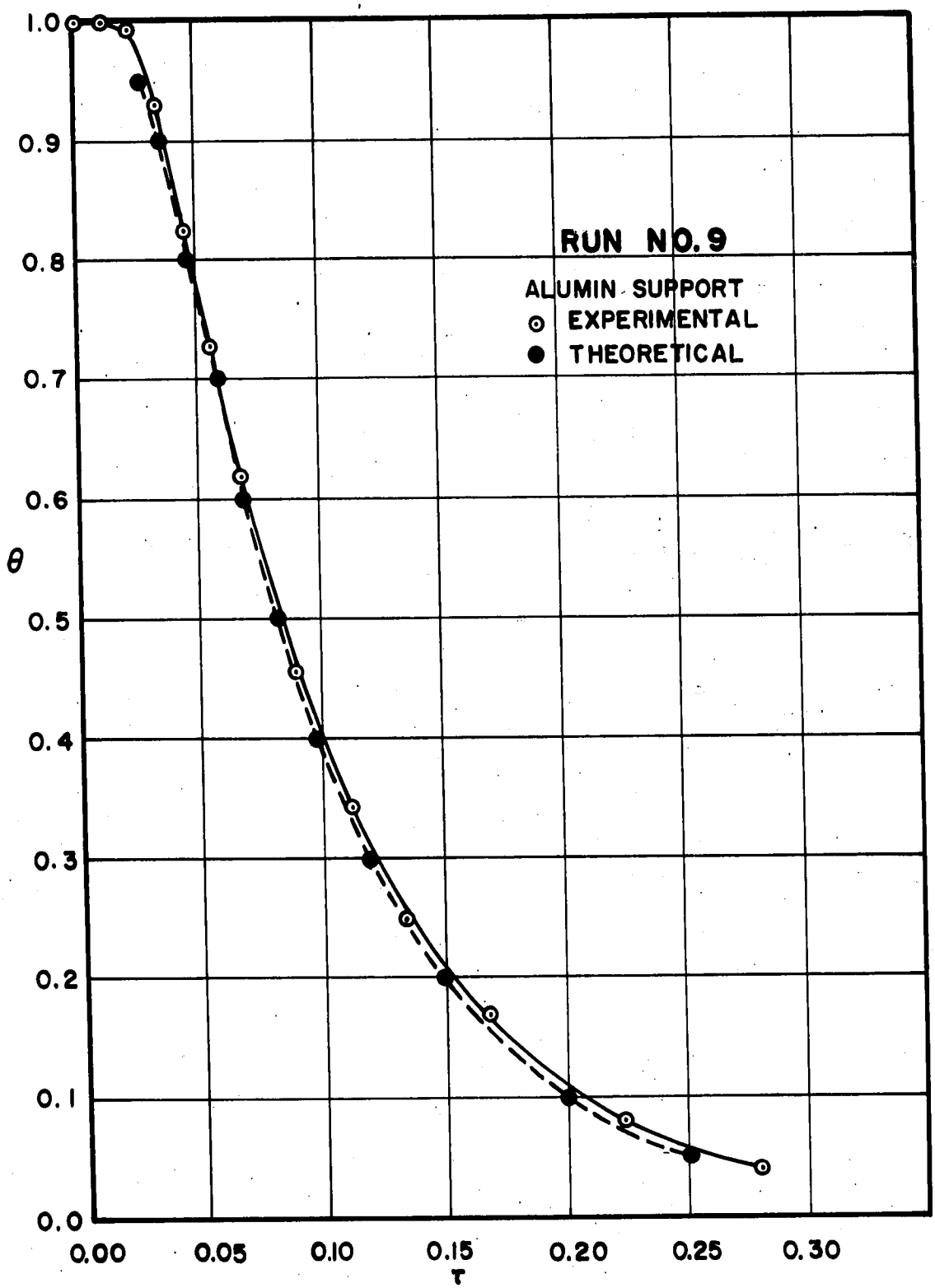

FIG 24—DIMENSIONLESS CENTERLINE TEMPERATURE TIME CURVES FOR HEAT LOSS FROM A CYLINDER

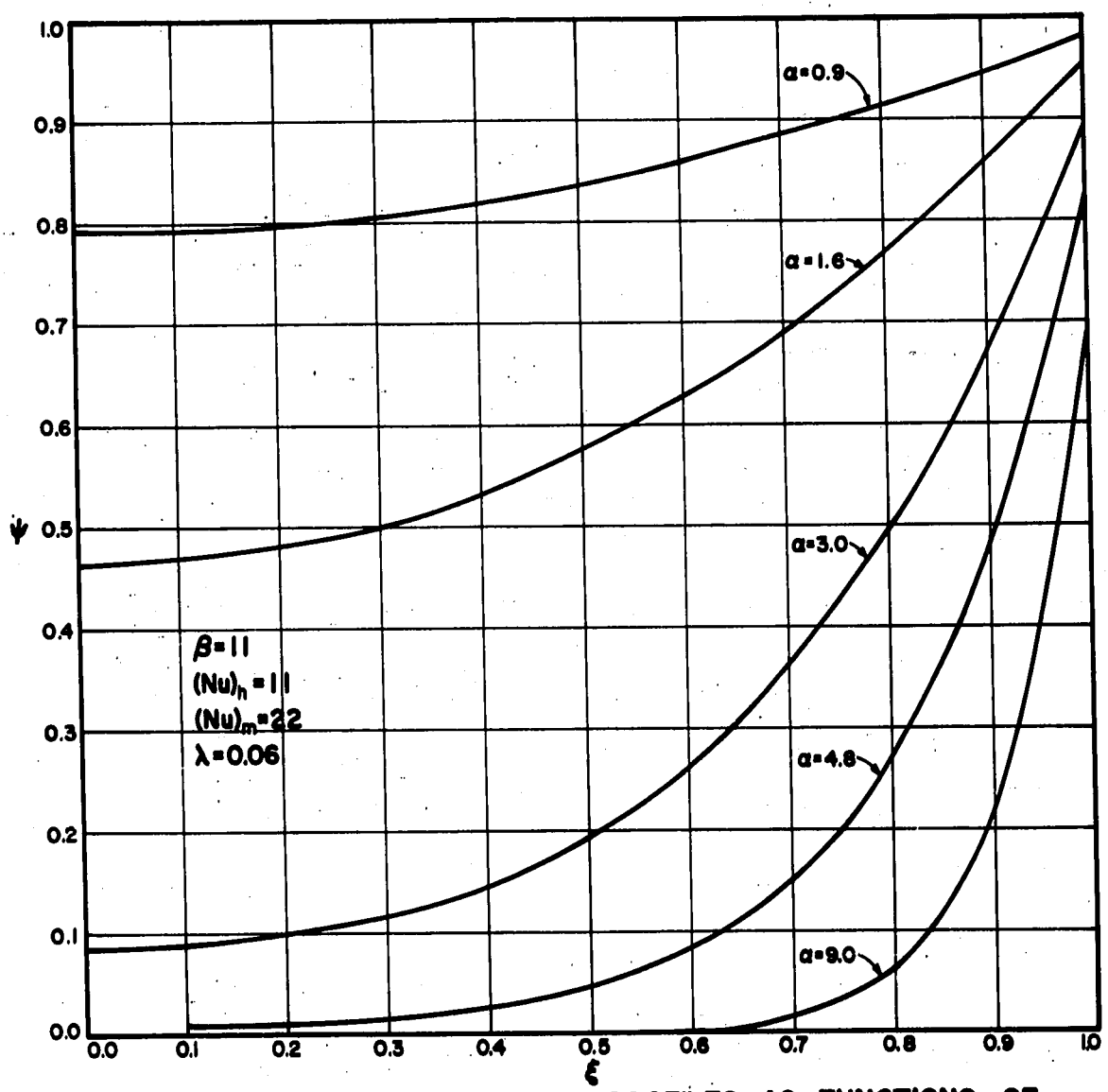

FIG. 25- RADIAL CONCENTRATION PROFILES AS FUNCTIONS OF α

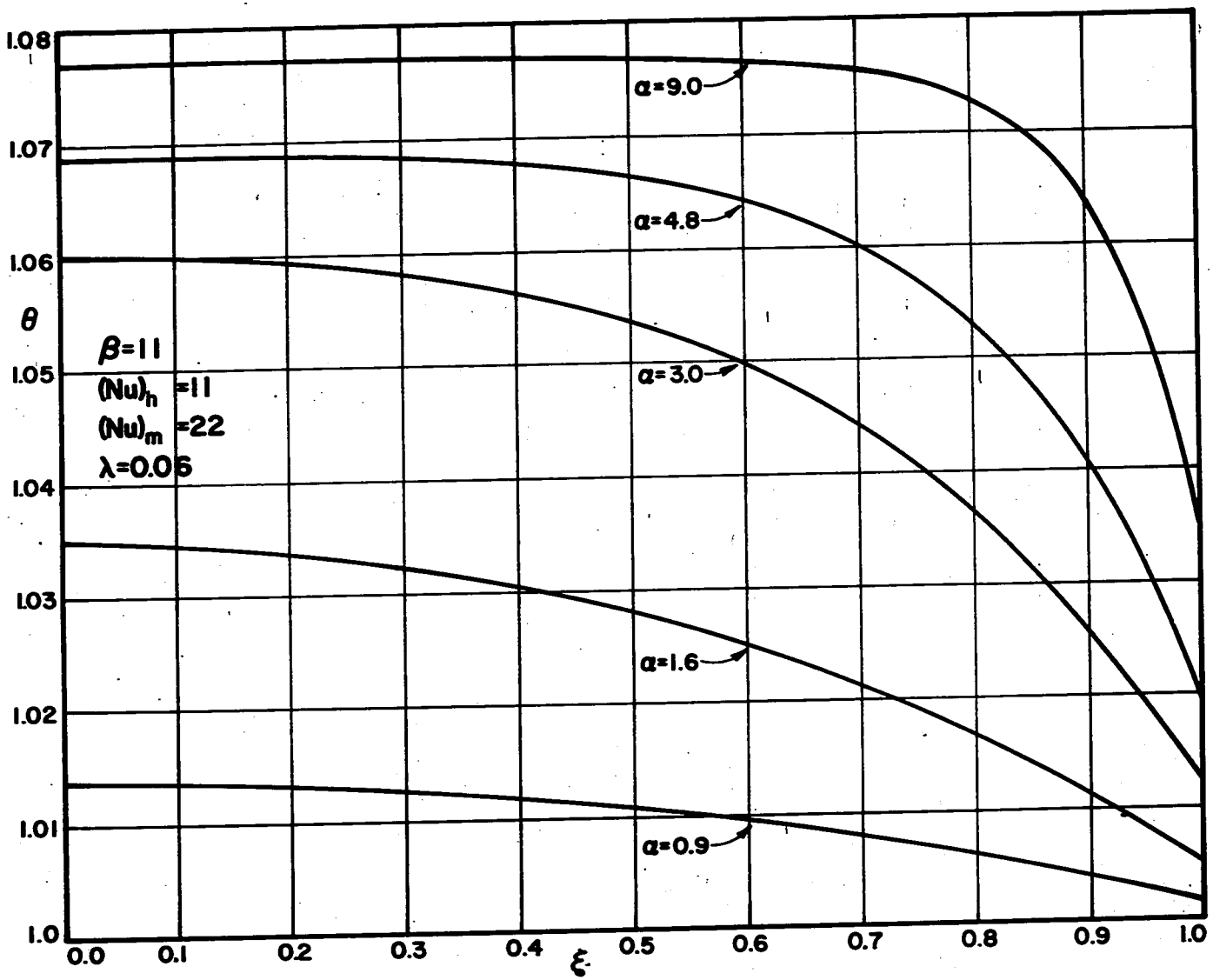

FIG. 26- RADIAL TEMPERATURE PROFILES AS FUNCTIONS OF α

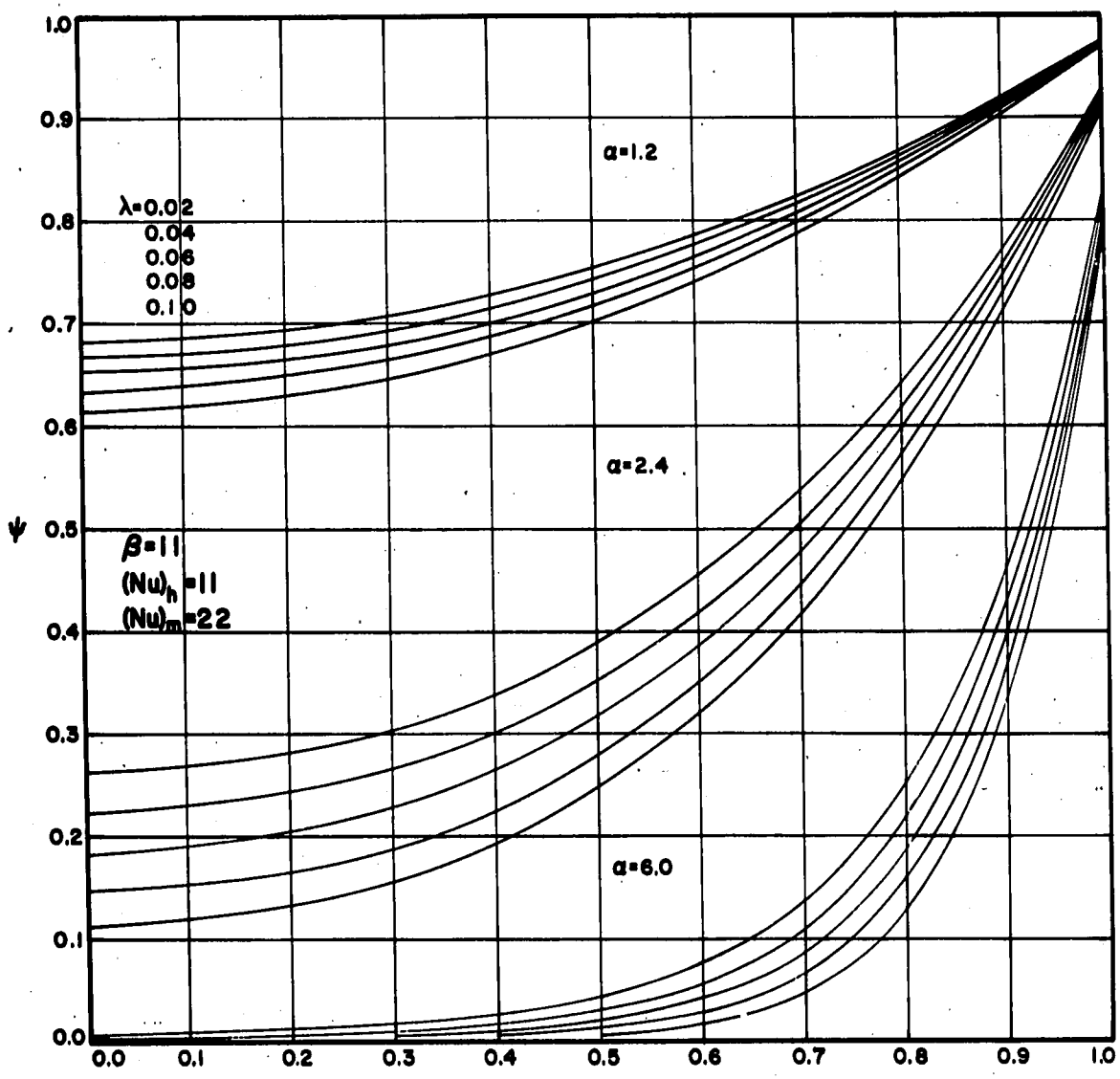

FIG. 27- RADIAL CONCENTRATION PROFILES AS FUNCTIONS OF α AND λ

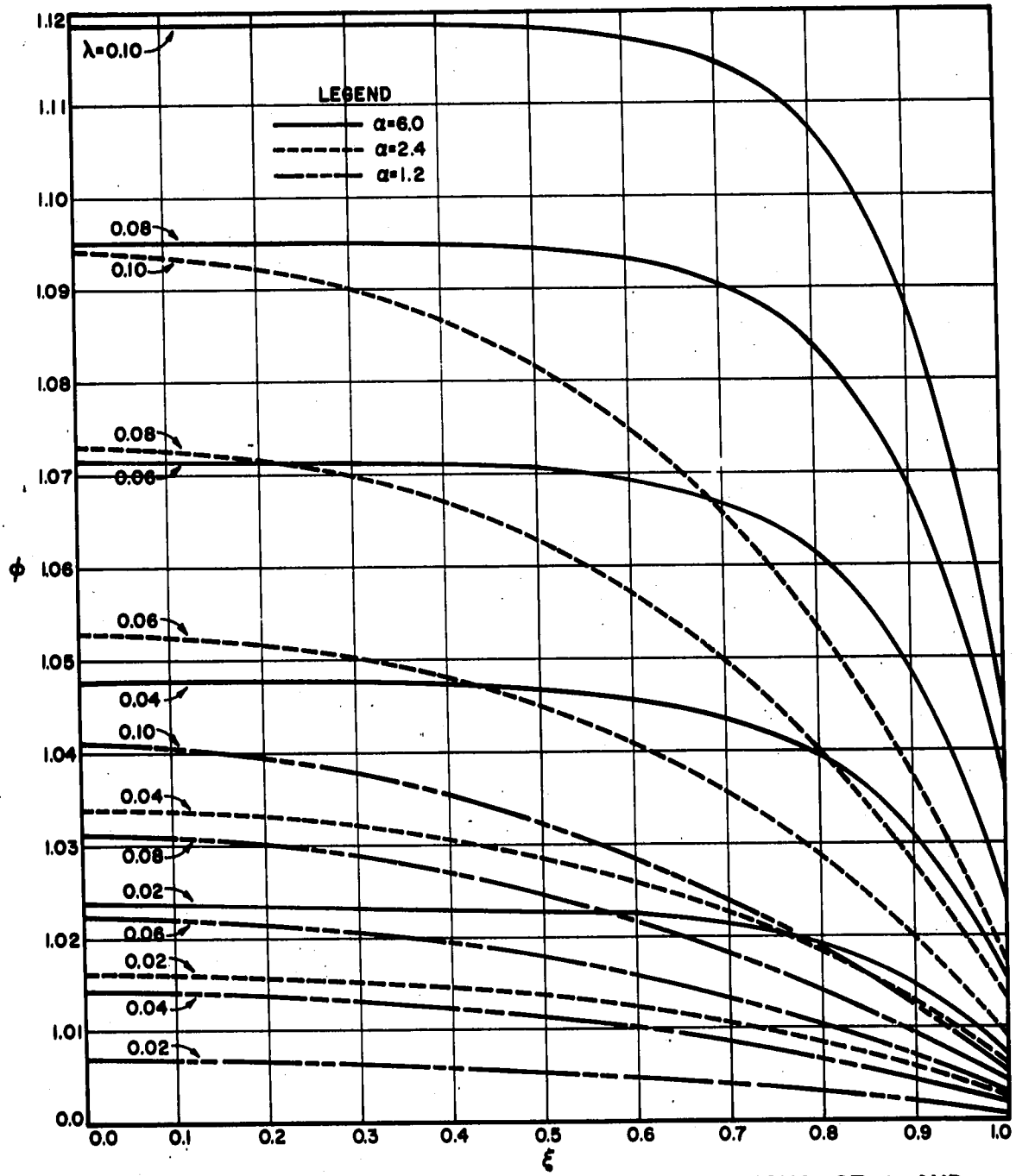

FIG. 28 - RADIAL TEMPERATURE PROFILES AS FUNCTIONS OF λ AND α

APPENDIX H - ORIGINAL REACTION DATA

RUN 20-1-3

Time, min.	T_s, mv	T_o, mv	(T_s-T_o)	ΔT(DIRECT) mv.	p, cm	Δp, cm oil	ΔF, in. H_2O
0	0.769	1.028	0.259	0.258	0.00	---	---
10	0.755	1.005	0.250	0.248	0.00	0.056	0.065
20	0.794	1.042	0.248	0.246	0.00	0.046	0.065
30	0.805	1.042	0.237	0.238	0.00	0.006	0.065
40	0.780	1.010	0.230	0.230	0.00	0.012	0.065
50	0.780	1.023	0.243	0.243	0.20	0.000	0.060
60	0.792	1.037	0.245	0.245	0.25	0.019	0.065
AVG.	0.782			0.244		0.023	

W_2 = 77.035g W_1 = 76.819g p = 1.14 atm

RUN 20-2-3

0	0.776	1.140	0.364	0.363	-0.05	---	---
5	0.779	1.176	0.377	0.379	0.00	---	---
10	0.811	1.192	0.381	0.381	0.00	0.091	0.165
17	0.800	1.188	0.388	0.389	0.00	0.084	0.165
20	0.794	1.186	0.392	0.391	0.00	---	---
25	0.796	1.193	0.397	0.396	0.00	0.097	0.165
30	0.796	1.195	0.399	0.398	0.00	---	---
37	0.811	1.212	0.401	0.400	0.00	0.076	0.165
40	0.815	1.215	0.400	0.400	0.00	---	---
45	0.811	1.214	0.403	0.402	0.00	0.076	0.170
50	0.796	1.208	0.412	0.411	0.00	---	---
56	0.788	1.206	0.418	0.420	0.00	---	0.170
AVG.	0.799			0.394		0.085	

W_2 = 83.402g W_1 = 82.735g p = 1.14atm

RUN 20-2-4

0	0.803	1.295	0.492	0.490	0.00	0.124	0.135
5	0.810	1.310	0.500	0.499	0.00	---	---
10	0.823	1.331	0.508	0.510	0.00	0.092	0.130
17	0.811	1.325	0.514	0.512	-0.05	---	---
20	0.809	1.327	0.518	0.520	-0.05	0.101	0.130
25	0.801	1.330	0.529	0.530	-0.05	---	---
30	0.796	1.337	0.541	0.539	-0.05	---	0.130
AVG.	0.808			0.514		0.106	

W_2 = 68.174g W_1 = 67.938g pp = 1.14atm

RUN 20-3-1

Time, min.	T_s, mv	T_o, mv	(T_s-T_o)	ΔT(DIRECT) mv	p, cm	Δp, cm oil	ΔF, in H O
0	0.773	1.557	0.784	0.784	0.05	---	---
10	0.770	1.557	0.787	0.785	0.05	0.345	0.125
20	0.772	1.544	0.772	0.770	0.00	0.290	0.115
30	0.786	1.541	0.755	0.756	0.00	0.241	0.115
40	0.787	1.528	0.741	0.741	0.00	0.212	0.115
50	0.770	1.509	0.739	0.738	0.00	0.194	0.115
60	0.790	1.527	0.737	0.740	0.00	0.205	0.115
AVG.	0.778			0.759		0.248	

W_2 = 82.521g W_1 = 81.857g p = 1.14atm

RUN 20-4-1

0	0.776	2.094	1.318	1.316	0.00	---	---
10	0.803	2.127	1.324	1.325	0.00	0.201	0.115
20	0.801	2.130	1.329	1.331	0.00	0.158	0.115
30	0.780	2.133	1.353	1.346	0.00	0.193	0.115
40	0.802	2.140	1.338	1.336	0.00	0.200	0.115
50	0.813	2.152	1.339	1.339	0.00	0.152	0.115
60	0.790	2.141	1.351	1.348	0.00	0.161	0.115
65	0.779	2.117	1.338	1.335	0.00	---	---
AVG.	0.794			1.333		0.178	

W_2 = 81.857g W_1 = 80.667g p 1.14atm

RUN 30-1-2

0	1.202	0.283	0.283	0.281	0.05	---	---
10	1.190	0.278	0.278	0.280	0.00	---	0.115
20	1.205	0.280	0.280	0.282	0.00	0.036	0.115
30	1.229	0.285	0.285	0.288	0.00	0.039	0.115
40	1.220	0.299	0.299	0.302	0.00	0.028	0.115
50	1.212	0.308	0.308	0.310	0.00	0.032	0.115
60	1.210	0.313	0.313	0.319	0.00	0.030	0.115
70	1.210	0.330	0.330	0.335	0.00	0.028	0.115
75	1.210	0.335	0.335	0.340	0.00	---	----
AVG.	1.209			0.302		0.038	

W_2 = 74.828g W_1 = 74.374g p = 1.12atm

RUN 30-2-5

0	1.206	---	---	0.440	---	---	---
10	1.201	1.633	0.432	0.437	-0.05	---	0.075
20	1.195	1.625	0.430	0.430	-0.20	---	---
30	1.189	1.613	0.426	0.426	-0.15	0.016	0.070
40	1.189	1.642	0.453	0.455	0.00	---	---
50	1.188	1.649	0.461	0.466	-0.05	---	---
60	1.189	1.664	0.475	0.478	0.00	---	0.075
70	1.188	1.669	0.480	0.483	0.00	---	---
80	1.188	1.675	0.487	0.489	0.00	---	---
AVG.	1.193			0.457		0.016	

W_2 = 65.975g W_1 = 64.355g p = 1.11atm

RUN 30-3-5

Time, min.	T_s, mv	T_o, mv	(T_s-T_o)	ΔT(DIRECT) mv	p, cm	Δp, cm oil	ΔF, in H_2O
0	1.190	1.965	0.775	0.776	0.10	0.124	0.095
10	1.190	1.966	0.776	0.779	0.00	0.092	0.115
20	1.194	1.982	0.788	0.791	0.00	0.059	0.115
30	1.201	1.996	0.795	0.796	0.00	0.038	0.115
40	1.209	2.004	0.795	0.796	0.00	0.037	0.115
50	1.216	2.013	0.797	0.797	0.00	0.020	0.115
60	---	---	---	0.798	---	---	---
AVG.	1.200			0.790		0.066	

W_2 = 65.025g W_1 = 64.200g p = 1.13atm

RUN 30-3-6

0	1.192	1.677	0.485	0.489	0.00	0.096	0.115
10	1.193	1.694	0.501	0.505	0.00	0.098	0.115
20	1.170	1.682	0.512	0.511	0.00	0.086	0.115
30	1.204	1.715	0.511	0.511	0.00	0.038	0.115
40	1.191	1.703	0.512	0.513	0.00	0.056	0.115
50	1.187	1.700	0.513	0.514	0.00	0.030	0.115
60	1.220	1.730	1.510	0.512	0.00	---	---
AVG.	1.194			0.508		0.066	0.115

W_2 = 68.952g W_1 = 68.390g p = 1.14 atm

RUN 30-4-6

0	1.217	2.373	1.156	1.161	0.00	---	0.110
10	1.224	2.418	1.194	1.195	0.00	0.120	0.115
20	1.217	2.411	1.194	1.195	0.00	0.086	0.115
30	1.222	2.416	1.194	1.195	0.00	---	---
40	1.220	2.423	1.203	1.204	0.00	0.087	0.115
50	1.218	2.419	1.201	1.202	0.00	0.051	0.115
60	1.232	2.427	1.195	1.200	0.00	0.038	0.115
AVG.	1.221			1.193		0.064	0.115

W_2 = 70.130g W_1 = 68.952 p = 1.14atm

RUN 50-1-1

0	1.977	2.211	0.234	0.235	0.00	---	---
10	1.963	2.190	0.227	0.228	0.00	0.004	0.165
20	1.988	2.210	0.222	0.216	0.00	0.014	0.165
30	1.978	2.188	0.210	0.211	0.00	0.031	0.160
40	1.951	2.167	0.216	0.216	0.05	---	---
50	1.946	2.167	0.221	0.219	0.05	0.013	0.165
60	1.965	2.182	0.217	0.219	0.00	0.034	0.165
AVG.	1.967			0.221		0.019	

W_2 = 80.447g W_1 = 80.220g p = 1.14atm

RUN 50-2-1

Time, min.	T_s, mv	T_o, mv	(T_s-T_o)	ΔT(DIRECT) mv	p, cm	Δp, cm oil	ΔF, in H_2O
0	1.942	2.419	0.477	0.476	0.00	---	---
10	1.945	2.417	0.472	0.469	0.00	---	0.125
20	1.945	2.400	0.455	0.455	-0.05	0.042	0.125
30	1.945	2.391	0.446	0.449	0.00	0.032	0.125
40	1.946	2.386	0.440	0.440	0.00	0.049	0.125
50	1.943	2.382	0.439	0.439	0.10	0.054	0.125
60	1.947	2.380	0.433	0.433	0.10	0.063	0.125
AVG.	1.945			0.452			

W_2 = 75.910g W_1 = 75.406g p = 1.14atm

RUN 50-3-1

0	1.956	2.646	0.690	0.693	0.00	0.068	0.175
10	1.956	2.650	0.694	0.693	0.00	---	---
20	1.940	2.623	0.683	0.685	0.00	0.086	0.175
30	1.961	2.644	0.683	0.685	0.00	0.089	0.175
40	1.943	2.630	0.687	0.686	0.00	0.098	0.175
50	1.945	2.620	0.675	0.678	0.00	0.100	0.175
60	1.965	2.630	0.665	0.667	0.00	---	---
AVG.	1.952			0.684		0.086	

W_2 = 81.283g W_1 = 80.477g p = 1.14atm

RUN 50-4-1

0	1.951	2.781	0.830	0.835	0.00	---	---
10	1.967	2.782	0.815	0.815	-0.05	0.035	0.150
20	1.960	2.765	0.805	0.807	0.05	0.000	0.150
30	1.958	2.764	0.806	0.808	0.00	0.017	0.150
40	1.963	2.771	0.808	0.805	0.00	0.056	0.150
50	1.970	2.776	0.806	0.805	0.00	0.057	0.150
60	1.947	2.761	0.815	0.820	0.00	0.069	0.150
AVG.	1.961			0.811		0.039	

W_2 = 80.617g W_1 = 79.689g p = 1.15atm

RUN 50-4-2

0	1.948	3.243	1.305	1.305	0.00	---	---
5	1.950	3.271	1.321	1.322	0.00	---	---
10	1.950	3.274	1.324	1.325	0.00	0.053	0.155
20	1.950	3.274	1.324	1.324	0.00	0.082	0.155
25	1.946	3.273	1.326	1.325	0.00	---	---
30	1.950	3.275	1.325	1.326	0.00	0.093	0.155
35	1.950	3.276	1.326	1.326	0.00	---	---
40	1.955	3.284	1.329	1.329	0.00	0.117	0.155
45	1.960	3.292	1.322	1.332	0.00	---	---
50	1.960	3.291	1.331	1.333	0.00	0.117	0.155
55	1.952	3.294	1.342	1.341	0.00	---	---
60	1.948	3.285	1.337	1.344	0.00	0.124	0.155
AVG.	1.951			1.327		0.099	

W_2 = 82.140g W_1 = 80.617g p = 1.15atm

RUN 60-1-1

Time, min.	T_s, mv	T_o, mv	(T_s-T_o)	ΔT(DIRECT) mv	p, cm	Δp, cm oil	ΔF, in H_2O
0	2.420	2.698	0.278	0.279	0.00	---	---
5	2.405	2.691	0.286	0.284	0.10	---	---
10	2.389	2.670	0.281	0.281	0.00	0.035	0.090
15	2.386	2.660	0.274	0.278	0.00	---	---
20	2.394	2.667	0.273	0.276	0.00	0.007	0.095
25	2.399	2.668	0.269	0.272	0.00	---	---
30	2.404	2.675	0.271	0.273	0.00	0.029	0.095
35	2.395	2.669	0.274	0.273	0.00	---	---
40	2.405	2.680	0.275	0.276	0.00	0.052	0.095
45	2.405	2.680	0.275	0.276	0.00	---	---
50	2.405	2.680	0.275	0.277	0.00	0.059	0.095
55	2.405	2.683	0.278	0.279	0.00	---	---
60	2.401	2.680	0.279	0.279	0.00	0.056	0.095
AVG.	2.401			0.277		0.040	

W_2 = 71.028 g W_1 = 70.635 g p = 1.14atm

RUN 60-2-1

0	2.429	2.867	0.438	0.439	0.00	---	---
5	2.452	2.887	0.435	0.437	-0.05	0.049	0.060
10	2.448	2.880	0.432	0.433	-0.05	---	---
15	2.406	2.838	0.432	0.433	-0.05	0.049	0.060
20	2.375	2.805	0.430	0.433	0.00	---	---
25	2.382	2.810	0.428	0.430	0.00	---	---
30	2.394	2.817	0.423	0.426	-0.05	---	---
AVG.	2.412			0.433		0.040	

W_2 = 71.328g W_1 = 71.028g p = 1.14atm

RUN 60-3-1

0	2.410	3.095	0.685	0.686	0.00	---	---
5	2.410	3.110	0.700	0.698	0.00	0.054	0.175
10	2.406	3.104	0.698	0.698	0.00	---	---
15	2.410	3.104	0.694	0.697	0.00	0.070	0.180
20	2.415	3.111	0.696	0.696	0.00	---	---
25	2.410	3.105	0.695	0.695	0.00	0.080	0.185
30	2.405	3.100	0.695	0.694	0.00	---	---
35	2.419	3.107	0.688	0.690	0.00	0.110	0.180
40	2.421	3.107	0.686	0.689	0.00	---	---
45	2.417	3.105	0.688	0.690	0.00	0.111	0.185
50	2.410	3.096	0.686	0.689	0.00	---	---
55	2.404	3.092	0.688	0.688	0.00	0.105	0.180
60	2.402	3.090	0.688	0.690	0.00	---	---
AVG.	2.411			0.692		0.089	

W_2 = 69.733g W_1 = 68.799g p = 1.15atm

RUN 60-4-1

Time, min.	T_s, mv	T_o, mv	(T_s-T_o)	ΔT(DIRECT) mv	p, cm	Δp, cm oil	ΔF, in H_2O
0	2.420	3.466	1.046	1.052	0.00	---	---
5	2.417	3.475	1.058	1.062	0.00	0.065	0.155
10	2.408	3.462	1.054	1.055	0.00	---	---
15	2.405	3.450	1.045	1.048	0.00	0.062	0.155
20	2.396	3.442	1.046	1.049	0.00	---	---
25	2.385	3.430	1.045	1.044	0.00	0.070	0.155
30	2.380	3.422	1.042	1.045	0.00	---	---
35	2.391	3.434	1.043	1.044	0.00	0.090	0.155
40	2.407	3.450	1.043	1.044	0.00	---	---
45	2.409	3.451	1.042	1.045	0.00	0.118	0.155
50	2.411	3.455	1.044	1.049	0.00	---	---
55	2.419	3.465	1.046	1.049	0.00	0.141	0.155
60	2.415	3.467	1.052	1.055	0.00	---	---
AVG.	2.405			1.053		0.091	
W_2 = 77.697g		W_1 = 76.427g		p = 1.14atm			

BLANK

0	1.175	---	---	0.001	0.05	---	---
10	1.169	---	---	0.000	0.00	---	---
20	1.147	---	---	0.000	-0.10	---	---
30	1.135	---	---	0.000	0.00	---	---
40	1.132	---	---	0.000	0.00	---	---
50	1.130	---	---	0.000	-0.10	---	---
60	1.135	---	---	0.000	0.00	---	---
AVG.	1.146			0.000			
W_2 = 77.832g		W_1 = 77.839g		p = 1.14 atm			

*All thermocouple conversions were accomplished through the Leeds and Northrup handbook.

SAMPLE ANALYSIS FOR INDIVIDUAL RUNS

The calibration curves for the gases are given in Figs. 29 and 30.

RUN NUMBER	VALVE USED	TOTAL PRESSURE cm Hg	INTEGRATOR COUNT O_2	INTEGRATOR COUNT N_2	PARTIAL PRESSURES cm Hg O_2	PARTIAL PRESSURES cm Hg N_2
20-1-3 A	L	20.005	515	655	0.187	0.150
B	R	20.004	580	640	0.181	0.147
C	L	20.012	530	650	0.192	0.149
20-2-3 A	L	20.061	1100	1840	0.325	0.423
B	R	20.145	1090	1850	0.305	0.425
C	L	20.117	1130	1925	0.332	0.443
D	R	20.262	1160	1930	0.320	0.444
20-2-4 A	R	20.185	1650	7385	0.434	1.70
B	L	20.100	1575	7210	0.436	1.66
C	R	20.102	1600	7310	0.428	1.68
D	L	20.224	1565	7270	0.434	1.67
20-3-1 A	L	19.840	2240	6515	0.594	1.50
B	R	19.800	2120	6420	0.549	1.47
C	L	20.040	2170	6550	0.576	1.50
D	R	20.155	2245	6600	0.578	1.52
20-4-1 A	L	19.968	3890	14,140	0.983	3.25
B	R	20.003	3985	14,310	0.988	3.29
C	L	20.163	3850	14,150	0.982	3.25
D	R	19.982	3880	14,060	0.965	3.23
30-1-2 A	R	20.304	1055	3825	0.293	0.920
B	L	20.302	1045	3730	0.312	0.922
C	R	20.375	1105	3875	0.306	0.932
D	L	20.376	1070	3870	0.317	0.950
E	R	20.373	1140	3920	0.315	0.942
30-2-5 A	L	19.975	1497	4507	0.420	5.38
B	R	20.075	1498	4615	0.400	5.24
C	L	20.195	1443	4420	0.406	5.17
D	R	19.883	1436	4432	0.382	5.27
30-3-5 A	R	20.114	2490	9715	0.621	2.21
B	R	18.359	2220	8960	0.571	2.04
C	R	20.274	2595	9905	0.646	2.26
D	L	20.457	2510	9610	0.640	2.19
30-3-6 A	L	20.123	1405	4330	0.397	1.00
B	R	19.992	1350	4340	0.365	1.00
C	R	19.904	1550	4640	0.411	1.08
D	L	20.410	1590	4775	0.442	1.10
E	R	20.215	1445	4460	0.397	1.03
30-4-6 A	R	20.359	3610	9140	0.900	2.10
B	L	20.583	3540	9190	0.902	2.11
C	L	19.911	3350	8640	0.855	1.99
D	R	19.838	3325	8590	0.832	1.98
E	L	19.889	3425	8810	0.872	2.03

RUN NUMBER	VALVE USED	TOTAL PRESSURE cm Hg	INTEGRATOR COUNT O_2	INTEGRATOR COUNT N_2	PARTIAL PRESSURES cm Hg O_2	PARTIAL PRESSURES cm Hg N_2
50-1-1 A	R	19.720	375	2485	0.132	0.572
B	L	20.168	360	2460	0.151	0.566
C	L	20.259	305	2355	0.138	0.540
50-2-1 A	R	19.924	1100	4450	0.305	1.02
B	L	19.978	1045	4355	0.312	1.00
C	R	20.273	1045	4405	0.294	1.01
D	L	20.042	1015	4330	0.307	1.00
50-3-1 A	R	20.090	1870	9040	0.487	2.08
B	L	20.013	1760	8970	0.480	2.06
C	R	20.017	1700	9040	0.449	2.08
D	L	20.068	1640	8740	0.453	2.01
E	R	19.741	1640	8760	0.433	2.01
F	L	19.955	1700	8980	0.467	2.06
G	R	20.124	1690	9060	0.446	2.08
50-4-1 A	L	20.122	1970	5690	0.530	1.31
B	R	20.172	2020	5765	0.522	1.32
C	L	20.106	2030	5730	0.542	1.32
50-4-2 A	L	20.172	3080	5255	0.791	1.21
B	R	20.076	3090	5260	0.778	1.21
C	L	20.070	3035	5180	0.780	1.19
D	R	20.023	3060	5200	0.770	1.20
60-1-1 A	L	20.332	515	4540	0.185	1.04
B	R	19.859	500	4695	0.163	1.08
C	R	20.063	520	4690	0.168	1.08
D	L	19.983	465	4545	0.176	1.04
60-2-1 A	L	19.904	715	1780	0.235	0.410
B	R	20.186	740	1800	0.220	0.414
C	L	20.043	690	1790	0.224	0.411
D	R	19.906	740	1830	0.220	0.420
60-3-1 A	L	20.128	1665	10,700	0.438	2.46
B	R	20.127	1440	10,080	0.405	2.32
C	L	20.201	1580	10,560	0.437	2.43
D	R	20.164	1515	10,535	0.403	2.42
E	L	20.115	1500	10,400	0.420	2.39
60-4-1 A	R	19.953	2110	6770	0.542	1.56
B	L	20.002	2210	6730	0.586	1.55
C	R	20.076	2090	6680	0.541	1.537
D	L	20.217	2070	6600	0.553	1.517
BLANK	L	20.237	3005	2230	0.770	0.513

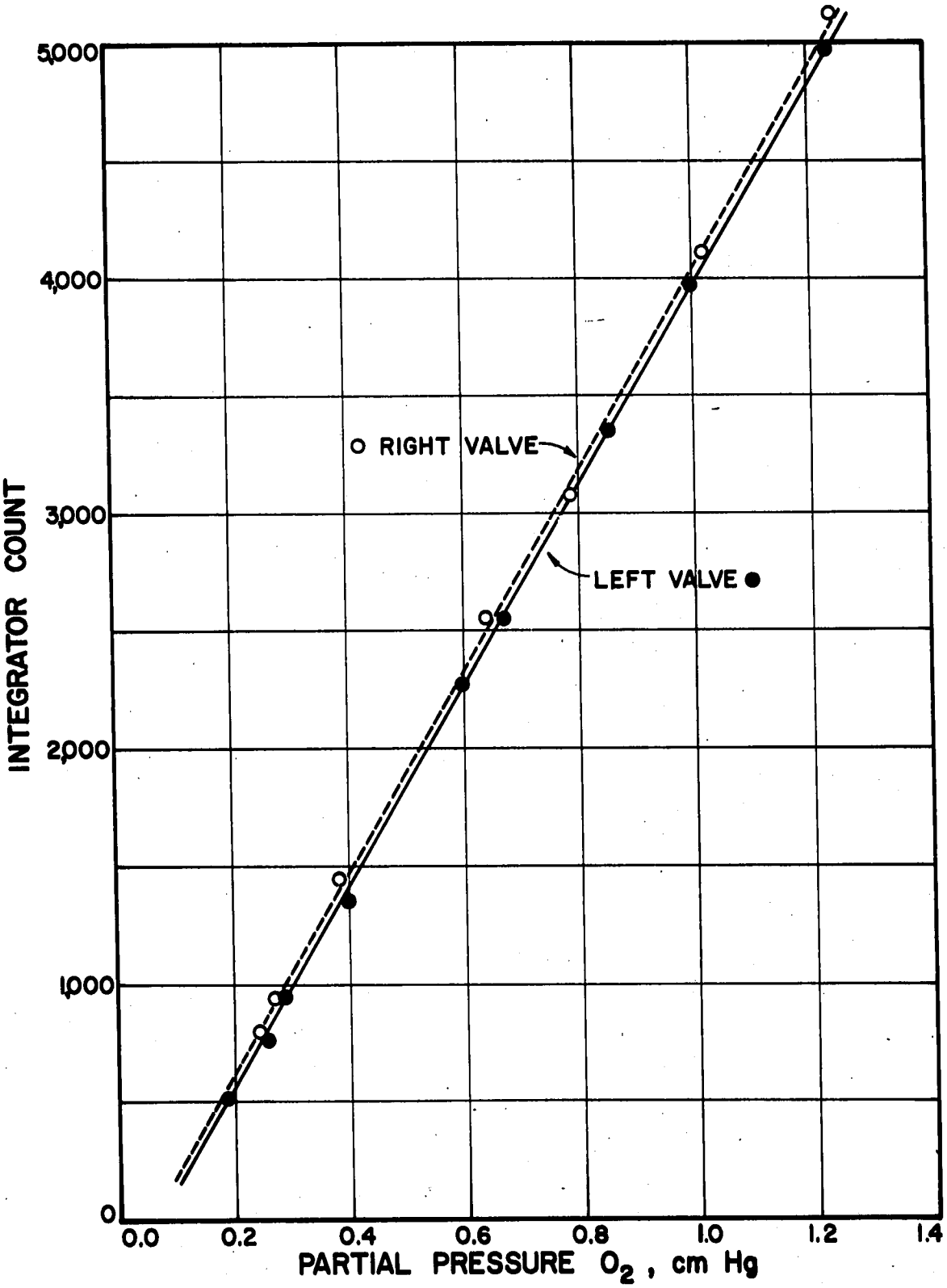

FIG. 29 – CHROMATOGRAPHIC CALIBRATION CURVES FOR OXYGEN CONTENT

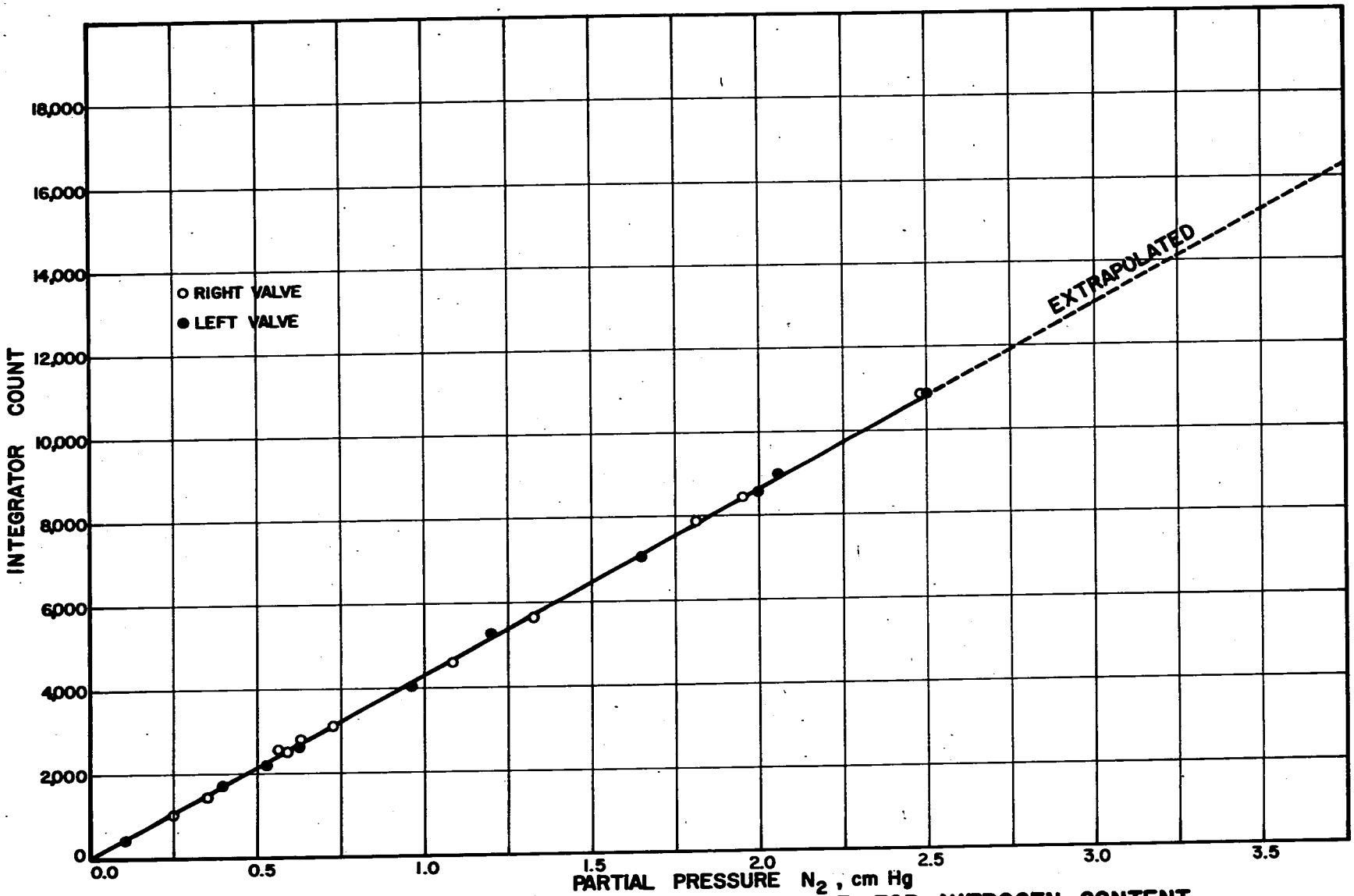

FIG. 30- CHROMATOGRAPHIC CALIBRATION CURVE FOR NITROGEN CONTENT

APPENDIX I - MAXIMUM TEMPERATURE RISE IN A PELLET

It was shown in Section V that the effects of bulk flow in the pellet are small enough that they may be neglected. The transport equations may be closely approximated by (c = constant)

$$\nabla^2 D_{Am}^{EFF} C_A = R \tag{I-1}$$

and

$$\nabla^2 k_e \bar{T} = - (-\Delta H) R \tag{I-2}$$

Multiplying (I-1) by $(-\Delta H)$ and coupling the equations gives

$$\nabla^2 \cdot \left[\frac{(-\Delta H) D_{Am}^{EFF} C_A}{k_e} + T \right] = 0$$

or

$$\left[\frac{(-\Delta H) D_{Am}^{EFF} C_{As} \psi}{k_e} + T_s \phi \right] = 0$$

This is Laplace's equation and has the solution

$$\frac{(-\Delta H) D_{Am}^{EFF} C_{As}}{k_e} \psi + T_s \phi = \text{constant}$$

and

$$\frac{(-\Delta H) D_{Am}^{EFF} C_{As}}{k_e T_s} \psi + \phi = \text{constant}$$

or

$$\lambda \psi + \phi = \text{constant}$$

This equation also applies at the surface

$$\lambda \psi_{ss} + \phi_{ss} = \text{constant}$$

Subtraction gives

$$\lambda (\psi_{ss} - \psi) = \phi - \phi_{ss} \tag{I-3}$$

The surfaces values are those given by the boundary conditions in the text. (See (21) and (23)), and the temperature rise will be a maximum when all oxygen is consumed ($\psi = 0$). Using the boundary conditions

$$\lambda\left[1 - \frac{1}{(Nu)_m}\frac{d\psi}{d\xi}\right] = -1 + \frac{1}{(Nu)_h}\frac{d\phi}{d\xi} + \phi$$

or

$$(\phi - 1)_{max} = \lambda - \frac{\lambda}{(Nu)_m}\frac{d\psi}{d\xi} - \frac{1}{(Nu)_h}\frac{d\phi}{d\xi} \qquad (I\text{-}4)$$

This expression for the maximum temperature rise in a pellet, independent of geometry and kinetics, is equivalent to that obtained by Prater (32), but includes the effect of the generalized boundary condition. The second term on the right side of (I-4) is small compared to the other terms. However, the term involving the temperature derivative can influence the maximum achievable temperature appreciably. Since $d\phi/d\xi$ is negative for exothermic reactions, values of $(\Delta T)_{max}$ may be low if this effect is ignored.

APPENDIX J - THE PERMEABILITY OF THE PELLETS

The apparatus used to measure the gas permeability of the porous catalyst pellets belonged to the Production Research Laboratories of the Humble Oil Company. For this reason, the apparatus will not be discussed in detail.

In general the equipment resembled that used in this work to measure the gas diffusivity. The samples again were single cylindrical pellets situated in a fixture which prevented gas from seeping around the edges of the pellet. Nitrogen at a predetermined high pressure was applied to one face of the speciman. The steady state rate at which it permeated to the atmospheric side of the pellet was measured.

The data taken is presented in Table 17. The first four runs are at various pressures to verify that Darcy's Law is applicable to the pellets. Then the permeability of several samples of each pellet type was measured. The permeabilities were calculated according to the formula:

$$K = 1.47(10^4)\frac{\mu Q L p_a}{tA(\Delta p)p_m} \qquad \text{(J-1)}$$

where

$$p_m = \frac{p_1 + p_2}{2}$$

From the measured permeabilities and porosity, an estimate of the pore radius which controls flow through the pellet can be made from the relationship

$$K = \frac{Pd^2}{96} \qquad \text{(J-2)}$$

Using a permeability of 0.005 Darcy's ($\simeq 5 \times 10^{-11} cm^2$) and a porosity of 0.5, the average diameter is approximately 10^{-4}cm whereas the mean free path is on the order of 10^{-5} giving an r/l ratio of about five. Thus, the application of equation (30) is borderline. However, Wakao and Smith (52) predicted a D_{AB}/D_{AB}^{EFF} ratio approximately equal to the square of the macropore porosity if ordinary diffusion prevails. In this case

$$\frac{D_{Am}^{EFF}}{D_{AB}} = 0.14 \simeq 0.12 = (.345)^2 = \epsilon_a^2$$

Both of these factors encouraged the selection of the diffusion equation (30) used in the text.

APPENDIX K - DETERMINATION OF RUN VELOCITIES

Pressure drops were measured for each run on a pitot tube connected to an inclined manometer equipped with five micron snubbers to dampen the oscillations. These measurements were only ggod on a relative basis, since the effects of the pulsations are appreciable.

An absolute velocity of 8.8 ft/sec was measured in the reactor with an anemometer at a pump suction pressure of one atmosphere which was close to actual run conditions. For this measurement, the bypass valve on the pump was set at the opening employed during most of the runs. It was assumed that the velocity of 8.8 ft/sec occurred during all runs having this valve setting.

From runs with equal velocities, a relationship between the fluid density and manometer pressure drop was available, and at a particular density, differences in the flow rate were assumed due only to changes in the bypass valve setting. Velocities at any flow rate were then available from the gas density from the relationship

$$v^2 = (v_m)^2 \frac{\Delta F}{\Delta F_m} = (8.8)^2 \frac{\Delta F}{\Delta F_m} \qquad \text{(K-1)}$$

where ΔF is the measured pressure drop and ΔF_m is the pressure drop obtained from the density-pressure drop relation mentioned above.

APPENDIX L - ORDER OF MAGNITUDE FOR THE BULK TRANSPORT OF HEAT

If viscous dissipations and gravitational effects are neglected, the energy equation may be written at steady state as

$$0 = - (\nabla \cdot \mathbf{q}) + \sum_i H_i [(\nabla \cdot \mathbf{J}_i - R_i)] \qquad \text{(L-1)}$$

or

$$0 = - \nabla \cdot [-k \nabla T + \sum_i H_i \mathbf{J}_i] + \sum_i H_i [\nabla \cdot \mathbf{J}_i - R_i]$$

where $\sum_i H_i \mathbf{J}_i$ is the energy flux of interdiffusion. This equation reduces to

$$k_e \nabla^2 T - \sum_i \mathbf{J}_i \cdot \nabla H_i - \sum_i H_i R_i = 0 \qquad \text{(L-2)}$$

which is in the same form as (2) with the additional bulk transport term. Since the mass average velocity at any point is zero, (L-2) may be expanded as follows

$$k_e \frac{1}{r} \frac{d}{dr}\left[r \frac{dT}{dr}\right] + \frac{p D_{Am}^{EFF}}{R_g T(1 - X_A)} \frac{dX_A}{dr} [C_{pA} + 2C_{pB} - 2C_{pC}] \frac{dT}{dr} - (-\Delta H) R_A = 0$$

which in dimentionless form is

$$\frac{d^2\phi}{d\xi^2} + \left[\frac{1}{\xi} + \frac{C_{As} D_{Am}^{EFF} \Delta C_p}{k \phi (1 - X_{As}\psi)} \frac{d\psi}{d\xi}\right] \frac{d\phi}{d\xi} = - \lambda \alpha^2 e^{\beta\left(1 - \frac{1}{\phi}\right)} \left[\frac{\psi}{\phi}\right]^n \qquad \text{(L-3)}$$

Equation (L-3) differs from (18) by a single term which has its maximum value at the solid surface. Thus, its significance may be estimated by comparison of its magnitude to unity. The size of the derivative may be estimated from the isothermal case where

$$\left.\frac{d\psi}{d\xi}\right|_{\xi=1} = \left[\frac{\alpha}{\tanh \alpha} - 1\right] \qquad \text{(L-4)}$$

The heat capacities were taken from Perry (31) as follows:

$$C_{pO_2} = 6.13 + 2.99(10^{-3})T - 0.806(10^{-6})T^2$$

$$C_{pH_2} = 6.92 + 0.218(10^{-3})T + 0.279(10^{-6})T^2$$

$$C_{pH_2O} = 8.22 + 0.15(10^{-3})T + 1.34(10^{-6})T^2$$

Using $\Delta C_p = 4.6$ cal/mole^{o}K at 298^{o}K, $D_{Am}^{EFF} = 0.1$ cm^2/sec, $k_e = 5.4(10^{-4})$ cal/sec cm^{o}K, $C_{As} = 3.0(10^{-6})$ moles/cm^3 and $\alpha = 10$ (larger than any measured) then the additional term

$$\frac{C_{As} D_{Am}^{EFF} \Delta C_p}{k_e} \left.\frac{d\psi}{d\xi}\right|_{\xi=i} < 0.006 << 1.0$$

which is sufficient evidence to consider the effect negligible.

APPENDIX M - TEMPERATURE DEPENDENCE OF THE HEAT OF REACTION

Kirchoff's equation for the heat of reaction at any temperature is

$$\Delta H_T = \Delta H_{T_o} + \Delta aT + \frac{\Delta b}{2}T^2 + \frac{\Delta c}{3}T^3 \qquad \text{(M-1)}$$

where Δa, Δb and Δc represent the difference in heat capacities of the products and the reactants. Using the heat capacities in Appendix L and the heat of formation of water at 25°C from Lange (25), the reference heat of formation may be calculated

$$\Delta H_{25°C} = -57,798 = \Delta H_{273°C} - (1.76)(298) - (0.78)(298)^2(10^{-3}) + (0.52)(10^{-6})(298)^3$$

$H_{273°C} = -57,217$ cal/mole.

The temperature range of interest in this work is 20°C to 100°C. Further calculations show that a change of less than 200 cal/mole occur over this range, or less than a 0.4% change.

APPENDIX N - SAMPLE CALCULATIONS

The run chosen to illustrate the sample calculations 1-16 is 50-2-1. The data may be found in Table 12 or Appendix H.

1) R^*, moles $O_2/cm^3 sec$

$W_2 - W_1 = 75.910 - 75.406 = 0.504g\ H_2O = 0.0140$ moles O_2

$$\text{Catalyst Volume} = \left[\frac{3}{8}\right]^2 \frac{\pi}{4} \left[5 \cdot \frac{3}{8}\right] (2.54)^3 = 3.38\ cm^3$$

time = 3600 sec.

$R^* = 11.47(10^{-5})$ moles $O_2/cm^3 sec$

2) $$C_{As} = \frac{X_{As} p}{R_g T_s}$$

$X_{As} = 0.0152$

$p = 1.14$ atm

$T_s = 321^oK$

$$R_g = 82.05\ \frac{cm^3\ atm}{^oK\ mole}$$

$C_{As} = 6.58(10^{-7})$ moles O_2/cm^3

3) $$\rho = \frac{\sum_i X_i M_i}{2.24(10^4)}$$

$$= \frac{(0.934)(2) + (0.0503)(28) + (0.0152)(32)}{2.24(10^4)} \cdot \frac{273}{321} \cdot \frac{1.14}{1.00}$$

$= 1.63(10^{-4}) g/cm^3$

4) $$\lambda = \frac{(-\Delta H) D_{Am}^{EFF} C_{As}}{k_e T_s}$$

$(-\Delta H) = 2(57,800)$ cal/mole

$D_{Am}^{EFF} = 0.0851\ cm^2/sec$ (see Fig. 8)

k_e = 0.13 BTU/hr ft^{o}F = 5.4(10^{-4}) cal/sec cm^{o}C

C_{As} = 6.58(10^{-7}) mole/cm^3

T_s = 321^{o}C

λ = 0.0376

5) $Re = \frac{Dv\rho}{\mu}$

$D = \frac{3}{8}$ in = 0.0312 ft

v = 8.8 ft/sec

ρ = 1.63(10^{-4}) g/cm = 0.0102 #/ft^3

μ = 6.05(10^{-6}) #/ft, sec (viscosity of hydrogen)

Re = 461

6) $Sc = \frac{\mu}{D_{Am}^{EFF}\rho}$

μ = 6.05(10^{-6}) #/ft sec

ρ = .0102 #/ft^3

D_{Am}^{EFF} = 0.0851 cm^2/sec = 9.15(10^{-5}) ft^2/sec

7) $Pr = \frac{C_p\mu}{k_e}$ (Used for all runs)

C_p = 3.9 $\frac{cal}{g^{o}C}$ (heat capacity of hydrogen)

μ = 6.05(10^{-6}) #/ft, sec = 96(10^{-6}) g/cm sec

k_e = 5.4(10^{-4}) cal/cm sec^{o}C

Pr = 0.70

8) $j_D = j_H$ = 0.026 [Bird, Stuart and Lightfoot (4) p. 408]

9) $(Nu)_h = j_H RePr^{\frac{1}{3}} = (0.026)(461)(0.70)^{\frac{1}{3}} = 10.63$

10) $(Nu)_m = j_D ReSc^{\frac{1}{3}} = (.0.026)(461)(6.7)^{\frac{1}{3}} = 22.7$

11) $\beta = \frac{E}{RT_s}$

$E = 6500$ cal/mole

$R = 1.987$ cal/mole, ^{o}K

$T_s = 321\ ^{o}K$

$\beta = 10.2$

12) $$\eta\alpha^2 = \frac{R^* R^2}{D_{Am}^{EFF} C_{As}}$$

$R^* = 11.47(10^{-7})$ moles/cm^3, sec

$$R^2 = \left[\frac{3}{16}\right]^2 (2.54)^2 = 0.227 \text{ cm}^2$$

$D_{Am}^{EFF} = 0.0851$ cm^2/sec

$C_{As} = 6.58(10^{-7})$ moles/cm^3

$\eta\alpha^2 = 4.65$

13) $\eta = 0.55$ (from curve such as Fig. 15)

14) $\alpha = 2.9$ (from curve such as Fig. 14)

15) $$k_s a = \frac{\alpha^2 D_{Am}^{EFF}}{R^2}$$

$\alpha = 2.9$

$D_{Am}^{EFF} = 0.0851$ cm^2/sec

$R^2 = 0.227$ cm^2

$k_s a = 3.2$ sec^{-1}

16) $$E = \frac{E^*}{1 + \frac{1}{2}\frac{\partial \ln\eta}{\partial \ln\alpha}}$$ (Table 14)

$E^* = 4000$ cal/mole

$$\frac{\partial \ln\eta}{\partial \ln\alpha} = -0.81$$ (from Fig. 14)

$E = 6700$ cal/mole

17) $D_{AB}^{EFF} = -\frac{N_A \omega L}{c} \ln \frac{1 + \omega}{1 + \omega X_A}$ (Table 9, Run 1) (30)

$$N_A L = \frac{(0.020)(59.5)}{(60)(22,400)} \cdot \frac{4}{(3/8)\pi(2.54)} \cdot \frac{273}{300} = 1.08(10^{-6}) \text{ moles/cm}^2\text{sec}$$

$$\omega = 1 + \frac{N_B}{N_A} = 1 - \left(\frac{M_A}{M_B}\right)^{\frac{1}{2}} = 1 - \left[\frac{32.00}{2.016}\right]^{\frac{1}{2}} = -3.00$$

$$c = \frac{p}{R_g T} = \frac{1.0}{(82)(300)} = 4.06(10^{-5}) \text{ moles/cm}^3$$

18) Thermal Diffusivity (Table 4, Run 2)

$$\alpha_d = \frac{\tau R^2}{t} \quad (\theta = 0.900)$$

$\tau = 0.092$

$R^2 = 2.72(10^{-4})$ ft^2

$t = 0.322/60$, hr (see Fig. 19)

$\alpha_d = 0.00468$ ft^2/hr

19) Thermal Conductivity (Table 6, Run 2)

$k_e = \alpha \rho C_p \quad (\theta = 0.900)$

$\alpha_d = 0.00468$ ft^2/hr (See Table 4)

$\rho = 81.7$ #/ft^3 (See Table 1)

$C_p = 0.218$ BTU/#$^\circ$F (See Table 5)

$k_e = 0.0830$ BTU/hr ft $^\circ$F

20) $$k_f = \frac{k_g}{1 + Z\left[\frac{2 - a}{a}\right]\left[\frac{\gamma}{1 + \gamma}\right]\left[\frac{T}{pdS^2(Pr)}\right]}$$

$$k_f = \frac{0.72(10^{-4})}{1 + \frac{(1.98)(10^{-24})(1.5)(0.58)}{(10.2)^2(10^{-20})(29.5)(10^{-8})}} = 0.110(10^{-4}) \text{ cal/cm sec}^{\circ}\text{C}$$

21) $k_t = 22.8\ k_f = (22.8)(0.110)(10^{-4})$

22) $k_e = k_e^{Air} - k_t^{Air} = 3.5(10^{-4}) - 2.5(10^{-4}) = 1.0(10^{-4})$

REFERENCES

1 Aris, R., Chem. Eng. Sci. 6, 202 (1957).

2 Beckman Instruments, Inc. "GC-2 Gas Chromatograph Instruction Manual" (1960).

3 Beek, J., A.I.Ch.E. J. 7, 337 (1961).

4 Bird, R. B, W. E. Stuart, and E. N. Lightfoot, "Transport Phenomena," John Wiley and Sons, New York (1960).

5 Boudart, M., Chem. Eng. Prog. 57, No. 8, 33 (1961).

6 Butt, J. B., Can. J. Chem. Eng. 41, 130 (1963).

7 Butt, J. B., A.I.Ch.E. J. 9, 707 (1963).

8 Carberry, J. J., Chem. & Proc. Eng., 306 (1963).

9 Carberry, J. J., A.I.Ch.E. J 7, 350 (1961).

10 Carberry, J. J., Chem. Eng. Sci. 17, 675 (1962).

11 Carberry, J. J., A.I.Ch.E. J. 8, 557 (1962).

12 Chambré, P. L., and A. Acrivos, Ind. & Eng. Chem. 49, 1025 (1957).

13 Damköhler, G, Z. Phys. Chem. A193, 16 (1943).

14 Eckert, E. R. G., and R. M. Drake, "Heat and Mass Transfer," McGraw-Hill, New York (1959).

15 Eggleton, A. E. J., and F. C. Tompkins, Trans. Far. Soc. 48, 738 (1952).

16 Frank-Kamenetskiĭ, D. A., "Diffusion and Heat Exchange in Chemical Kinetics," Chapt. II, Princeton Univ. Press, Princeton University (1955).

17 Fulkerson, W., Oak Ridge National Laboratories, Private Communication.

18 Godbee, H. W., Oak Ridge National Laboratories, Private Communication.

19 Grilly, E. R., W. J. Taylor, and H. L. Johnston, J. Chem. Phys. 14, 435 (1946).

20 Henry, J. P., B. Chennakesavan, and J. M. Smith, A.I.Ch.E. J. 7, 10 (1961).

21 Hildebrand, E. B., "Advanced Calculus for Engineers," Prentice-Hall Englewood Cliffs, N. J. (1948).

22 Hoogschagen, J., Ind. & Eng. Chem. 47, 906 (1955).

23 Hougan, O. A., Ind. & Eng. Chem. 53, No. 7, 509 (1961).

24 Hsu, H. W., and R. W. Bird, A.I.Ch.E. J. 6, 516 (1960).

25 Lange, N. A., "Handbook of Chemistry," 9th Ed., McGraw-Hill, New York (1956).

26 Masamune, S., and J. M. Smith, A.I.Ch.E. J. 8, 217 (1962).

27 Mingle, J. O., and J. M. Smith, A.I.Ch.E. J. 7, 243 (1961).

28 Mischke, R. A., and J. M. Smith, I.&E.C. Fund. 1, 288 (1962).

29 Olsen, F. C. W., and O. T. Shultz, Ind. & Eng. Chem. 34, 874 (1942).

30 Park, E. L., M.S. Thesis, Rice University (1962).

31 Perry, J. H., "Chemical Engineers Handbook," 3rd Ed., McGraw-Hill, New York (1950).

32 Prater, C. D., Chem. Eng. Sci., 8, 284 (1958).

33 Rao, M. R., and J. M. Smith, A.I.Ch.E. J. 9, 485 (1963).

34 Rao, M. R., and J. M. Smith, A.I.Ch.E. J. 10, 293 (1964).

35 Rao, M. R., N. Wakao, and J. M. Smith, I.&E.C. Fund. 3, 127 (1964).

36 Richtmyer, R. D., "Difference Methods For Initial Value Problems," Interscience Publishers, New York (1957).

37 Roiter, V. A., and G. P. Korneichuk, Zhur. Fiz. Khim. 28, 1812 (1954).

38 Rosner, D. E., A.I.Ch.E. J.9, 321 (1963).

39 Rosner, D. E., Chem. Eng. Sci. 19, 1 (1964).

40 Rothfeld, L. B., A.I.Ch.E. J. 9, 19 (1963).

41 Schilson, R. E., and N. R. Amundson, Chem. Eng. Sci 18, 226 (1961).

42 Schneider, P. J., "Temperature Response Charts," John Wiley and Sons, New York (1962).

43 Schotte, W., A.I.Ch.E. J. 6, 66-67 (1960).

44 Scott, D. S., Can. J. Chem. Eng. 40, 173 (1962).

45 Scott, D. S., and K. E. Cox, Can. J. Ch. Eng. 38, 201 (1960).

46 Scott, D. S., and F. A. L. Dullien, A.I.Ch.E. J. 8, 113 (1962).

47 Sehr, R. A., Chem. Eng. Sci. 9, 145 (1958).

48 Smith, N. L., and N. R. Amundson, Chem. Eng. Sci. 13, 226 (1961).

49 Thiele, E. W., Ind. & Eng. Chem. 31, 916 (1939).

50 Tinkler, J. D., and A. B. Metzner, Ind. & Eng. Chem. 53, 663 (1961).

51 Trotter, I. P., Ph.D. Thesis, Princeton University (1958).

52 Wakao, N., and J. M. Smith, Chem. Eng. Sci. 17, 825 (1962).

53 Wakao, N. and J. M. Smith, I.&E.C. Fund. 3, 123 (1964).

54 Watson, G. M., R. B. Evans, III, and E. A. Mason, J. Chem. Phys. 35, 2076 (1961).

55 Weisz, P. B., Z. physik Chem. 11, 1 (1957).

56 Weisz, P. B., and J. S. Hicks, Chem. Eng. Sci. 17, 265 (1962).

57 Weisz, P. B., and C. D. Prater, "Advances in Catalysis," Vol.6, Academic Press, New York (1954).

58 Weisz, P. B., and A. B. Schwartz, Jour. Cat. 1, 399 (1962).

59 Wheeler, A. "Advances in Catalysis," 3, Academic Press, New York (1950).

60 Wheeler, A., "Catalysis," 2, Reinhold, New York (1955).

61 Wicke, E., and R. Kallenback, Kolloid Z. 97, 135 (1941).